# The hemodynamic influence of the intrapelvic bleeding volume measured with three dimensional (3D) CT Volumetry by mechanic partially stable or instable pelvic ring fractures

Dissertation to obtain the grade Doctor of Medicine
From the Justus Liebig University
Medical Faculty
Gießen

Prepared from Georgievski Goran
Born in Skopje, North Macedonia

Gießen, 2025

From the Experimental Trauma Surgery, Justus- Liebig- University of Giessen
Department of Trauma-, Hand-, and Reconstructive Surgery,
University of Giessen GmbH

Correspondent 1: Univ-. Prof. Dr. med. Dr. h.c. Chirstian Heiß
Correspondent 2: PD Dr. Fritz Roller

Disputation Day: 17.12.2025

# Contents

1 **Introduction** ..... 1
1.1 Epidemiology ..... 2
1.2 Anatomy of the Pelvis ..... 3
1.2.1 Bony Anatomy – Pelvic Bones ..... 4
1.2.2 Ilium ..... 5
1.2.3 Pubis ..... 6
1.2.4 Ischium ..... 6
1.2.5 Sacrum ..... 6
1.2.6 Coccyx ..... 7
1.2.7 Joints ..... 7
1.2.8 Anatomical Variations ..... 8
1.3 Muscles of the pelvis ..... 9
1.4 Anatomy of the Blood Vessels in the Pelvic Region ..... 11
1.4.1 Arteries ..... 11
1.4.2 Veins ..... 14
1.4.3 Nerves ..... 14
1.4.4 Nerves of the Pelvic Region ..... 15
1.5 Definitions, Etiology and Diagnosis of Pelvic Fractures ..... 17
1.5.1 Key Terms and Definitions ..... 17
1.6 Mechanism of Injury ..... 17
1.7 Classification of Pelvic Fractures ..... 18
1.7.1 Tile Classification ..... 18
1.7.2 AO Classification of Pelvic Ring Fractures ..... 20
1.7.3 Fragility Fracture Classification of the Pelvis (FFP) ..... 25
1.8 Clinical Features and Diagnosis of Pelvic Fractures ..... 27
1.8.1 Clinical Features ..... 27
1.8.2 Diagnosis ..... 28
1.9 Therapy ..... 29
1.9.1 Emergency Therapy of Unstable Pelvic Ring Fractures ..... 29
2 **Research Question and Study Aim** ..... 31
3 **Material and Methods** ..... 33
3.1 Study Design and Setting ..... 33
3.1.1 Inclusion and Exclusion Criteria ..... 33
3.2 Data Collection and Analysis ..... 34
3.3 Parameters Evaluated ..... 35

3.4 Data Analysis Using 3D Slicer ..... 35
3.5 Statistical Analysis ..... 40
4 **Results** ..... 41
4.1 Epidemiological Findings ..... 41
4.1.1 Gender and Age Distribution ..... 41
4.2 Classification of Fractures ..... 45
4.2.1 AO Classification ..... 45
4.2.2 FFP Classification ..... 46
5 **Discussion** ..... 52
5.1 Polytrauma and Maximum Care Hospitals ..... 52
5.2 Morbidity, Mortality, and Economic Burden ..... 53
5.3 Gender and Age Distribution ..... 53
5.4 Mechanisms of Injury ..... 54
5.5 High-Energy Versus Low-Energy Trauma ..... 54
5.6 Economic and Clinical Burden ..... 54
5.7 Challenges in Early Detection ..... 55
5.8 Hidden Shock and Diagnostic Innovations ..... 55
5.9 CT Volumetry: Historical and Current Applications ..... 56
5.10 3D CT Volumetry in Evaluating Bleeding Volumes ..... 56
5.11 Methodology and Training ..... 56
5.12 Limitations of 3D Slicer for Clinical Use ..... 57
5.13 Bleeding Volume by Fracture Classification ..... 57
5.14 Comparison with Prior Studies ..... 58
5.15 Fragility Fracture Classification and Age-Related Variations ..... 58
5.16 Mechanisms of Injury and Clinical Impact ..... 58
5.17 Age-Related Variations in Pelvic Fractures ..... 59
5.18 Findings in the Literature ..... 60
5.19 Treatment Strategies for Complex Pelvic Fractures ..... 60
5.20 Advances in the Treatment of Unstable Pelvic Fractures ..... 60
5.21 Current Radiological Interventions ..... 61
5.22 Polytraumatized Patients and Injury Patterns ..... 61
5.23 Comparison with Epidemiological Studies ..... 62
5.24 Clinical Outcomes, Limitations, and Conclusion ..... 62
5.25 Study Limitations ..... 62
5.26 Future Implications ..... 63
5.27 Proposed Diagnostic and Therapeutic Algorithm ..... 63
6 **Conclusion** ..... 65

7 **References** ..... 66
8 **Summary** ..... 71
9 **Zusammenfassung** ..... 73
10 **List of Figures** ..... 76
11 **List of Tables** ..... 81
12 **Abbreviation Index** ..... 82
13 **Ehrenwörtliche Erklärung** ..... 84
14 **Acknowledgements** ..... 85

# 1 Introduction

Pelvic fractures represent a persistent challenge for trauma and orthopedic surgeons due to their complexity and the critical importance of timely and adequate treatment. These injuries not only affect patient survival but also significantly influence postoperative outcomes and complications, such as infections, revision surgeries, and post-traumatic arthrosis (Verma et al., 2020). The treatment of such patients frequently requires intensive care unit (ICU) management and early inpatient rehabilitation, placing a substantial burden on healthcare systems (McMinn et al., 2020). Furthermore, the multifaceted complications associated with pelvic fractures pose considerable challenges for patients, impacting their long-term quality of life (Sobantu et al., 2017).

In the setting of a trauma center, a large proportion of patients presenting with pelvic fractures are polytraumatized individuals, with complex pelvic fractures being a leading cause of mortality in this group (Giannoudis et al., 2007). However, an increasing number of cases involve isolated pelvic injuries, particularly in older adults with osteoporotic fractures. This demographic shift, driven by an aging population, underscores the growing prevalence of low-energy trauma as a causative factor for pelvic fractures (World Health Organization, 2011; Andrich et al., 2015). Treating these patients is inherently more complex due to comorbidities and the fragile nature of osteoporotic bone (Oberkircher et al., 2018; Rollmann et al., 2017).

Advancements in modern medicine have emphasized the importance of early diagnosis and management of pelvic fractures. The timely recognition of intrapelvic bleeding, alongside innovative systems such as the Resuscitative Endovascular Balloon Occlusion of the Aorta (REBOA), is pivotal in improving patient outcomes (Wortmann et al., 2020; Pieper et al., 2018). These developments highlight the critical need for accurate diagnostic tools and tailored treatment protocols to manage these injuries.

The research conducted in this context aimed to investigate the incidence and characteristics of polytrauma cases in the Region of Middle Hesse. It sought to determine whether the use of 3D CT segmentation for assessing the bleeding volume in pelvic fractures significantly influences subsequent treatment strategies. Specifically, the study explored whether this technique could alter the diagnostic and therapeutic algorithms employed in managing these complex fractures, potentially leading to improved outcomes. The goal was to assess the impact of advanced imaging technologies on clinical

decision-making and to evaluate their role in shaping treatment protocols for patients with pelvic polytrauma (Veith et al., 2016; Blackmore et al., 2003; Iwano et al., 2009).

### *1.1 Epidemiology*

Pelvic fractures account for approximately 1.5–3% of all skeletal injuries and are often life-threatening, particularly in polytraumatized patients (Hodgson, 2009). Hodgson et al. (2009) identified road traffic accidents (RTAs) as the predominant cause of high-energy pelvic fractures, followed by falls from height and heavy object trauma. These patterns remain consistent over time. However, recent studies suggest an increasing prevalence of low-energy fractures, particularly in elderly populations, reflecting a global trend toward an aging society (Kannus et al., 2000; Dong et al., 2022).

Epidemiological data indicate that pelvic fractures predominantly affect younger male populations, with high-energy trauma such as car and motorcycle accidents being the primary cause (Yoshihara & Yoneoka, 2014; Sunil & Shetty, 2000). In contrast, older adults, particularly women, are more likely to sustain pelvic fractures due to low-energy mechanisms, such as ground-level falls, often compounded by osteoporosis (Dzupa et al., 2009; Andrich et al., 2021). These fractures carry significant socioeconomic implications, particularly in younger individuals, as they frequently lead to prolonged recovery periods and impaired productivity (Ghosh et al., 2019).

Notably, low-energy fractures are associated with lower mortality rates. For instance, a Brazilian study reported a mortality rate of only 3% for type A fractures, which typically result from low-energy trauma and are often free from complications. In contrast, high-energy fractures, such as type C injuries, are associated with severe trauma and significantly higher mortality rates (Pereira et al., 2017). Pohlemann et al. (1996) found that pelvic ring injuries without significant soft tissue involvement comprised 63.6% type A fractures (stable fractures), 21% type B (partially stable fractures), and 15.5% type C (instable pelvic fractures). Operative stabilization was required in 3.9%, 37.3%, and 54.3% of these cases, respectively (Pohlemann et al., 1996).

In Germany, the incidence of osteoporotic pelvic fractures is rising. Andrich et al. (2015) reported an annual incidence of 22.4 osteoporosis-associated fractures per 10,000 individuals over the age of 60, with similar trends observed in Finland, where rates among individuals aged 80 and above increased from 73 to 364 per 100,000 per year between 1970 and 1997 (Kannus et al., 2000; Burge et al., 2007). These findings underscore the

increasing clinical and societal burden posed by pelvic fractures in an aging population (Destatis website, 2023).

### *1.2 Anatomy of the Pelvis*

The anatomy of the pelvis is highly complex, as it serves as the structural connection between the torso and the lower extremities while proximally adjoining the abdominal region **(Figure 1, Gray, 2013).** From a biomechanical perspective, the pelvis is crucial for transmitting forces from the torso to the legs and providing stability during movement. It is composed of the pelvic bones and the terminal parts of the vertebral column. Structurally, the pelvic region is divided into two subregions:

1. **Greater Pelvis (Latin: Pelvis Major):** The greater pelvis is the upper region of the pelvic area, formed by the upper parts of the pelvic bones and the lower lumbar vertebrae. Functionally, it is considered part of the lower abdomen and supports abdominal viscera.
2. **Lesser Pelvis (Latin: Pelvis Minor):** The lesser pelvis, also known as the true pelvis, constitutes the inferior portion of the pelvic region. Components of the pelvic bones, the sacrum, and the coccyx form it. This region encloses and protects the pelvic cavity, which houses the reproductive organs, bladder, and rectum (Gray, 2013).

Two specific anatomic structures are particularly relevant to the study of pelvic trauma and clinical management:

- **Retroperitoneal Space:** Positioned posterior to the peritoneum, the retroperitoneal space contains critical anatomical structures, including significant blood vessels such as the abdominal aorta and the inferior vena cava. These vessels are significant in the management of polytraumatized patients, as injuries in this area often result in life-threatening hemorrhages.
- **Perineum:** The perineum comprises the region containing the openings of the gastrointestinal, reproductive, and urinary tracts, as well as the roots of the external genitalia. This area is of clinical interest due to its involvement in trauma-related injuries (Gray, 2013).

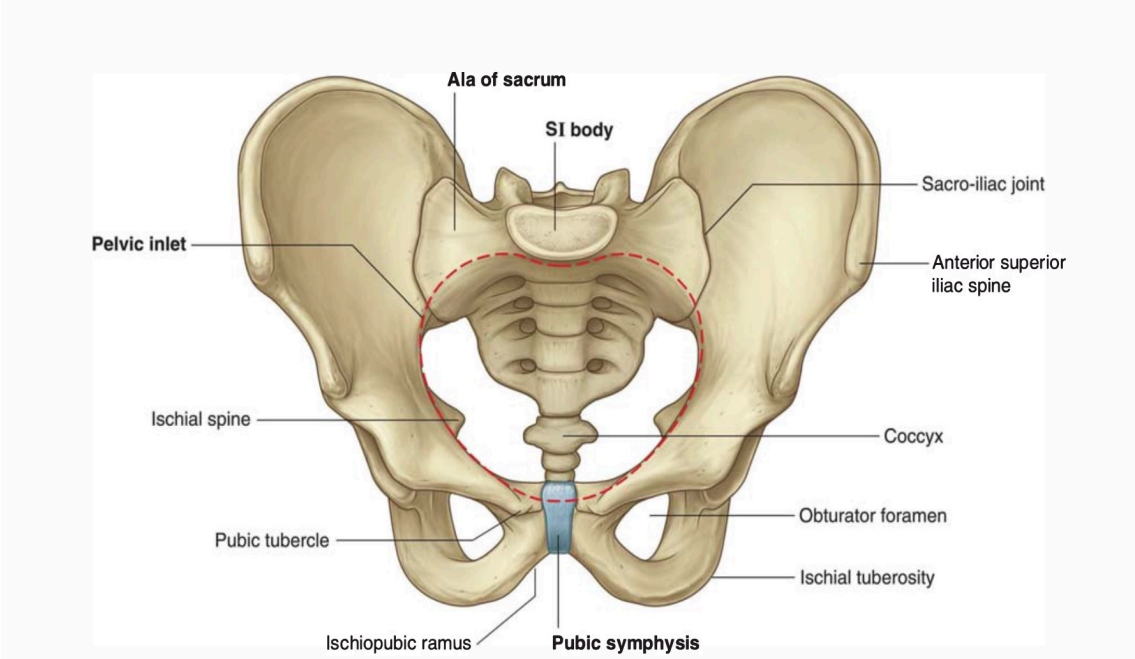


**Figure 1: Pelvic inlet and associated anatomical structures.** The figure illustrates the main anatomical landmarks of the pelvic inlet, including the sacro-iliac joint, pubic symphysis, ischiopubic ramus, and obturator foramen, among others. Adapted from Gray, Henry (2013), *Gray's Anatomy*, London, England: Arcturus Publishing.

### *1.2.1 **Bony Anatomy – Pelvic Bones***

As previously defined, the greater and lesser pelvis connect to the sacrum and coccyx to form the pelvic girdle. Anatomically, the pelvic bone is irregular and divided into two regions by an oblique line on its medial surface. The area above this line constitutes the lateral wall of the false pelvis (greater pelvis), while the area below it forms part of the true pelvis (lesser pelvis), **(Figure 1, Gray, 2013).**

A central feature of the pelvic bone is the acetabulum, which is formed by the fusion of three components of the pelvic bone: the ilium, ischium, and pubis. Together with the head of the femur, the acetabulum forms the hip joint, enabling movement and weight-bearing functions. The acetabulum is located on the lateral surface of the pelvic bone, and inferior to it lies the large obturator foramen. This foramen is enclosed by the obturator membrane (membrana obturatoria), serving as a passage for neurovascular structures.

The posterior margin of the pelvic bone contains two key features: the greater sciatic notch and the lesser sciatic notch, which are separated by the ischial spine. Inferiorly, the posterior margin is defined by the ischial tuberosity, a prominent structure that serves as a weight-bearing surface during sitting (Gray, 2013).

On the anterior side, the pelvic bone has an irregular margin marked by the anterior superior iliac spine (spina iliaca anterior superior), the anterior inferior iliac spine (spina iliaca anterior inferior), and the pubic tubercle **(Figure 2, Gray, 2013).**

The ilium, ischium, and pubis initially develop as separate components connected by cartilage around the acetabulum. By approximately 18 years of age, they fuse into a single pelvic bone, contributing to the mature structure of the pelvis (Gray, 2013).

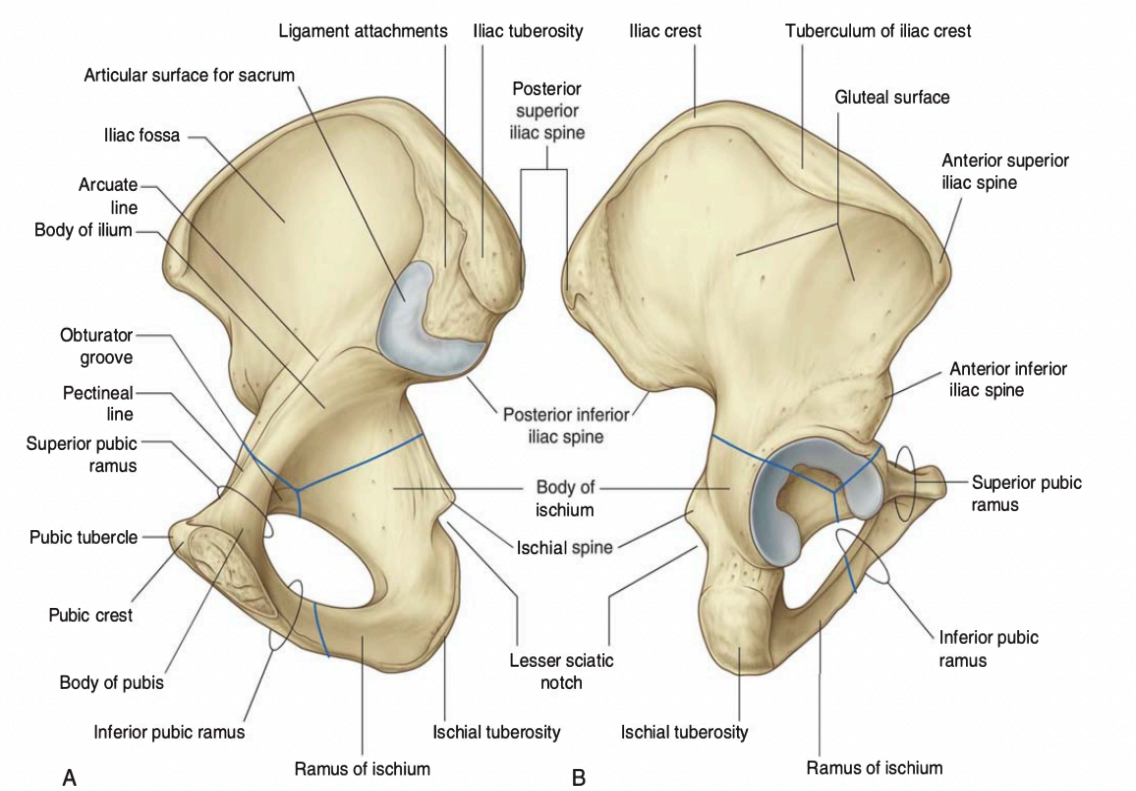


**Figure 2: Anatomical components of the pelvic bone**. (A) Medial surface of the pelvic bone, highlighting structures such as the iliac fossa, arcuate line, and pubic crest. (B) The lateral surface of the pelvic bone illustrates features including the gluteal surface, anterior superior iliac spine, and acetabulum. Adapted from Gray, Henry (2013), Gray's Anatomy, London, England: Arcturus Publishing.

### *1.2.2 Ilium*

The ilium (Latin: Os Ilium) is the superior portion of the pelvic bone and is divided into upper and lower parts by a prominent line on its medial surface **(Figure 2, Gray, 2013).** The upper portion forms part of the false pelvis, providing attachment points for muscles associated with the lower limb. The iliac fossa, located on the anteromedial surface of the

wing (Latin: Ala Ossis Ilii), is concave in shape. The external surface of the ilium connects to the gluteal region, playing a crucial role in the movement of the lower limb. The iliac crest, the superior margin of the ilium, is an attachment site for the abdomen, back, and lower limb muscles and fascia.

This crest terminates anteriorly at the anterior superior iliac spine (Spina Iliaca Anterior Superior) and posteriorly at the posterior superior iliac spine (Spina Iliaca Posterior Superior). The iliac crest's tuberculum marks the iliac crest's lateral end, while the posterior end features the iliac tuberosity (Gray, 2013).

### *1.2.3 Pubis*

The pubis (Latin: Os Pubis) consists of a body and two arms **(Latin: Rami, Gray, 2013, Figure 2).** The body of the pubis articulates with the pubic symphysis, and its superior surface extends laterally to form the prominent pubic tubercle.

The superior pubic ramus and inferior pubic ramus join posteriorly with the ilium and ischium. The superior margin of the superior pubic ramus, known as the pecten pubis or pectineal line, contributes to the linea terminalis of the pelvic bone. The inferior surface of the superior pubic ramus forms the upper margin of the obturator groove, a key passage for neurovascular structures.

### *1.2.4 Ischium*

The ischium (Latin: Os Ischii) forms the inferior and posterior portion of the pelvic bone (Gray, 2013, Figure 2). It consists of a large body that joins superiorly with the ilium and superior pubic ramus, and anteriorly, a ramus that fuses with the inferior pubic ramus. A prominent anatomical landmark is the ischial tuberosity, located on the posteroinferior aspect of the bone. This structure is a primary attachment site for lower limb muscles and bears the body's weight while sitting (Gray, 2013).

### *1.2.5 Sacrum*

The sacrum is a triangular bone that forms part of the spine **(Figure 2 and 3, Gray, 2013).** It is composed of five fused sacral vertebrae and articulates proximally with the lumbar vertebrae (L5) and distally with the coccyx. Each lateral surface of the sacrum articulates with the ilium via a large, L-shaped facet, forming the sacroiliac joint. Posterior to the facet lies a roughened area for the attachment of ligaments.

On the superior surface of the first sacral body, wing-like transverse processes known as the ala are located laterally. Another key feature is the promontory, the anterior edge of the first sacral vertebral body, which contributes to the pelvic inlet **(Figure 3, Gray, 2013).**

### *1.2.6 Coccyx*

The **coccyx**, or the tailbone, is the spine's rudimentary, terminal portion **(Figure 3, Gray, 2013).** It has the shape of an inverted triangle and is composed of four fused coccygeal vertebrae. The coccyx articulates proximally with the sacrum, forming the base of the spinal column (Gray, 2013).

### *1.2.7 Joints*

From a surgical perspective, the sacroiliac joint and the pubic symphysis are critical structures as they close the pelvic ring and play a key role in the biomechanics and stability of the pelvic girdle. The forces transmitted from the lower limbs are conveyed through the sacroiliac joints. Superiorly, the pelvic ring articulates with the sacrum and the fifth lumbar vertebra (L5) to form the lumbosacral joint (Gray, 2013).

Several ligaments, including the anterior sacroiliac ligament, the posterior sacroiliac ligament, and the interosseous sacroiliac ligament ensure the stability of the sacroiliac joint. The pubic symphysis, located anteriorly between the surfaces of the pubic bones, is a fibrocartilaginous joint reinforced by the superior pubic ligament and inferior pubic ligament. These joints and their associated ligaments contribute to the pelvic girdle's structural integrity and functional dynamics **(Figure 3, Gray, 2013).**

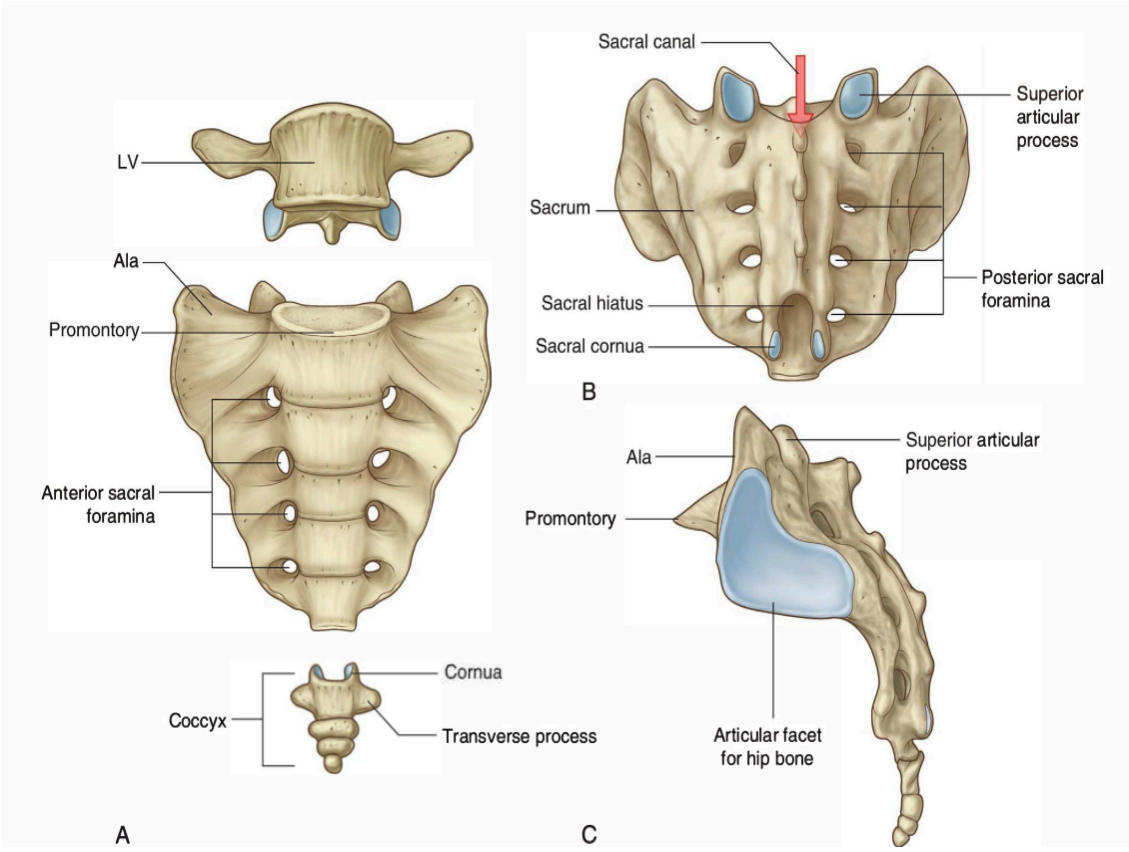


**Figure 3: Sacrum and Sacro-iliac joint anatomy.** (A) Anterior view of the sacrum, illustrating key structures such as the anterior sacral foramina, promontory, and ala. (B) The posterior view of the sacrum highlights the sacral hiatus, sacral cornua, and posterior sacral foramina. (C) The lateral view of the sacrum shows the superior articular process, articular facet for the hip bone, and the promontory. Adapted from Gray, Henry (2013), Gray's Anatomy, London, England: Arcturus Publishing.

### *1.2.8 Anatomical Variations*

Significant anatomical differences exist between the male and female pelvis, with critical implications, particularly during childbirth. The female pelvis is uniquely adapted to facilitate the passage of the fetus through the pelvic cavity. Key differences include:

1. **Shape of the Pelvic Inlet:** The female pelvis has a circular-shaped pelvic inlet, while the male pelvis has a heart-shaped pelvic inlet. Additionally, the **promontory** in the female pelvis is less pronounced, and the wings of the ilium are broader and more flared.

2. **Subpubic Angle:** The angle formed by the inferior pubic rami is more significant in females (approximately 80–85°) compared to males (50–60°), facilitating a wider birth canal.

3. **Anterior Superior Iliac Spine (ASIS):** In males, the **spina iliaca anterior superior** is generally positioned more medially compared to females, reflecting the narrower overall dimensions of the male pelvis.

These differences underline the functional and structural adaptations of the female pelvis for reproductive purposes **(Figure 4, Gray, 2013).**

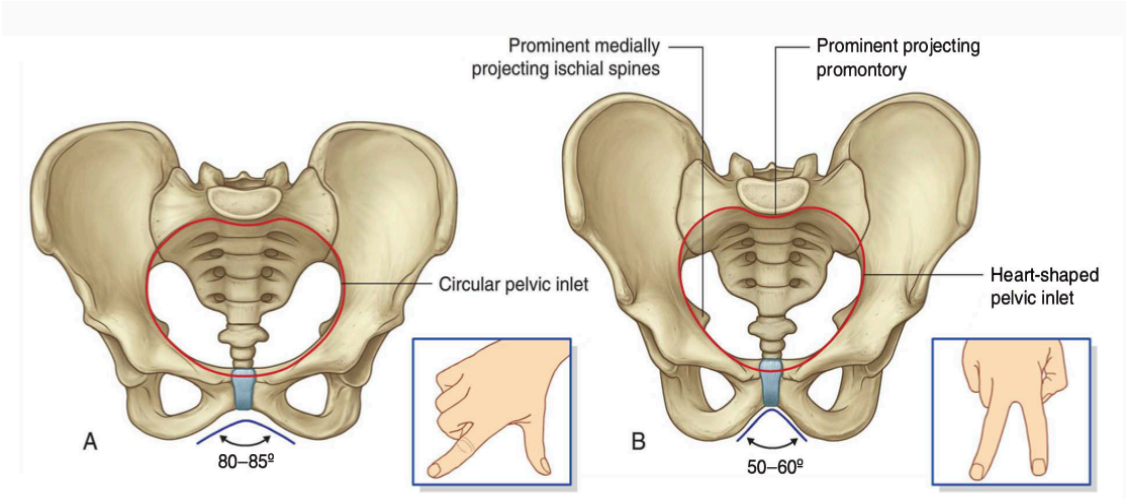


**Figure 4: Comparison of the bony pelvis between women and men.** (A) The female pelvis has a circular pelvic inlet and a wider pubic arch angle (80–85°). (B) Male pelvis with a heart-shaped pelvic inlet and a narrower pubic arch angle (50–60°). The inset illustrations approximate the pubic arch angle: the angle between the thumb and index finger for women, and the angle between the index and middle fingers for men. Adapted from Gray, Henry (2013), Gray's Anatomy, London, England: Arcturus Publishing.

### *1.3 Muscles of the pelvis*

The pelvis muscles are categorized into several functional groups, each contributing to the pelvic region's movement, stabilization, and support **(Figure 5).** These muscles are vital for maintaining posture, facilitating locomotion, and supporting pelvic organs.

**The gluteal group** is located on the lateral side of the pelvic bone (os ilium) and is divided into superficial and deep layers. The superficial group includes the gluteus maximus, gluteus medius, gluteus minimus, and the tensor fasciae latae. These muscles are responsible for hip extension, abduction, internal rotation, and pelvis stabilization during walking. The deep layer consists of smaller muscles such as the piriformis, superior and inferior gemelli, obturator internus and externus, and quadratus femoris. These muscles

contribute to external rotation and stabilization of the hip joint. The gluteal muscles are essential for dynamic movement and maintaining balance during physical activity **(Figure 5, Gray, 2013).**

**The adductor group** comprises the pectineus, adductor longus, adductor brevis, adductor magnus, and gracilis muscles. These muscles primarily adduct the hip, facilitating movements such as crossing the legs and maintaining pelvic stability during locomotion. They are situated in the medial compartment of the thigh, connecting the pelvis to the femur and playing an essential role in coordinating lower-limb movements (Gray, 2013). Another significant group is the iliopsoas, which is formed by the iliacus and psoas major muscles. Together, they are often referred to as the iliopsoas. This muscle group is a powerful hip flexor, stabilizing the lumbar spine and ensuring proper posture and alignment while standing and walking (Gray, 2013).

**The ischiocural group,** commonly known as the hamstrings, includes semitendinosus, semimembranosus, and biceps femoris muscles. These muscles extend the hip and flex the knee, making them critical for walking, running, and climbing. Positioned along the posterior thigh, they stabilize the pelvis and lower limb during dynamic activities (Gray, 2013).

**The pelvic floor muscles,** or pelvic diaphragm, comprise coccygeus and levator ani muscles. These muscles form a supportive sling that separates the pelvic cavity from the perineum. They are essential in supporting the pelvic organs, maintaining continence, and assisting in childbirth (Gray, 2013).

Clinically, the pelvic muscles are of great significance due to their innervation and vascularization. Injuries to these muscles, often seen in pelvic trauma, can lead to extra- or intramuscular bleeding, which may be overlooked but can profoundly affect patient

outcomes. Proper evaluation and management of muscle injuries are crucial in the treatment of pelvic trauma to ensure optimal recovery (Gray, 2013).

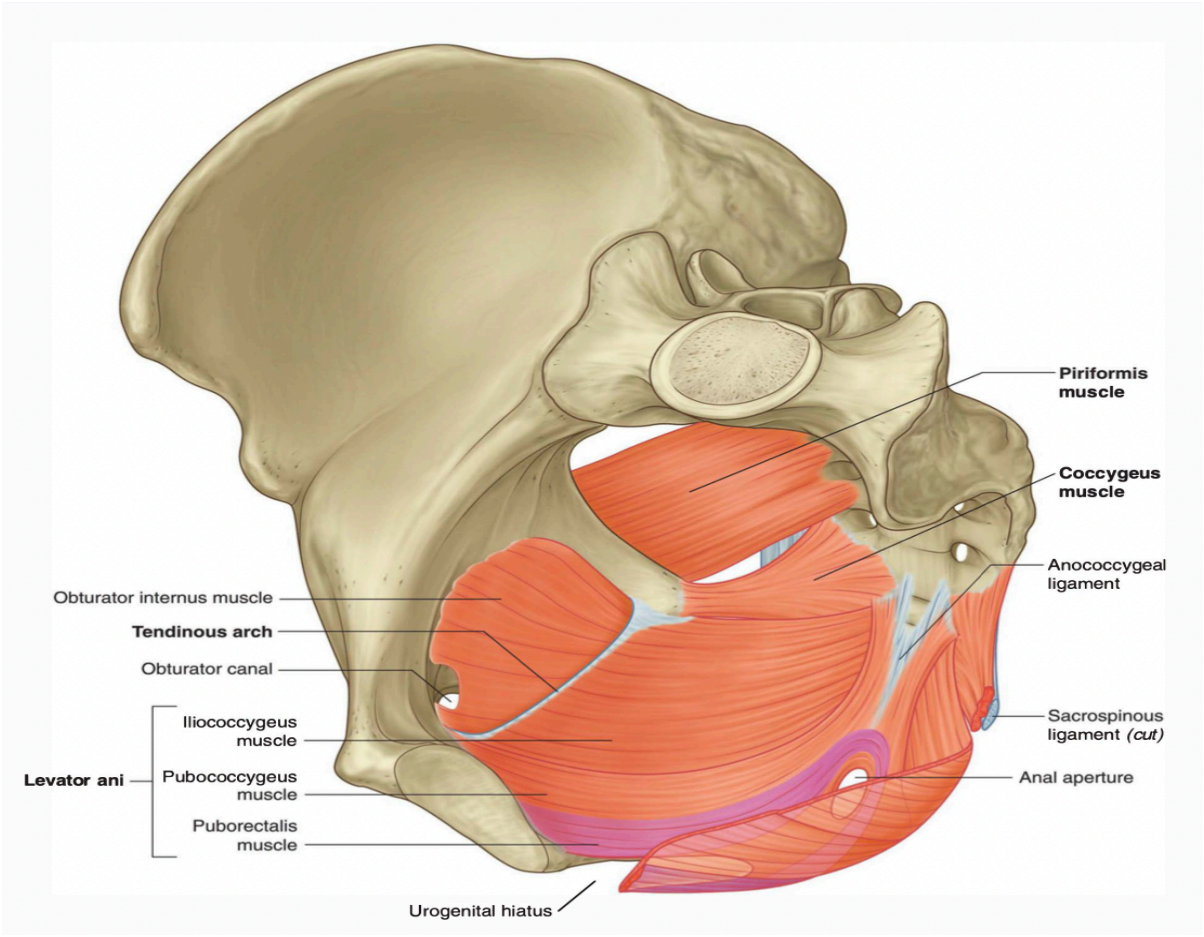


**Figure 5: Muscles of the pelvic region (medial view of the right side of the pelvis).** The illustration highlights key muscles of the pelvic area, including the obturator internus, piriformis, coccygeus, and components of the levator ani (iliococcygeus, pubococcygeus, and puborectalis muscles). Additional structures shown include the tendinous arch, urogenital hiatus, and sacrospinous ligament, which has been partially cut for clarity. Adapted from Gray, Henry (2013), Gray's Anatomy, London, England: Arcturus Publishing.

## *1.4 Anatomy of the Blood Vessels in the Pelvic Region*

### *1.4.1 Arteries*

The primary arterial structure in the pelvic region is the internal iliac artery, which branches extensively to supply the pelvic viscera, walls, floor, and the perineum **(Figure 6, Gray, 2013).** Additionally, the median sacral artery contributes to the vascularization of pelvic structures, while in females, the ovarian arteries, originating from the abdominal

aorta, provide further blood supply. The internal iliac artery follows a distinct pathway, dividing into two main trunks: the posterior and anterior trunks (Gray, 2013).

The posterior trunk of the internal iliac artery gives rise to several key branches, including the iliolumbar artery, which supplies the lower posterior abdominal wall; the lateral sacral artery, which vascularizes the sacrum and spinal nerves; and the superior gluteal artery, the largest branch, which supplies the gluteal region and associated muscles. These branches play a crucial role in maintaining the vascular integrity of the pelvis and its surrounding structures, ensuring adequate blood flow to support various functions. The arterial anatomy of the pelvic region and its branching patterns are illustrated in Figure *6*.

#### *1.4.1.1 Anterior Trunk of the Internal Iliac Artery*

The anterior trunk of the internal iliac artery is primarily responsible for supplying blood to the pelvic viscera. It gives rise to several key branches, each serving specific structures within the pelvis.

These branches include the umbilical artery, which continues as the medial umbilical ligament after giving off superior vesical branches; the superior and inferior vesical arteries, which supply the bladder and associated structures; the middle rectal artery, which provides blood to the rectum; the internal pudendal artery, which supplies the perineum; and the inferior gluteal artery, which contributes to the blood supply of the gluteal region. In females, the uterine artery arises from the anterior trunk and supplies the uterus, with additional branches to the vagina and surrounding structures **(Figure 7, Gray, 2013).** The extensive branching pattern of the anterior trunk ensures a reliable vascular supply to the pelvic organs and surrounding regions, supporting their critical functions. The anatomical distribution of these branches is illustrated in Figure 6 and Figure 7, demonstrating their relationships with neighboring structures (Gray, 2013).

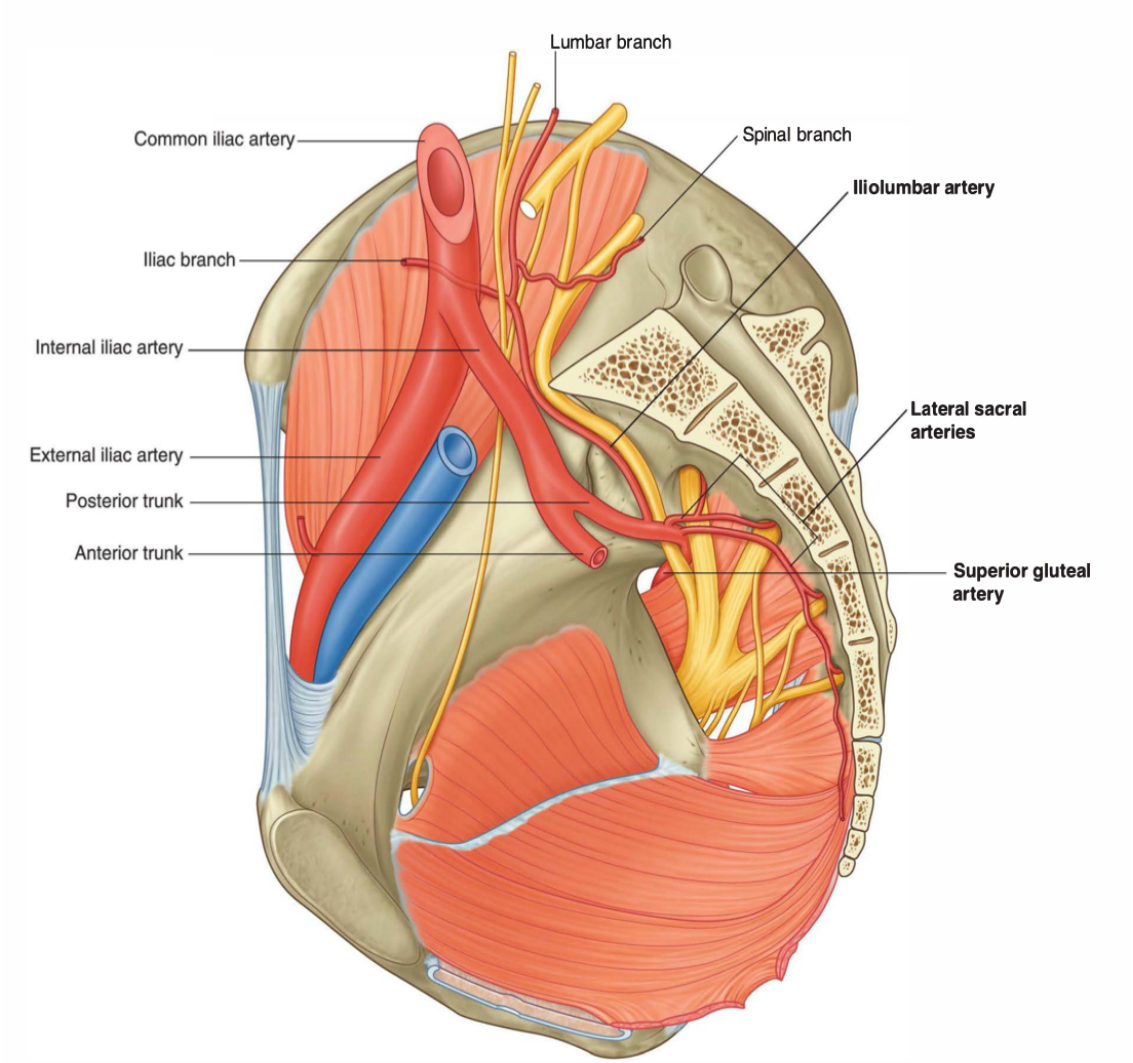


**Figure 6: Branches of the internal iliac artery and associated structures (male pelvis).** The illustration highlights the internal iliac artery, which divides into the posterior and anterior trunks. Key branches of the posterior trunk include the iliolumbar artery, lateral sacral arteries, and superior gluteal artery, which supply the posterior abdominal wall, sacrum, and gluteal region. The vascular anatomy of the pelvis demonstrates the close relationship between arterial branches and surrounding structures. Adapted from Gray, Henry (2013), Gray's Anatomy, London, England: Arcturus Publishing.

#### *1.4.1.2 Corona Mortis*

Darmanis et al. (2007) conducted an anatomical study with significant clinical implications, focusing on the corona mortis, also known as the "crown of death." This vascular anastomosis can be either arterial or venous, connecting the obturator vessels and the external iliac or inferior epigastric arteries or veins. Anatomically, the corona mortis varies in location and distance but is typically found in the retropubic region.

From a surgical perspective, injury to this anastomosis poses a substantial risk of severe bleeding, which, if left untreated, can lead to fatal outcomes. This vascular structure's awareness and careful handling are crucial during surgical approaches to the pelvis and acetabulum (Darmanis et al., 2007; Gray, 2013).

### *1.4.2 Veins*

Veins typically accompany arteries throughout the body; the pelvis is no exception. However, exceptions to this rule include the umbilical artery and the iliolumbar artery, which do not have accompanying veins.

Within the pelvic cavity, venous plexuses are intricately connected to the surfaces of pelvic organs. In females, these plexuses are associated with the vagina and uterus, while in males, they are related to the prostate. Additionally, both sexes have venous connections to the bladder and rectum.

One particularly notable venous structure is the plexus venosus sacralis, located on the anterior surface of the sacrum. Fractures of the sacrum can result in injury to this venous plexus, leading to significant clinical complications. The importance of recognizing and addressing such venous injuries during pelvic trauma management cannot be overstated (Gray, 2013).

### *1.4.3 Nerves*

The somatic nerves of the pelvic region, including the sacral and coccygeal plexuses, are responsible for innervating the lower limbs as well as the muscles of the pelvis and perineum. These plexuses are formed by the ventral rami of spinal nerves S1 to Co, with contributions from the lumbar plexus via L4 and L5. Together, these structures form the lumbosacral plexus.

The sacral plexus also provides innervation to specific muscles, such as the musculus piriformis, which plays a key role in hip stabilization and movement.

The intricate anatomy and functional significance of the pelvic nerve plexuses are essential for understanding both normal function and the consequences of nerve injuries in pelvic trauma **(Figure 8, Gray, 2013).**

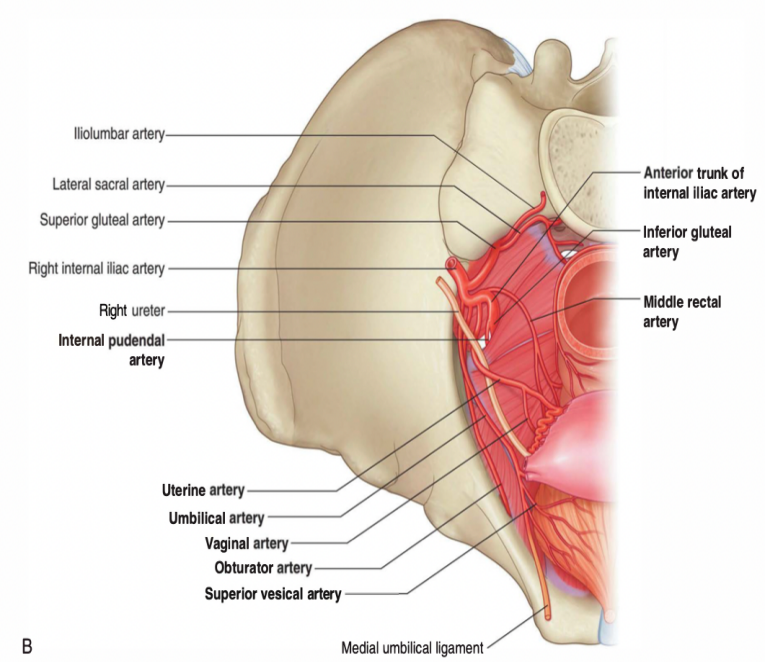


**Figure 7: Branches of the anterior trunk of the internal iliac artery in females.** This illustration highlights the arterial branching of the anterior trunk of the internal iliac artery, including the uterine artery, vaginal artery, umbilical artery, obturator artery, middle rectal artery, internal pudendal artery, and inferior gluteal artery. These arteries supply blood to the pelvic viscera, perineum, and adjacent structures. The medial umbilical ligament is also depicted, showing its continuation from the umbilical artery. Adapted from Gray, Henry (2013), Gray's Anatomy, London, England: Arcturus Publishing.

### *1.4.4 Nerves of the Pelvic Region*

The lumbosacral trunk forms the sacral plexus, comprising contributions from L4 and L5, and the anterior rami of spinal nerves S1 to S4. This plexus gives rise to several important branches, including the sciatic nerve, the pudendal nerve, and the superior and inferior gluteal nerves. Additional branches include the nerve to obturator internus, the nerve to quadratus femoris and gemellus muscles, the posterior femoral cutaneous nerve (also known as the posterior cutaneous nerve of the thigh), the perforating cutaneous nerve, and the nerve to piriformis.

These branches innervate various muscles of the pelvis, lower limb, and perineum **(Figure 8, Gray, 2013).**

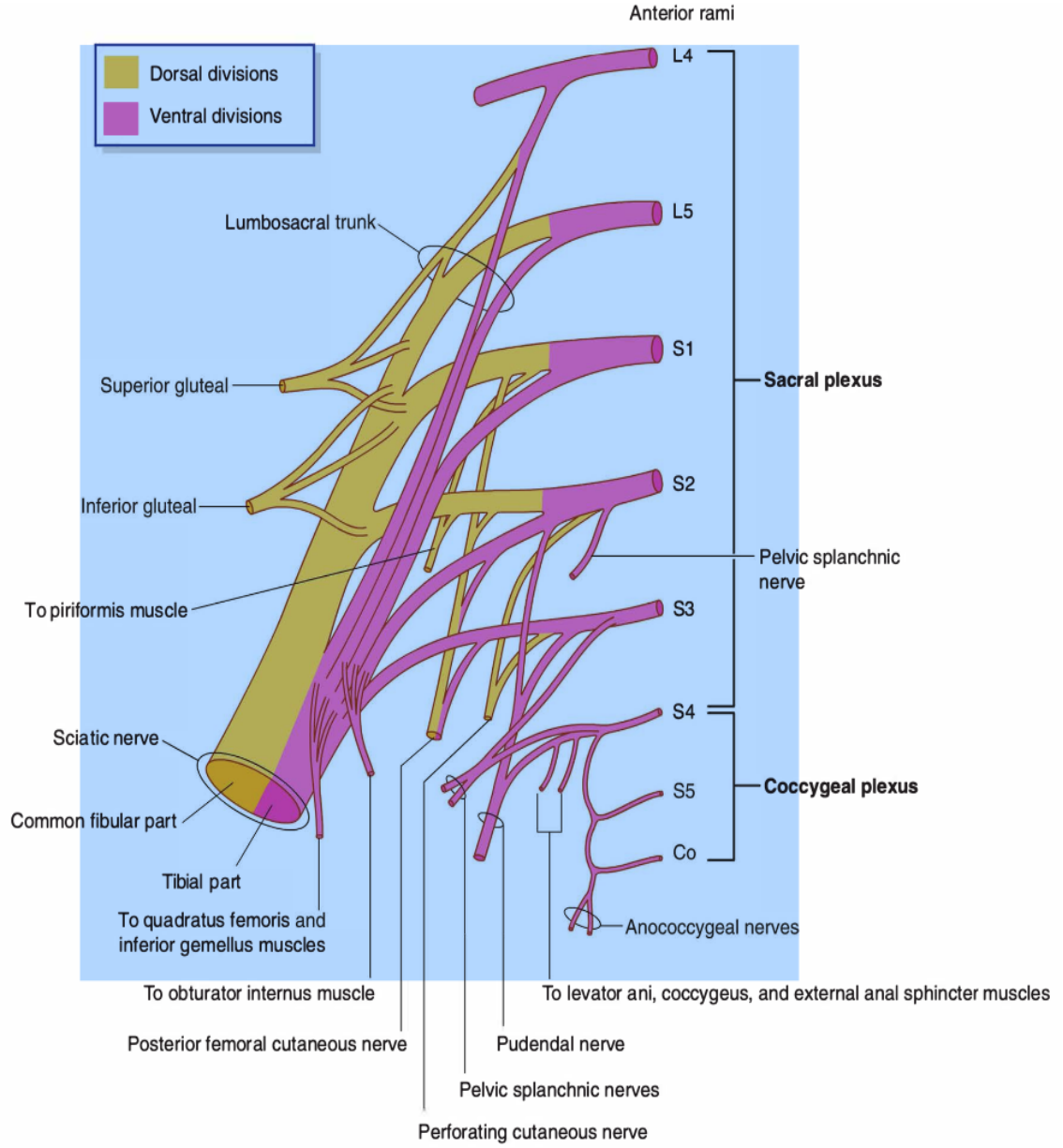


**Figure 8: Components and branches of the sacral and coccygeal plexuses.** This diagram illustrates the anatomical composition of the sacral and coccygeal plexuses, including contributions from the lumbosacral trunk (L4 and L5), ventral rami of S1 to Co, and their major branches. Key nerves such as the sciatic nerve, superior and inferior gluteal nerves, pudendal nerve, and pelvic splanchnic nerves are shown, along with their targets, including the musculus piriformis, levator ani, and external anal sphincter. Dorsal and ventral divisions are color-coded for clarity. Adapted from Gray, Henry (2013), *Gray's Anatomy*, London, England: Arcturus Publishing.

## *1.5 Definitions, Etiology and Diagnosis of Pelvic Fractures*

### *1.5.1 Key Terms and Definitions*

A pelvic fracture refers to a break in one or more bones of the pelvic ring. Depending on the mechanism of injury, these fractures can range from minor, such as osteoporotic fractures caused by low-energy trauma, to complex fractures resulting from high-energy trauma such as car accidents. As previously discussed in the anatomy of the pelvis, pelvic stability relies on both bony and ligamentous structures, with the weight-bearing portion concentrated in the posterior arch (J Trauma Acute Care Surg, 2014).
A stable pelvic fracture is characterized by minimal or no displacement and typically does not involve disruption of the pelvic ring. In contrast, an unstable pelvic fracture involves significant displacement of the pelvic ring and is often associated with injuries to major blood vessels, nerves, and visceral organs. These are commonly referred to as complex pelvic injuries (J Trauma Acute Care Surg, 2014).

Polytrauma is defined as injuries affecting multiple body regions or organ systems, with one or more of these injuries being life-threatening. Tscherne (1998) further specified polytrauma as significant injuries in three or more points across two or more anatomic AIS regions, in combination with additional physiological impairments (Pohlemann et al., 1998).

## *1.6 Mechanism of Injury*

The most common mechanisms of pelvic fractures are lateral compression and anteroposterior compression, often resulting from road traffic accidents. These mechanisms can disrupt the pelvic ring. Vertical shear forces, frequently observed in falls from heights, and inferior forces also contribute to pelvic fractures. In some cases, pathologic fractures of the pelvic ring occur due to underlying bone diseases such as osteoporosis, osteomalacia, or tumors. These fractures are usually associated with low-energy trauma and occur predominantly in elderly patients (Pohlemann et al., 1998).

## *1.7 Classification of Pelvic Fractures*

### *1.7.1 Tile Classification*

The literature includes several classifications for pelvic fractures. This study highlights three major classification systems: Tile Classification, AO Classification, and Fragility Fracture of the Pelvis (FFP) Classification.

Marvin Tile (1986) proposed a classification system based on the mechanism of injury and the stability of the fracture:

**1) Type A: Stable Fractures.** These fractures maintain the continuity and stability of the pelvic ring. Examples include avulsion injuries and isolated fractures of the iliac wing. Osteoporotic pelvic fractures caused by low-energy trauma, such as a direct fall, also fall under this category **(Figure 9a, jramc.bmj.com).**

- A1: Fractures not involving the pelvic ring.
- A2: Stable fractures with minimal displacement (Tile, 1988).

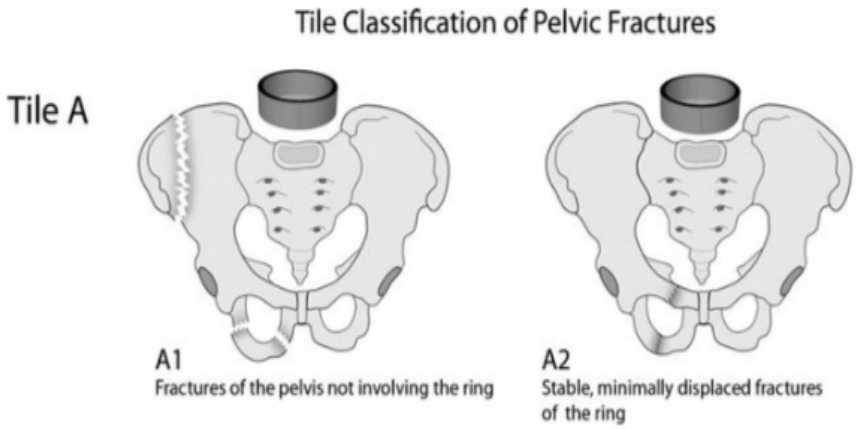


**Figure 9a: Tile Classification of Pelvic Fractures.** The illustration depicts the Tile classification of pelvic fractures based on fracture stability and mechanism of injury. Type A: Stable fractures, including A1 (fractures not involving the pelvic ring) and A2 (stable, minimally displaced fractures of the ring). Adapted from Journal of the Royal Army Medical Corps (jramc.bmj.com).

**2) Type B: Rotationally Unstable but Vertically Stable Fractures**
These fractures involve rotational instability without disrupting the pelvic ring's vertical stability. They commonly occur due to frontal or front-lateral trauma **(Figure 9b, jramc.bmj.com).**

- B1: Open book injuries.
- B2: Lateral compression – Ipsilateral.
- B3: Lateral compression – Contralateral (Bucket handle injuries) (Tile, 1988).

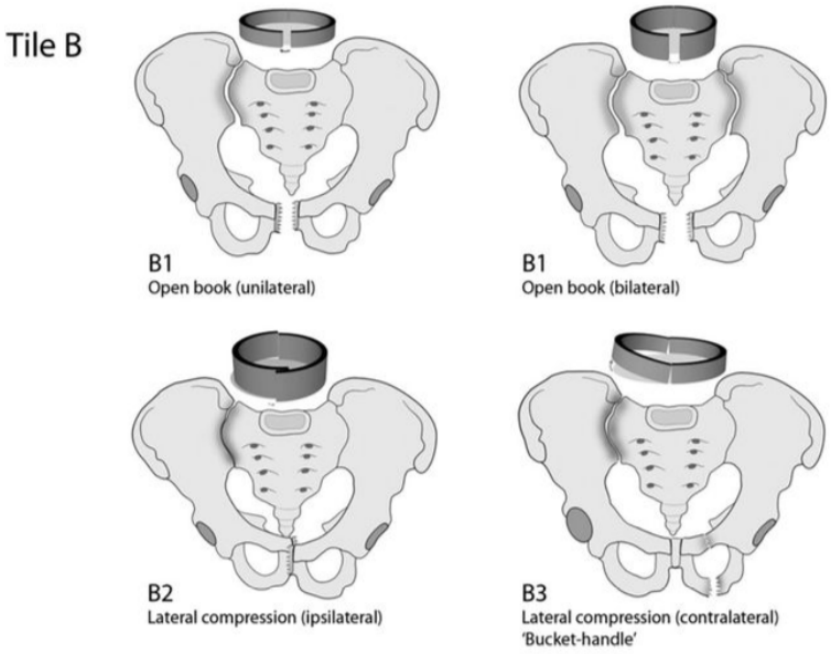


**Figure 9b: Tile Classification of Pelvic Fractures.** The illustration depicts the Tile classification of pelvic fractures based on fracture stability and mechanism of injury. Type B: Rotationally unstable but vertically stable fractures, subdivided into B1 (open book injuries), B2 (ipsilateral lateral compression), and B3 (contralateral lateral compression or bucket-handle injuries). Adapted from Journal of the Royal Army Medical Corps (jramc.bmj.com).

**3) Type C: Rotationally and Vertically Unstable Fractures**
These fractures result from high-energy trauma, such as falls from great heights or motorbike accidents. They are highly unstable and require urgent intervention **(Figure 9c, jramc.bmj.com).**

- C1: Rotationally and vertically unstable.
- C2: Bilateral instability.
- C3: Associated with acetabular fractures (Tile, 1988).

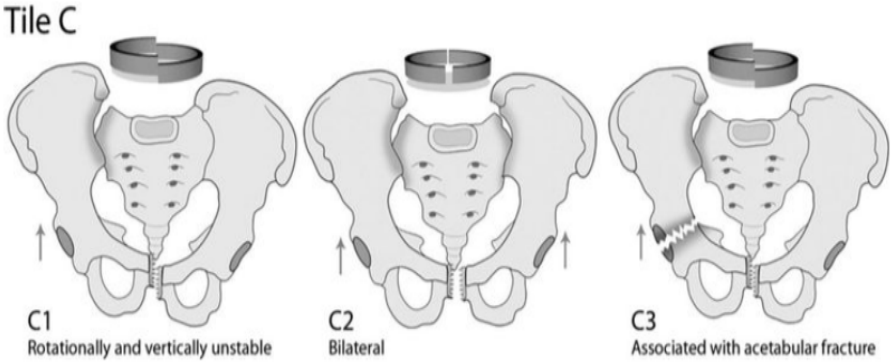


**Figure 9c: Tile Classification of Pelvic Fractures.** The illustration depicts the Tile classification of pelvic fractures based on fracture stability and mechanism of injury. Type C: Rotationally and vertically unstable fractures, including C1 (unilateral instability), C2 (bilateral instability), and C3 (associated with acetabular fractures). Adapted from Journal of the Royal Army Medical Corps (jramc.bmj.com).

### *1.7.2 AO Classification of Pelvic Ring Fractures*

In 1996, the AO Foundation and the Orthopaedic Trauma Association introduced a standardized, internationally recognized classification system for pelvic ring fractures **(Figures 10a, 10b, and 10c, jramc.bmj.com).**

This system categorizes fractures based on their anatomical location, stability, and injury mechanism. It is divided into three primary types, each with three subtypes, allowing for detailed categorization of pelvic injuries. The classification helps guide treatment decisions and provides a framework for research and clinical communication (J Orthop Trauma, 2018 Volume 32, Number 1 Supplement, January 2018).

**1) Type A: Stable Fractures**

Type A fractures involve an intact posterior arch and are considered stable. These include avulsion fractures, isolated fractures of the anterior arch, and transverse fractures of the sacrum or coccyx.

- A1: Innominate bone avulsion fractures (e.g., anterior superior iliac spine or ischial tuberosity fractures).
- A2: Innominate bone fractures involving unilateral or bilateral anterior arch disruption.
- A3: Transverse fractures of the sacrum or coccyx.

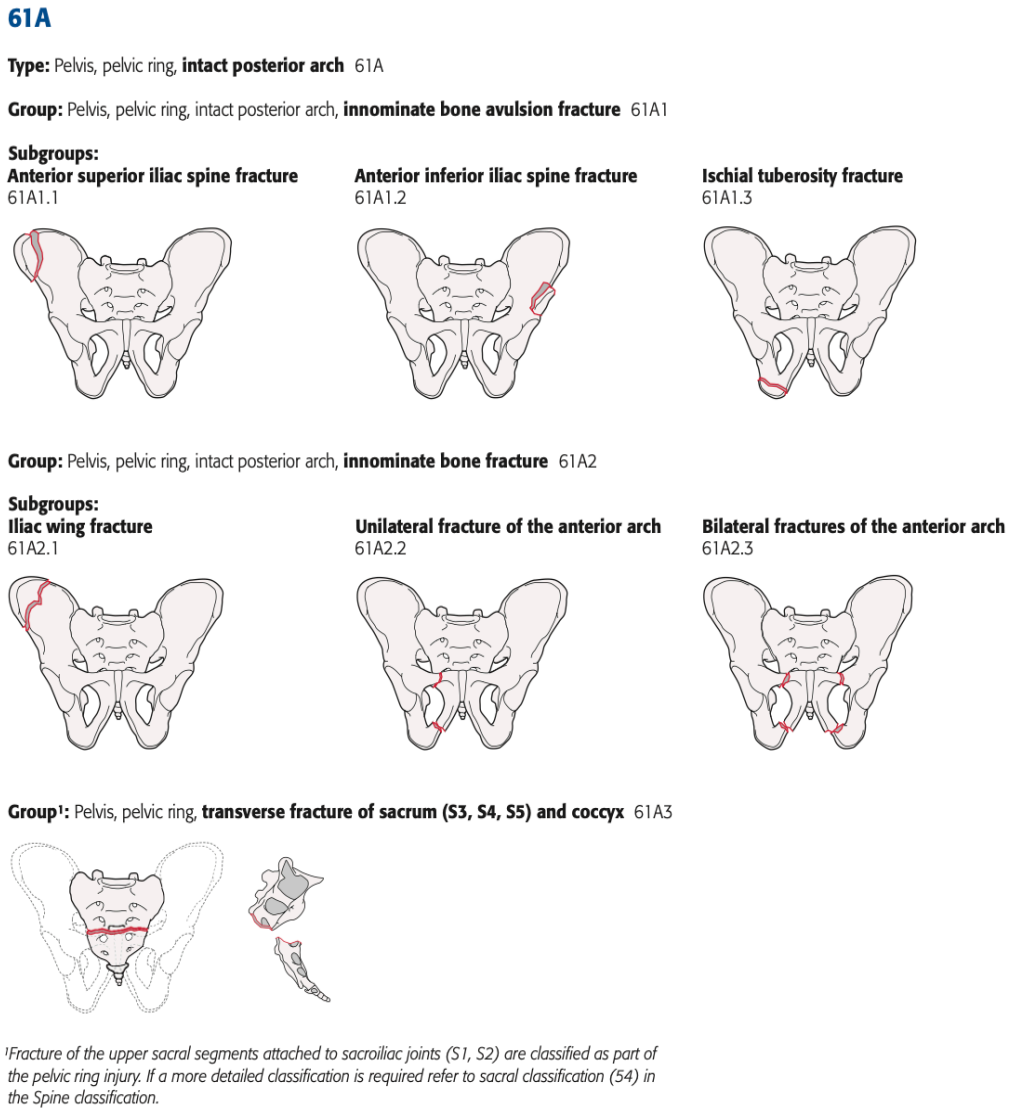


**Figure 10a: Type 61A - Stable Fractures with Intact Posterior Arch. This figure illustrates Type 61A fractures, which maintain posterior arch stability.** Subgroups include avulsion fractures of the anterior superior iliac spine, anterior inferior iliac spine, or ischial tuberosity (61A1); iliac wing fractures and unilateral or bilateral anterior arch fractures (61A2); and transverse fractures of the sacrum or coccyx (61A3). Adapted from J Orthop Trauma • Volume 32, Number 1 Supplement, January 2018 (Copyright © 2017 by AO Foundation, Davos, Switzerland; Orthopaedic Trauma Association, IL, US www.jorthotrauma.com)

## 2) Type B: Partially Stable (Rotationally Unstable) Fractures

Type B fractures involve incomplete disruption of the posterior arch, resulting in rotational instability but preserved vertical stability. These injuries often result from lateral compression or anteroposterior compression mechanisms (J Orthop Trauma, 2018).

- B1: No rotational instability (e.g., lateral compression or open book fractures).
- B2: Rotationally unstable, unilateral posterior injury (e.g., lateral compression with internal rotation instability).
- B3: Rotationally unstable, bilateral posterior injury (e.g., contralateral lateral compression fractures).

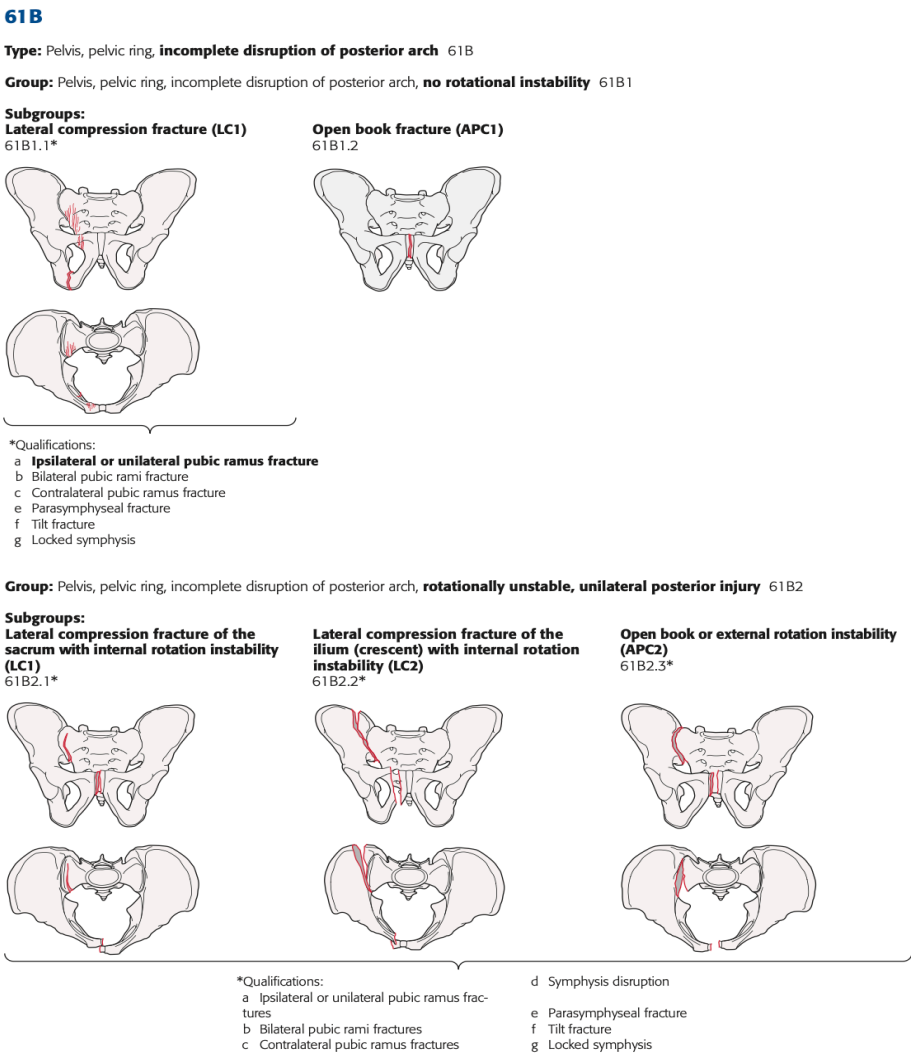


**Figure 10b: Type 61B - Partially Stable Fractures with Rotational Instability Depicts Type 61B fractures.** Characterized by incomplete posterior arch disruption and rotational instability. Subgroups include lateral compression fractures (LC1), open book fractures (APC1), and unilateral posterior injuries with varying rotational instability (LC2 and APC2). Adapted from J Orthop Trauma • Volume 32, Number 1 Supplement, January 2018 (Copyright © 2017 by AO Foundation, Davos, Switzerland; Orthopaedic Trauma Association, IL, US www.jorthotrauma.com)

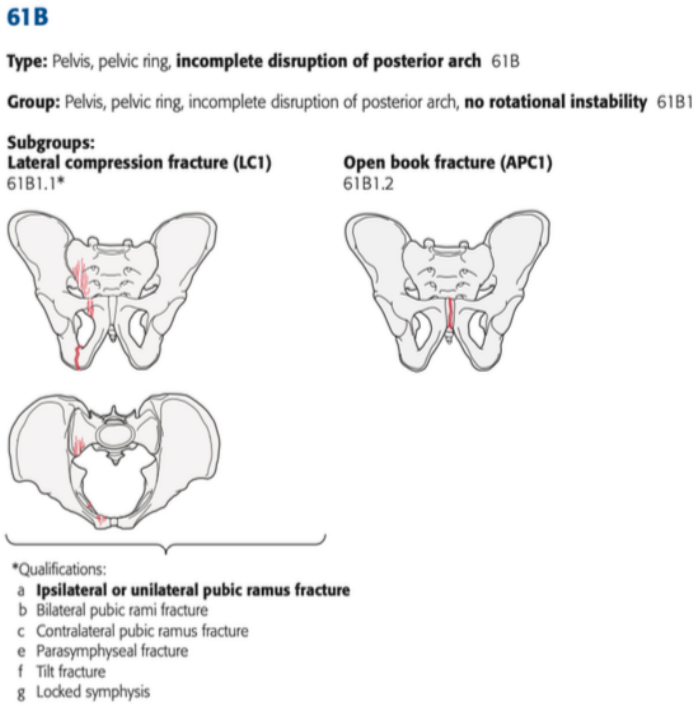


**Figure 10c: Type 61B (Continued) - Bilateral Posterior Injuries with Rotational Instability.** Shows bilateral posterior injuries (61B3) involving combinations of lateral compression (LC3) and external rotation instability (APC2). These injuries result in complex patterns of instability on both sides of the pelvis. Adapted from J Orthop Trauma • Volume 32, Number 1 Supplement, January 2018 (Copyright © 2017 by AO Foundation, Davos, Switzerland; Orthopaedic Trauma Association, IL, US www.jorthotrauma.com)

### 3) Type C: Complete Instability (Rotationally and Vertically Unstable Fractures)

Type C fractures involve complete disruption of the posterior arch and are both rotationally and vertically unstable. These injuries are often caused by high-energy trauma, such as falls from heights or motor vehicle collisions (J Orthop Trauma, 2018).

- C1: Unilateral posterior injury (e.g., iliac fractures or sacroiliac joint disruptions).
- C2: Bilateral posterior injury with asymmetric disruption (e.g., sacral fractures or complete sacroiliac disruption).
- C3: Bilateral posterior injury with complete instability on both sides.

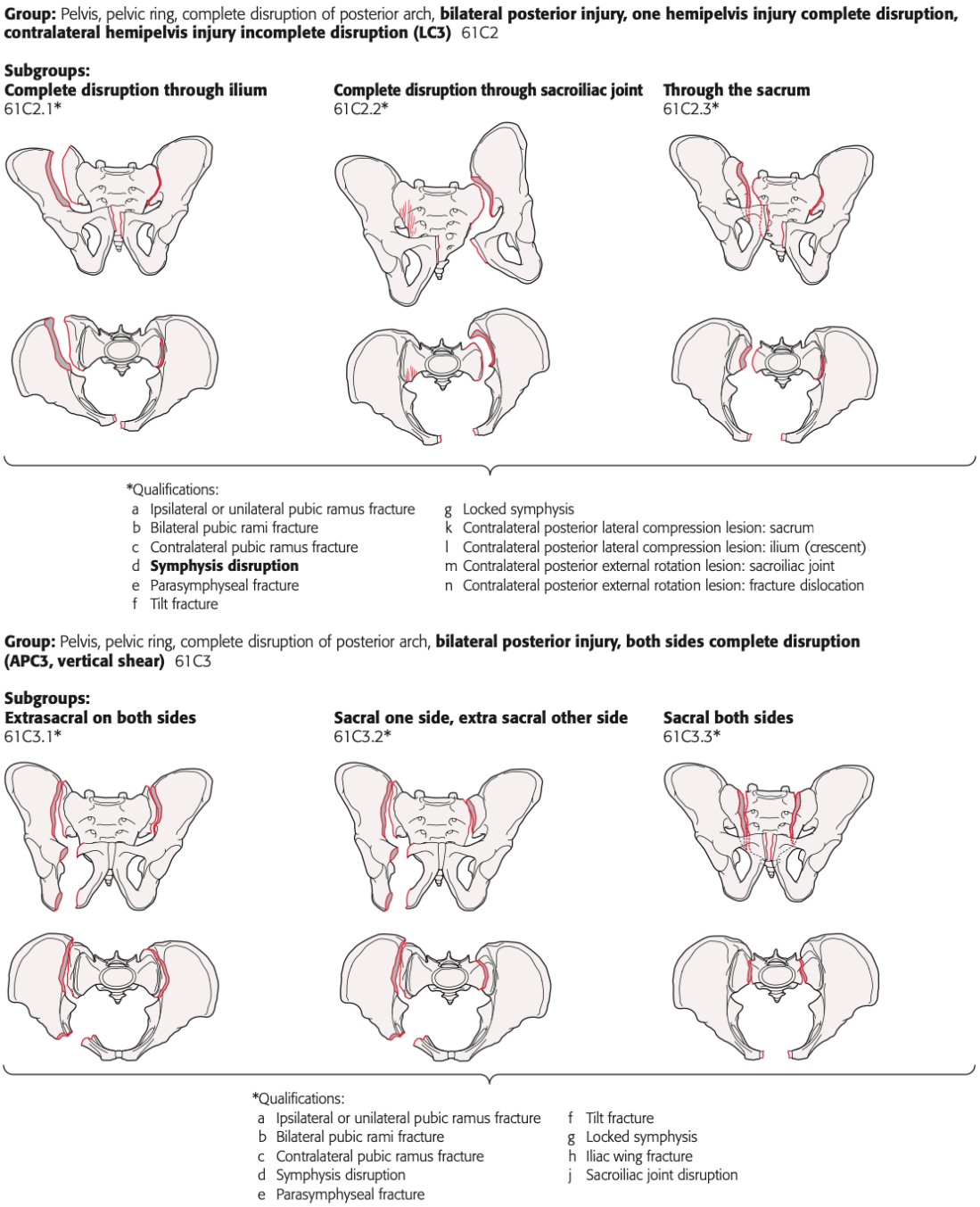


**Figure 10d: Type 61C - Complete Posterior Arch Disruption (Unilateral). Illustrates Type 61C fractures, where the posterior arch is completely disrupted.** Subgroups include injuries through the iliac bone, sacroiliac joint, or sacrum (61C1). Bilateral Posterior Injuries with Asymmetric Disruption depict bilateral injuries with complete disruption on one side and partial or complete disruption on the contralateral side. Subgroups include disruptions through the ilium, sacroiliac joint, or sacrum (61C2): Bilateral Posterior Injuries with Complete Disruption: This shows bilateral posterior injuries involving complete instability on both sides. Subgroups include extrasacral and sacral fractures (61C3). These injuries represent the most severe patterns of pelvic ring disruption. Adapted from J Orthop Trauma • Volume 32, Number 1 Supplement, January 2018 (Copyright © 2017 by AO Foundation, Davos, Switzerland; Orthopaedic Trauma Association, IL, US, www.jorthotrauma.com)

### *1.7.3 Fragility Fracture Classification of the Pelvis (FFP)*

Population ageing is an irreversible global phenomenon, particularly pronounced in countries such as Germany. This demographic shift has led to an increased incidence of osteoporotic fractures, prompting orthopedic and trauma surgeons to develop targeted classification systems such as the Fracture Fragility of the Pelvis (FFP) classification.

The primary focus is often on identifying which fractures occur from minimal trauma, indicating a higher level of bone fragility.

Understanding fracture fragility is crucial for clinicians in diagnosing, treating, and managing osteoporosis and other skeletal conditions, aiming to reduce the incidence of fractures and enhance patient quality of life.

This classification is particularly important in the context of age-related osteoporosis and other conditions that weaken bone integrity.The Fracture Fragility of the Pelvis classification has become increasingly relevant in clinical practice due to its continuous evolution and updates. Initial contributions by Finiels and Linstrom focused predominantly on sacral fractures, as highlighted in their publications (Finiels et al., 1997; Linstrom et al., 2009).

However, Rommens and Hofmann significantly expanded the classification framework in their seminal works published in 2013 and updated further in 2021, focusing on the entire pelvic ring to enhance diagnostic accuracy and facilitate more effective treatment protocols (Rommens & Hofmann, 2013, 2023).

The classification provides a systematic approach to identifying and managing fragility fractures of the pelvis, allowing clinicians to tailor interventions based on specific fracture patterns and patient characteristics. **Figure 11** presents a detailed visualization and description of the Fracture Fragility of the Pelvis classification.

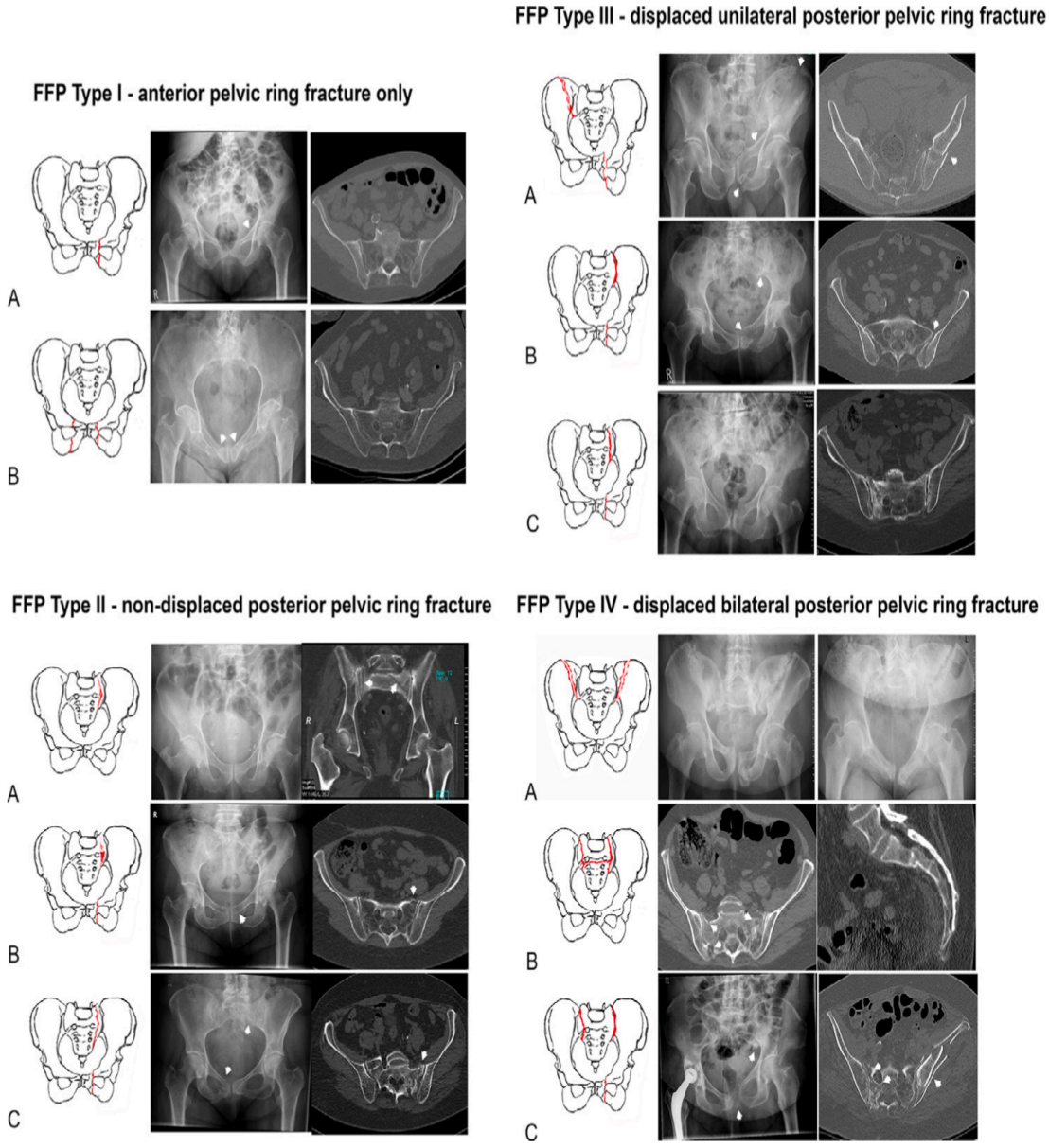


**Figure 11: FFP Classification of Pelvic Ring Fractures.** This figure illustrates the FFP (Fragility Fracture of the Pelvis) classification, which categorizes fractures based on the location and displacement of pelvic ring injuries: FFP Type I: Anterior pelvic ring fractures only, with no involvement of the posterior pelvic ring. (A-C) Examples show variations in fracture patterns with corresponding radiographs and CT images. FFP Type II: Non-displaced posterior pelvic ring fractures, where the posterior ring is involved without significant displacement. (A-C) Subcategories illustrate different posterior injury patterns with detailed imaging. FFP Type III: Displaced unilateral posterior pelvic ring fractures affect one side of the posterior ring with displacement. (A-C) Examples demonstrate unilateral posterior fractures with associated anterior ring involvement. FFP Type IV: Displaced bilateral posterior pelvic ring fractures, where both sides of the posterior ring show significant displacement. (A-C) Imaging highlights bilateral instability and severe disruptions in the pelvic ring. The figure integrates schematic illustrations, radiographs, and CT images to visualize each FFP classification subtype comprehensively. Injury. 2013;44(12):1733–44.

## *1.8 Clinical Features and Diagnosis of Pelvic Fractures*

### *1.8.1 Clinical Features*

Patients with pelvic fractures often present to the emergency department in critical condition, typically due to hypovolemic shock, and are frequently unable to describe the mechanism of injury. In addition, clinical signs of genitourinary and intra-abdominal injuries are commonly observed.

While hypovolemic shock is a well-recognized indicator of severe trauma, a specific clinical feature indicative of significant pelvic injury is the presence of "Milch's sign." In line with the principle of "treat first what kills first," the management of patients with partially stable or unstable pelvic fractures adheres to the Advanced Trauma Life Support (ATLS) protocol and the ABCDE schema for prioritizing life-threatening injuries (Rossaint et al., 2006; Rossaint et al., 2007).

In patients with stable pelvic fractures, clinical tests such as compression tests, distraction tests, and direct pressure tests can be safely performed. Conversely, complex pelvic injuries are suggested by findings such as pelvic ring instability, asymmetry, or active bleeding from the anus, vagina, or penis.

At the Department of Traumatology, Hand and Reconstructive Surgery, University of Giessen, the ATLS protocol is strictly followed. Upon arrival in the emergency unit, patients are managed by a multidisciplinary trauma team, which typically includes:

- Trauma Surgeon (Team Leader)
- Anaesthesiologist
- General Surgeon
- Neurosurgeon
- Radiologist
- Nursing personnel for each specialty

The trauma team can be rapidly expanded based on the severity and complexity of the case. Each team member has clearly defined responsibilities during the examination and treatment of the patient according to the ABCDE schema.

Patients are generally transported to the emergency unit by rescue services, accompanied by an emergency physician. They are preregistered using the IVENA platform, a state emergency registry. This system ensures timely communication with the trauma team, providing critical information about the mechanism of injury, the patient’s personal details, and their condition from the crash scene onward.

Upon arrival, the trauma team conducts a primary survey and performs an extended Focused Assessment with Sonography for Trauma (e-FAST) examination. The team leader evaluates the findings to determine subsequent steps, such as initiating fluid therapy, conducting immediate surgical interventions, or ordering urgent radiological assessments (Pohlemann et al., 1998).

### *1.8.2 Diagnosis*

1. **FAST Exam (Focused Assessment with Sonography for Trauma):** The FAST exam is a widely adopted method for detecting free fluid in the thoracic and abdominal cavities. However, in the context of pelvic fractures, this modality is neither highly sensitive nor specific. Nevertheless, detecting free fluid may indirectly indicate vascular injuries or damage to abdominal organs (Rossaint et al., 2007; Johnson et al., 2013).
2. **Conventional Radiography:** Standard radiography is the initial imaging modality for suspected pelvic fractures. In hemodynamically unstable patients with clinical indications of an unstable pelvic ring fracture, an anteroposterior pelvic X-ray is typically performed. Specialized views, such as inlet and outlet projections, can be utilized to better visualize the anterior and posterior pelvic ring (J Trauma Acute Care Surg, 2014).
3. **CT scan:** Computed tomography (CT) with contrast is the gold standard for diagnosing and classifying pelvic fractures in emergency settings, particularly in hemodynamically unstable polytrauma patients. A full-body CT scan can be completed within seconds, providing a comprehensive assessment of the injuries, including the capability for three-dimensional reconstruction (Breiman et al., 1982; Blackmore et al., 2003; Hori et al., 2011; Veith et al., 2016).
4. **MRI Scan:** Magnetic resonance imaging (MRI) is primarily indicated for evaluating osteoporotic fractures, particularly those involving the posterior pelvic ring in elderly patients. However, its use in emergencies for diagnosing or managing pelvic ring fractures is generally not recommended (Ge et al., 2014; Iwano et al., 2009).

## *1.9 Therapy*

### *1.9.1 Emergency Therapy of Unstable Pelvic Ring Fractures*

Pelvic fractures frequently occur in conjunction with other injuries in polytraumatised patients, often leading to hypovolemic shock. In such cases, the initial treatment focus must be on managing hypovolemic shock and stabilizing vital parameters. Primary stabilization, such as internal fixation, is contraindicated during the resuscitation phase for patients in hypovolemic shock. Once the patient has been stabilized, attention shifts to the management of the pelvic fracture, as it is often the source of the instability (Pohlemann et al., 1998; Culemann et al., 2003).

In cases of unstable pelvic fractures responsible for the patient's instability, immediate intervention is critical (J Trauma Acute Care Surg, 2014). Patients presenting with pelvic ring fractures, significant associated bleeding, and hemoglobin levels below 8 g/dl at admission are treated in accordance with the pelvic trauma algorithm. This includes a concise, goal-oriented diagnostic procedure to guide subsequent treatment steps (Pohlemann et al., 1998; Culemann et al., 2003).

Surgical intervention should be initiated immediately upon deciding that it is necessary. Emergency surgical treatment options include external fixation and the Pelvic C-Clamp, which are effective in stabilising the pelvic ring in acute settings.

Vascular injuries often accompany unstable pelvic fractures. In such cases, surgical intervention alone may be insufficient to address hemorrhage. Approximately 80–90% of unstable pelvic trauma cases involve massive venous bleeding from the prevesical and presacral venous plexuses, as well as the spongy fracture surfaces of the pelvis. If external fixation fails to control bleeding or stabilize circulation, the small pelvis can be accessed via an infraumbilical longitudinal incision (Stoppa approach). This approach involves packing the retroperitoneal, presacral, and prevesical spaces with rolls and abdominal towels to control venous bleeding. This straightforward surgical method can be performed in various settings and is highly effective (Pohlemann et al., 1998; Culeman et al., 2008).

Computed tomography (CT) with a contrast medium in the emergency room facilitates the early diagnosis of active bleeding by visualizing contrast medium leakage from damaged blood vessels. Following angiography, bleeding can be localized and addressed with transarterial catheter embolization (TAE), a minimally invasive procedure that

effectively controls arterial hemorrhage (Westhoff et al., 2008; Usui & Kondo, 2024; Costantini et al., 2016).

In recent years, the Resuscitative Endovascular Balloon Occlusion of the Aorta (REBOA) system has emerged as a valuable tool in managing uncontrollable hemorrhage (*Figure 12*). This endovascular procedure involves placing and inflating a balloon in the aorta via a groin approach, thereby reducing blood loss in traumatic and non-traumatic abdominal and pelvic bleeding while improving cerebral and coronary blood flow (Wortmann et al., 2020; Pieper et al., 2018).

Once the patient's primary condition is stabilized, definitive surgical treatment can be performed, such as open reduction and internal fixation. Patients with non-displaced pelvic ring fractures can often be managed conservatively with rest and non-steroidal anti-inflammatory drugs (NSAIDs) (J Trauma Acute Care Surg, 2014).

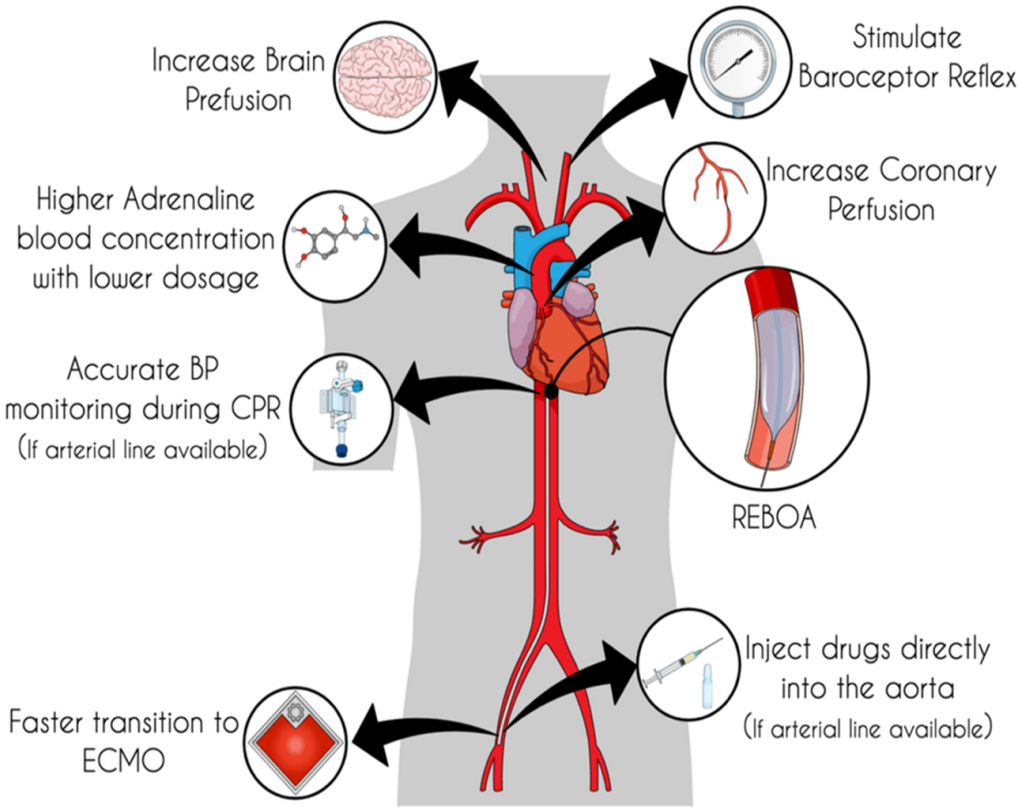


**Figure 12: REBOA during Non-Traumatic Cardiac Arrest (NTCA) can enhance hemodynamics and improve organ perfusion, particularly to the heart and brain, by occluding the aorta.** This placement allows for targeted redirection of blood flow, effectively managing hemorrhagic shock and stabilizing patients until further interventions. It also facilitates advanced resuscitation techniques like ECMO, potentially improving survival rates in critical situations. Overall, REBOA serves as a valuable tool in emergency care for managing cardiac arrest. J. Clin. Med. 2022, 11(3), 742; https://doi.org/10.3390/jcm11030742

# 2 Research Questions and Study Aim

The measurement of bleeding volume in partially unstable and completely unstable pelvic fractures represents a critical milestone in the treatment of such injuries. This evaluation, in conjunction with other diagnostic and clinical parameters, provides crucial insights into patient management strategies (Blackmore et al., 2003; Veith et al., 2016).

Younger patients often present challenges in initial assessment due to compensatory mechanisms that may mask the severity of their clinical condition. In contrast, elderly patients are more vulnerable to trauma and typically experience worse clinical outcomes. This is compounded by their generally poorer overall health status compared to younger individuals (Rommens & Hofmann, 2013; Andrich et al., 2015).

The existing literature includes studies examining unstable pelvic fractures, where bleeding volumes were measured and correlated with patients' clinical statuses and laboratory parameters. These findings underscore precise assessment's importance in guiding therapeutic decisions (Westhoff et al., 2008; Costantini et al., 2016; Veith et al., 2016).

In the region of central Hesse, patients with pelvic fractures are typically transported to a specialized trauma room, level I care unit, equipped for primary stabilization and diagnosis. The multidisciplinary trauma team adheres to the ABCDE schema for patient management. The diagnostic algorithm includes computed tomography (CT) scans, allowing for the rapid establishment of a definitive diagnosis (Breiman et al., 1982; J Trauma Acute Care Surg, 2014).

Pelvic fractures, characterized by their vascular complexity, often involve arterial injuries leading to significant intrapelvic bleeding. While intra-abdominal "free" bleeding volumes are commonly assessed, intramuscular bleeding and fracture hematoma volumes are often overlooked, despite their potential impact on patient outcomes (Pohlemann et al., 1998; Wortmann et al., 2020).

**Aim of the Study**

This study aims to leverage 3D Slicer Volumetry to measure bleeding volumes in partially unstable and completely unstable pelvic fractures. The bleeding volume will be analyzed in relation to fracture type and subtype, clinical status, and patient outcomes.

Specifically, the study addresses the following research questions:

1. **Comparison of Bleeding Volumes**: Is there a difference in bleeding volume between Type B and Type C pelvic fractures as classified by the AO Classification system?

2. **Utility of 3D Slicer Volumetry**: Can 3D Slicer Volumetry Segmentation be considered an optimal method for defining bleeding volume in pelvic fractures, or is it primarily suited for research purposes?

3. **Assessment of Blood Loss**: Does the free intrapelvic bleeding volume accurately reflect the true blood loss in pelvic fractures?

The importance of this topic is still there, because of the changing technology. Furthermore, evaluating the practicality, reliability, and accuracy of 3D Slicer Volumetry will determine its feasibility for routine clinical application. If validated, this technology could transform trauma assessment by providing rapid, objective, and reproducible measurements that complement traditional clinical and imaging evaluations.
Importantly, establishing a strong correlation between volumetric bleeding measurements and actual blood loss will reinforce the clinical relevance of this approach.

Ultimately, the integration of advanced volumetric analysis into pelvic fracture management holds promise for enhancing patient outcomes through more precise hemorrhage assessment and tailored treatment strategies. The findings of this study could pave the way for wider adoption of 3D imaging technologies in trauma care, contributing to more effective and evidence-based treatment protocols.

# 3 Material and Methods

## *3.1 Study Design and Setting*

This retrospective and exploratory study was conducted from 2016 to 2021 at the Department for Trauma, Hand and Reconstructive Surgery in the University Hospital of Giessen, as well as the Experimental Traumatology Laboratory at the Justus Liebig University in Giessen. Patient data was pseudonymized at the outset to ensure confidentiality.

The research study officially started after the positive ethics (reference number: AZ 269/21) vote from Justus Liebig University of Giessen. This crucial endorsement validates the integrity of the project.

### *3.1.1 Inclusion and Exclusion Criteria*

Patients included in this study were those with partially unstable or completely unstable pelvic fractures as the primary criterion. Data was collected from the German Trauma Register for severely injured patients (1,536 patients over 5 years) and primarily from the clinic's operative programme.

**The inclusion criteria were:**

- Patients aged 14 years or older
- Admitted to the hospital with predominantly Type B or Type C pelvic fractures
- according to the AO Classification, or FFP3 and FFP4 pelvic fractures as per the
- Fracture Fragility of the Pelvis (FFP) Classification
- Clinical stability upon hospital admission, allowing for a full-body CT scan with intravenous contrast

**Exclusion criteria were:**

- Patients with Type A pelvic fractures as per the AO Classification
- Patients transferred to the clinic more than 2 hours after the injury
- Patients with penetrating trauma in the pelvic region
- Patients with known vascular malformations or pre-existing vascular diseases in the pelvic region

### *3.2 Data Collection and Analysis*

Patient data, including clinical parameters from those admitted to the intensive care unit (ICU), were collected during admission and subsequent hospitalization.

All patients underwent a full-body CT scan with contrast upon arrival at the hospital, providing high-quality imaging data.

CT scan data was processed using the 3D Slicer® software platform, a free and open-source application for analyzing and visualizing medical images. This platform supports interactive segmentation, volume rendering, and quantitative analysis, making it suitable for research in image-guided therapy. The 3D Slicer version used was 4.11.20210226, which supports various data types, including 2D, 3D, and 4D visualizations, and can be used on desktop or virtual reality systems.

3D Slicer is free and open-source software designed for image analysis and scientific visualization. It is utilized in various medical applications, such as autism, cancer, and neurosurgery (Fedorov et al., 2012).

This modular software (under a BSD-style license) supports both interactive and batch processing, allowing the development of customized tools. Key features include image registration and processing of diffusion tractography (DTI), compatibility with DICOM images and multiple formats, interactive visualization of volumetric images and polygonal meshes, data fusion and co-registration with rigid and non-rigid algorithms, and automatic image segmentation.

3D Slicer is compatible with Windows, Linux, and macOS. While it is freely available for academic and commercial use, users must ensure compliance with local regulations, as the software is not FDA-approved for clinical use.

To assess interobserver variability, five CT scans were randomly selected for volume measurement. These were analyzed under identical conditions, and the measurements were repeated and reviewed for consistency.

Original authors of the Slicer are the Slicer Community, and it is realized throughout BSD licenses. BSD licenses are a group of permissive free software licenses that place few restrictions on how the software can be used and distributed. This approach differs from copyleft licenses, which mandate that derivative works be shared alike. The original BSD license was created for the Berkeley Software Distribution (BSD), a Unix-like operating system. Over time, this initial version has been updated, leading to what are now known as modified BSD licenses.

### *3.3 Parameters Evaluated*

Archived patient data was thoroughly reviewed and statistically evaluated. An Excel database was created containing the following variables:

- Age and sex
- Date and time of injury
- Initial treatment in the clinic or transfer details
- Fracture type (AO and FFP Classification)
- Haemoglobin levels
- Base excess levels
- Blood pressure at admission
- Mechanism of trauma
- Duration of hospitalization and ICU stay
- Initial surgical treatment type
- ASA (American Society of Anesthesiologists) Classification
- Neurological status and Glasgow Coma Scale (GCS) score

### *3.4 Data Analysis Using 3D Slicer*

The CT scans were analyzed following supervised training in the use of 3D Slicer. Official documentation and video tutorials for pelvic segmentation and volume analysis were accessed through slicer.org. A tutorial specifically tailored to the pelvic region and femur segmentation was applied. Segmentation and analysis were performed to quantify bleeding volumes and assess fracture-related parameters. The process initially took about four hours per patient, reduced to two hours post-training (Blackmore et al., 2003; Veith et al., 2016).

In the evolving field of trauma medicine, accurate assessment of injury severity, particularly bleeding volume, is critical.

The following illustrative example shows the integration of CT and 3D Slicer into trauma care: A patient arrives in hypovolemic shock following a road traffic accident. A CT scan reveals a pelvic fracture. 3D Slicer is used to segment and quantify hematomas, guiding whether surgical or conservative management is appropriate. This software's thresholding, painting, and segmentation growth functions support accurate 3D reconstructions and precise blood volume quantification (Blackmore et al., 2003; Veith et al., 2016) **(Figure 13).**

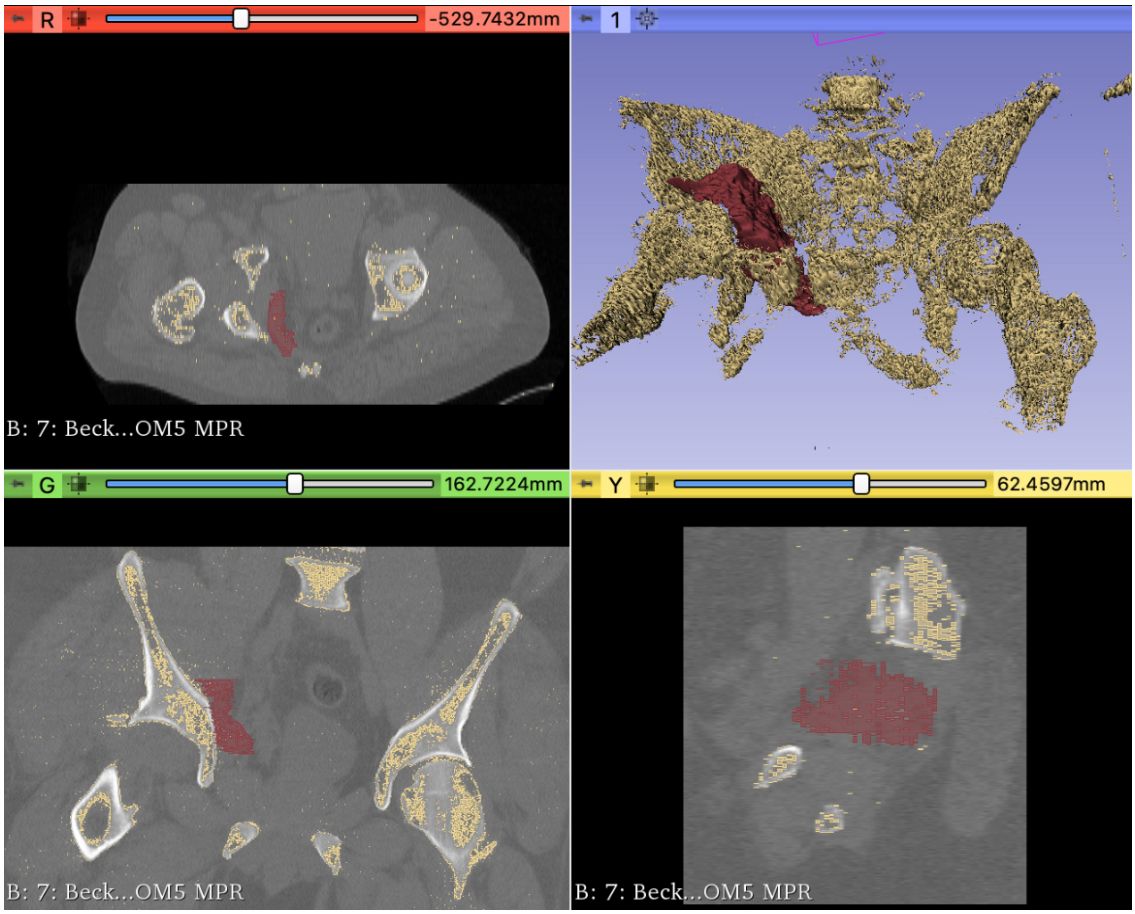


**Figure 13: Example of Segmentation and 3D Reconstruction in a Patient with Pelvic Bleeding.** The figure demonstrates a multi-planar CT segmentation and 3D reconstruction of a patient with pelvic bleeding. Top Left: Axial CT view showing the bleeding region highlighted in red. Top Right: 3D reconstruction illustrating the bleeding distribution in relation to the skeletal anatomy. Bottom Left: Coronal CT view emphasizing the extent of the hemorrhage and its anatomical relationships. Bottom Right: Sagittal CT view detailing the vertical spread of the bleeding along the pelvic structures. This visualization highlights the utility of the "Thresholding" function, helping us to distinguish the different tissues.

When working with multiple tissues that have similar densities, it's advisable to utilize the "Use for masking" feature within the threshold effect. This option allows the brush tool to adapt to areas within the selected threshold range, ensuring that only the specified regions are marked. After that, the user can select the "Paint" effect to begin marking relevant areas on the image that should be assigned the chosen color. Care must be taken to stay within the boundaries of the organ or material being marked, especially when adjacent tissues share similar densities that may lead to unintended overlaps. If mistakes occur, users can rectify them using the "Erase" effect, which functions similarly to the paint tool. It's essential not to mark each slice individually; instead, marking selected slides is sufficient, but it's crucial to perform this on all three planes-sagittal, coronal, and

axial-so that subsequent steps can be completed effectively. Once initial markings are made, users can apply the "Grow from seeds" effect to compile the organ from the chosen slices by clicking the "Initialize" button. The resulting outline will appear across all three imaging planes, and if the user is satisfied, they can apply it. If adjustments are needed, they can either manually refine the results, add additional slices, or experiment with different threshold ranges to achieve the desired segmentation. Following this, the approach differs slightly for simpler segmentations, such as modeling a knee joint. In such cases, one can directly apply the threshold to create a base model. After selecting the color and the appropriate threshold range, users can assemble a preliminary model in the chosen color via the "Apply" button. This model can be visualized in a designated area by using the "Show 3D" function, allowing for adjustments and refinements as needed. To refine colors of other segments, users can use the "Paint" function again by selecting the color under "Editable Area" and specifying which regions need to be altered. This can be done by either painting directly on the 3D model or in the respective imaging planes. The process involves selecting the new color for the segment and adjusting the brush size with the slider, ensuring a 3D brushing effect is activated for more accurate and natural results. This step should continue until all segments desired have been appropriately colored.

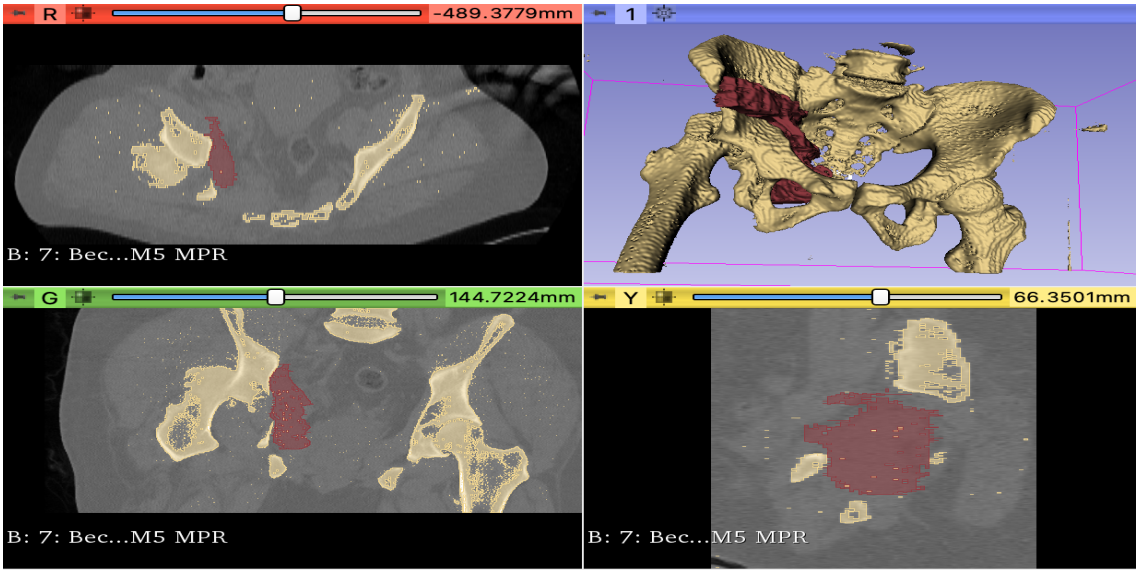


**Figure 14: Example of Segmentation and 3D Reconstruction in a Patient with Pelvic Bleeding.** The figure demonstrates a multi-planar CT segmentation and 3D reconstruction of a patient with pelvic bleeding. Top Left: Axial CT view showing the bleeding region highlighted in red. Top Right: 3D reconstruction illustrating the bleeding distribution in relation to the skeletal anatomy. Bottom Left: Coronal CT view emphasizes the hemorrhage's extent and its anatomical relationships. Bottom Right: Sagittal CT view detailing the vertical spread of the bleeding along the pelvic structures. This visualization highlights the utility of the "Smoothing and Closing" function, helping us to distinguish the different tissues.

Separating individual segments and assigning distinct colors aids in evaluating specific segments from multiple angles, allowing for a more precise assessment and preventing interference when the segments are hidden from view during the editing process. While there is a quicker, albeit less accurate, method to achieve this by using the "Islands" function to add segments directly on the imaging planes, the segments must be completely separate without any connections.

Lastly, various tools are available within the software to enhance the model. Initially, small fragments surrounding the model can be removed using the "Islands" effect. The "Remove Small Islands" function can eliminate these fragments based on specified voxel sizes depending on the desired outcome. Additionally, smoothing effects can polish the model's surface without significantly altering its structure. The "Smoothing" and "Closing" functions provide capabilities for refining edges and filling in gaps, allowing users to test their efficacy based on their preferences **(Figure 14).**

Manual adjustments can also be performed with the "Paint" and "Erase" functions, although saving these for the final stages is advisable to optimize efficiency. This comprehensive approach ultimately ensures the segmentation is accurate, refined, and ready for further analysis or presentation.

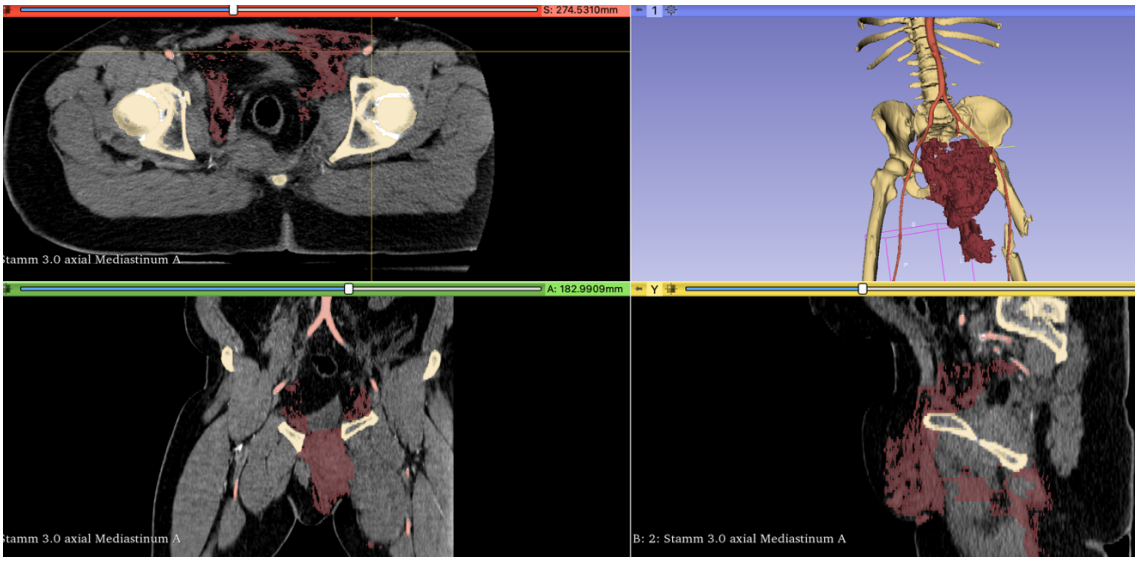


**Figure 15: Example of Segmentation and 3D Reconstruction in a Patient with Pelvic Bleeding.** The figure demonstrates a multi-planar CT segmentation and 3D reconstruction of a patient with pelvic bleeding. Top Left: Axial CT view showing the bleeding region highlighted in red. Top Right: 3D reconstruction illustrating the bleeding distribution in relation to the skeletal anatomy. Bottom Left: Coronal CT view emphasizing the extent of the hemorrhage and its anatomical relationships. Bottom Right: Sagittal CT view detailing the vertical spread of the bleeding along the pelvic structures. This visualization highlights the utility of segmentation and 3D reconstruction for identifying and localizing hemorrhagic sites, crucial for surgical planning and trauma management.

**Figure 15** illustrates the capabilities of the 3D Slicer, highlighting its ability to handle image segmentation, bleeding volume measurement, and three-dimensional reconstruction for research purposes.

After completing the segmentation process, the bleeding volume can be quantified using the program. The software automatically calculates the volume in cubic millimeters ($mm^3$), where 1 $mm^3$ corresponds to 1 milliliter (ml) of blood. This quantification enables precise measurement of blood loss, including the volume associated with bone or other anatomical structures analyzed during segmentation.

Figure 16 illustrates an example of segmentation, highlighting the bleeding volume and including a detailed three-dimensional reconstruction for further analysis.

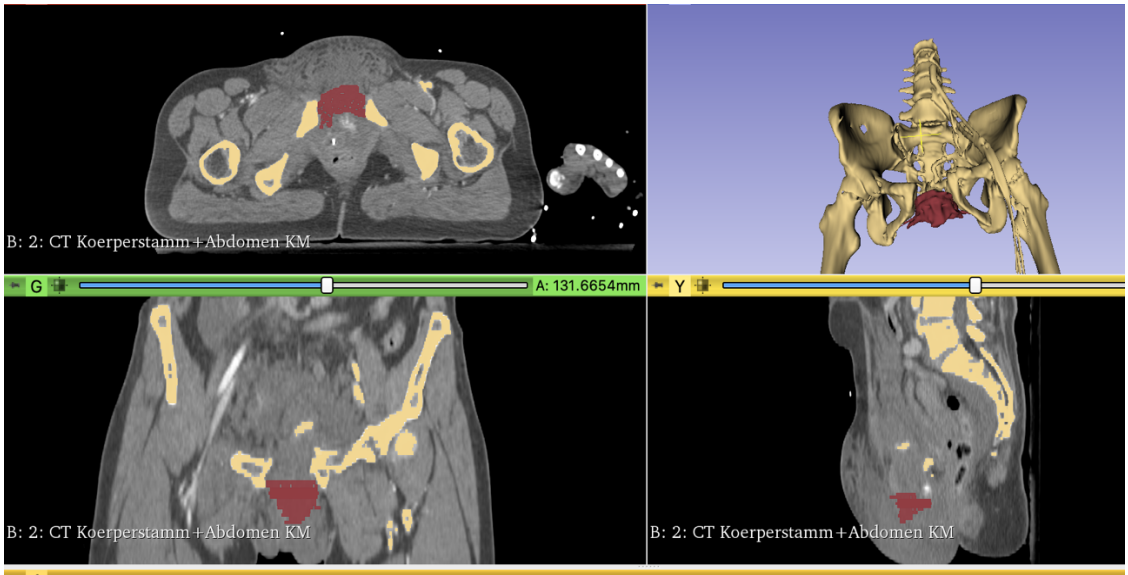


| | A | B | C | D | E | F | G |
|---|---|---|---|---|---|---|---|
| 1 | **Segment** | **Number of voxels [voxels]** | **Volume [mm3] (1)** | **Volume [cm3] (1)** | **Surface area [mm2]** | **Volume [mm3] (2)** | **Volume [cm3] (2)** |
| 2 | Bone | 391204 | 1.11924e+06 | 1119.24 | 337644 | 1.11641e+06 | 1116.41 |
| 3 | clot | 5539 | 15847.2 | 15.8472 | 4977.74 | 14950.9 | 14.9509 |

**Figure 16: 3D Reconstruction and Quantification of Bleeding in a Patient with an Unstable Pelvic Fracture.** This figure illustrates the 3D reconstruction and segmentation of pelvic bleeding in a patient with an unstable pelvic fracture, combined with quantitative analysis of the bleeding volume: Top Left: Axial CT view highlighting the bleeding (red) and skeletal structures (yellow). Top Right: 3D reconstruction showing the spatial distribution of the bleeding relative to the pelvis. Bottom Left: Coronal CT view visualizing the vertical extent of the hemorrhage. Bottom Right: Sagittal CT view providing additional anatomical context of the bleeding region. Table: The table below quantifies the bleeding, presenting the number of voxels, volume in cubic millimeters (mm3), and cubic centimeters (cm3), as well as the surface area of the segmented structures (bone and clot). This quantification is critical for assessing injury severity and planning treatment strategies.

### *3.5 Statistical Analysis*

The statistical analysis for this study was conducted using non-parametric methods to address the ordinal nature of the data and potential deviations from normality in variable distributions. The Mann-Whitney U test, a robust non-parametric alternative to the independent samples t-test, was employed to compare medians between two independent groups. This method does not rely on the assumption of normality, making it particularly well-suited for the data analyzed in this research.

Data preparation involved organizing and encoding variables from the dataset, which were processed using SPSS software. Key variables included age at admission, encoded gender, diagnostic categories, and clinical parameters such as systolic blood pressure, Glasgow Coma Scale (GCS) scores, operation categories, and laboratory findings like base excess levels. To ensure the integrity of the analysis, user-defined missing values were treated as missing data, and cases with invalid values for specific variables were excluded from the statistical tests.

The Mann-Whitney U test was applied to all encoded variables to assess differences in medians between two independent groups. For each variable, the test generated the Mann-Whitney U value, the Wilcoxon W statistic, the Z-score, and asymptotic and exact significance values (two-tailed). When computationally feasible, the exact methodology was used to provide precise p-values, particularly in cases with smaller sample sizes or tied ranks, enhancing the robustness of the analysis. To mitigate potential issues from multiple comparisons, the Bonferroni correction was considered to control Type I error rates across the various tests conducted. Missing data were addressed by excluding cases with missing values for specific variables, and no imputation techniques were applied.

Results were interpreted using a significance threshold of 0.05 and ranks and effect sizes were reported to contextualise the magnitude of observed differences between groups. The analysis was conducted with the non-parametric testing module in SPSS V29 IBM, enabling precise computation of results while maintaining defined memory constraints to ensure accuracy and reproducibility. This rigorous approach to statistical analysis provided a robust framework for evaluating relationships and differences across the studied variables, thereby contributing to the overall reliability and validity of the study's conclusions.

# 4 Results

## *4.1 Epidemiological Findings*

Out of the 1,536 registered patients recorded in the trauma register at our university hospital in Giessen between 2017 and 2022, only 70 patients met the study's inclusion criteria. This accounts for 4.55% of the total patient population analyzed.

### *4.1.1 Gender and Age Distribution*

The average age of the study population was 49.98 years, with a standard deviation (SD) of ±21.47 years. The age range spanned from 15 to 88 years, as shown in **Figure 17.** The age distribution exhibited two distinct peaks, with one occurring between the ages of 18 and 35 and the other between 50 and 60 years. Regarding gender distribution, 75.7% of the patients were male, corresponding to 53 individuals, while 24.3% were female, comprising 17 individuals. The gender distribution is summarized in **Table 1.**

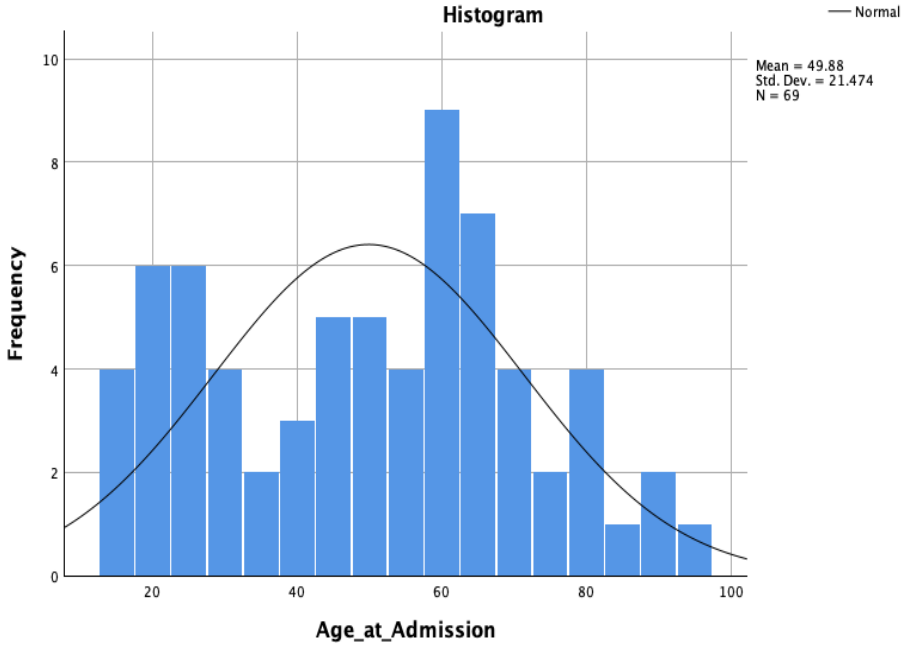


**Figure 17: Histogram of Age at Admission.** The histogram illustrates the age distribution of the study population, highlighting two distinct peaks: one between 18 and 35 years and another between 50 and 60 years. The superimposed curve represents the normal distribution for comparison, with a mean age of 49.88 years and a standard deviation of ±21.47 years. The dataset includes a total of 69 patients, showcasing a wide age range from 15 to 88 years. This distribution indicates potential differences in injury patterns and demographics across age group.

**Table 1: Description of gender distribution**

| Gender | | | | | |
|---|---|---|---|---|---|
| | | Frequency | Percent | Valid Percent | Cumulative Percent |
| Valid | Female | 17 | 24.3 | 24.3 | 24.3 |
| | Male | 53 | 75.7 | 75.7 | 100.0 |
| | Total | 70 | 100.0 | 100.0 | |

The primary cause of pelvic fractures in this patient group was traffic accidents, accounting for 57.14% (40 out of 70) of cases. Of these, 20 patients were car occupants, 13 were motorcyclists, and four were pedestrians struck by vehicles. Additionally, two cyclists and one scooterist sustained pelvic fractures after being hit by vehicles. Falls from heights exceeding three meters were the second most common cause, affecting 25.71% (18 out of 70) of patients. A fall from less than three meters was sufficient to cause a type B or C pelvic fracture in 17.14% (12 out of 70) of patients, as illustrated in **Figure 18.**

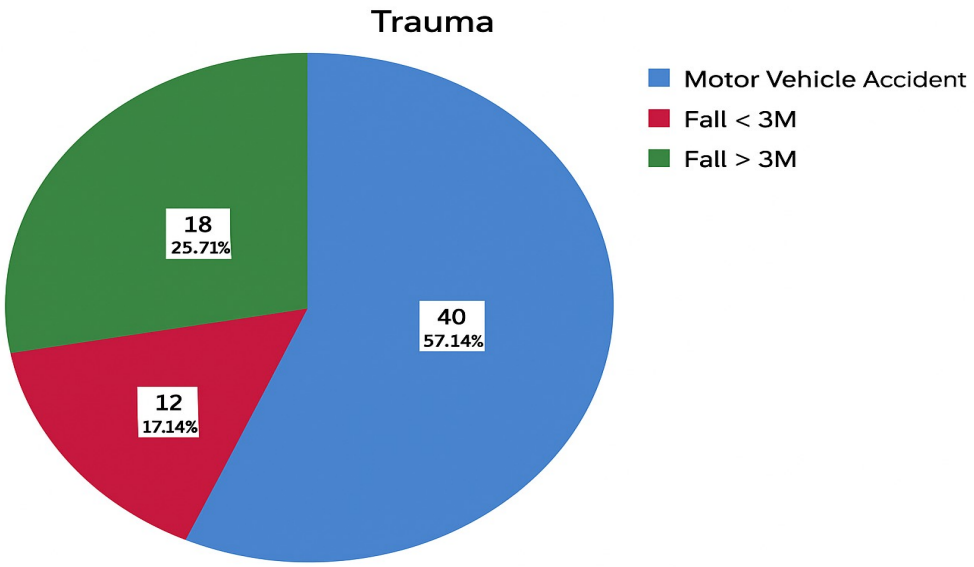


**Figure 18: Distribution of patients based on the mechanism of injury.** The chart illustrates that 57.14% of pelvic fractures were caused by traffic accidents (blue segment), 25.71% resulted from falls exceeding three meters (green segment), and 17.14% were due to falls of less than three meters (red segment).

An isolated pelvic injury was the most common type of trauma, occurring in 25 cases (35.7% of patients). The majority of these cases involved partially unstable pelvic fractures (Type B, according to the AO Classification). Among the associated injuries, 13 patients (18.5% of cases) presented with thoracic trauma, most commonly serial rib fractures and lung contusions. Osseous injuries to the spine were observed in two patients (2.9%), while transverse process fractures of the 4th and 5th lumbar vertebrae, indicative

of pelvic involvement, were identified in three patients (4.3%). Other injury combinations included extremity injuries, reported in 11 patients (15.7%), and abdominal injuries, found in six patients (8.6%). These findings are summarized in **Table 2.**

**Table 2: Number and dispersion of accompanying injuries by patient with a pelvic fracture**

| **Associated injury** | | | | |
|---|---|---|---|---|
| | Frequency | Percent | Valid Percent | Cumulative Percent |
| Pelvis | 25 | 35.7 | 35.7 | 35.7 |
| Pelvis and Abdomen | 6 | 8.6 | 8.6 | 44.3 |
| Pelvis und Extremities | 11 | 15.7 | 15.7 | 60.0 |
| Pelvis and Hip Injuries | 5 | 7.1 | 7.1 | 67.1 |
| Pelvis und Thorax | 13 | 18.5 | 18.5 | 85.7 |
| Pelvis- und Spine | 2 | 2.9 | 2.9 | 88.6 |
| Pelvis and Head | 7 | 10.0 | 10.0 | 98.6 |
| Spine | 1 | 1.4 | 1.4 | 100.0 |
| Total | 70 | 100.0 | 100.0 | |

The average hospital stay for this patient group was 33.55 days (±21.68), calculated from the day of admission to the emergency room. This is illustrated in **Figure 19.**

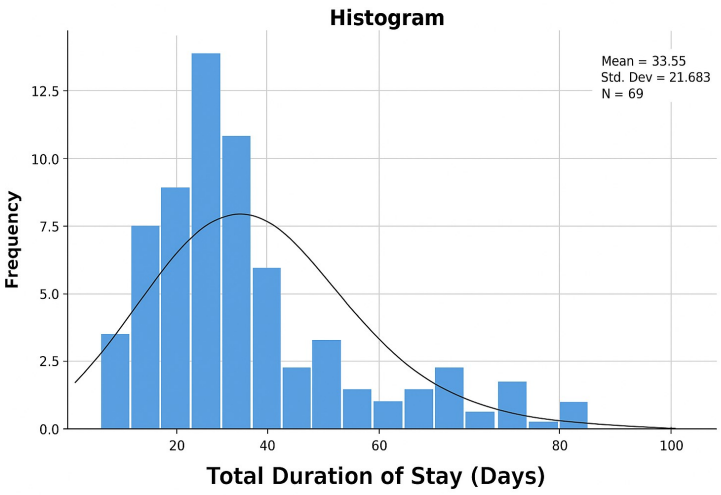


**Figure 19: Distribution of the total length of hospital stay (in days) for the patient group.** The mean duration of hospitalisation was 33.55 days, with a standard deviation of ±21.68. The histogram illustrates the frequency of hospital stays and includes a normal distribution curve for reference.

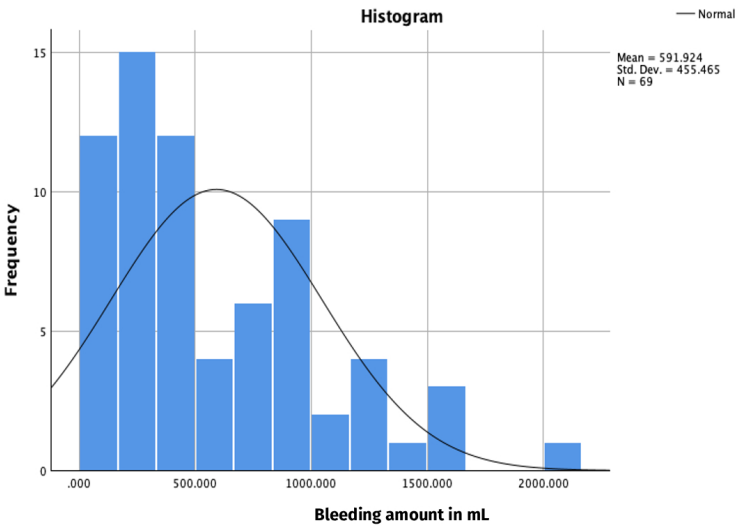


**Figure 20: Distribution of the amount of bleeding (in ml) in patients with pelvic fractures.** The mean bleeding volume was 591.9 ml, with a standard deviation of ±455.4 ml. The histogram depicts the frequency of bleeding volumes, overlaid with a normal distribution curve for reference.

The average amount of bleeding in the patient group was 591.9 ml (±455.4 ml), as measured using the 3D Slicer software for patients with pelvic fractures, this is illustrated in **Figure 20.** Systolic blood pressure at the time of admission to the emergency room was also observed. A total of 63 patients (90.00%) had a systolic blood pressure greater than 89 mmHg, while 5 patients (7.14%) presented with systolic pressures between 75 and 89 mmHg. Only 2 patients (2.86%) had a systolic blood pressure below 75 mmHg (Figure 21).

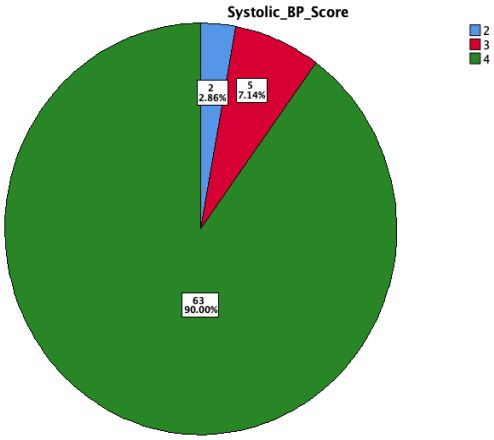


**Figure 21: Distribution of systolic blood pressure in patients upon admission to the emergency room.** The majority of patients (63, 90.00%) had systolic blood pressure values above 89 mmHg. A smaller proportion of patients (5, 7.14%) had systolic pressures between 75 and 89 mmHg, while only 2 patients (2.86%) had systolic blood pressure below 75 mmHg.

### *4.2 Classification of Fractures*

Currently, the most commonly used and structured systems for classifying pelvic fractures are the AO Classification and the Fracture Fragility of the Pelvis (FFP) Classification.

#### *4.2.1 AO Classification*

Out of the 70 patients included in this study, 30 patients (42.86%) were classified as having a Type B pelvic fracture (Table 3). These were further subcategorized as follows: B1 fractures: 15 patients (24.3% of the total cohort). B2 fractures: 10 patients (14.3% of the total cohort). B3 fractures: 3 patients (4.3% of the total cohort).

**Table 3: Distribution of pelvic fracture type for patients according to the AO Classification.**

| AO | | | | | |
|---|---|---|---|---|---|
| | | Frequency | Percent | Valid Percent | Cumulative Percent |
| Valid | A61-B1.1 | 15 | 21.4 | 21.4 | 21.4 |
| | A61-B1.3 | 2 | 2.9 | 2.9 | 24.3 |
| | A61-B2.1 | 4 | 5.7 | 5.7 | 30.0 |
| | A61-B2.2 | 2 | 2.9 | 2.9 | 32.9 |
| | A61-B2.3 | 4 | 5.7 | 5.7 | 38.6 |
| | A61-B3.1 | 3 | 4.3 | 4.3 | 42.9 |
| | A61-C1.1 | 9 | 12.9 | 12.9 | 55.7 |
| | A61-C1.2 | 4 | 5.7 | 5.7 | 61.4 |
| | A61-C1.3 | 1 | 1.4 | 1.4 | 62.9 |
| | A61-C2.1 | 9 | 12.9 | 12.9 | 75.7 |
| | A61-C2.2 | 3 | 4.3 | 4.3 | 80.0 |
| | A61-C3.1 | 5 | 7.1 | 7.1 | 87.1 |
| | A61-C3.2 | 3 | 4.3 | 4.3 | 91.4 |
| | A61-C3.3 | 5 | 7.1 | 7.1 | 98.6 |
| | A61C3. 3 | 1 | 1.4 | 1.4 | 100.0 |
| | Total | 70 | 100.0 | 100.0 | |

Based on the data in **Table 3,** 40 patients (57.14%) were classified as having a Type C pelvic fracture. These were further subcategorised as follows: C1 fractures: 14 patients

(20.3% of the total cohort). C2 fractures: 12 patients (17.2% of the total cohort). C3 fractures: 14 patients (19.9% of the total cohort) **(Table 3).**

### *4.2.2 FFP Classification*

Analysis of pelvic fractures according to the Fracture Fragility of the Pelvis (FFP) Classification revealed the following distribution: FFP2 fractures: 10 patients (14.3% of the total cohort). FFP3 fractures: 28 patients (40.0% of the total cohort). FFP4 fractures: 32 patients (45.7% of the total cohort) **(Table 4).** As previously mentioned, the use of 3D Slicer enabled the detection of free blood in the pelvis caused by hemorrhage, as well as bleeding in the muscles located near the site of the fracture.

**Table 4: Distribution of pelvic fracture type for patients according to the FFP Classification.**

| Classification | | | | | |
|---|---|---|---|---|---|
| | | Frequency | Percent | Valid Percent | Cumulative Percent |
| Valid | FFP2B | 7 | 10.0 | 10.0 | 10.0 |
| | FFP2C | 3 | 4.3 | 4.3 | 14.3 |
| | FFP3A | 4 | 5.7 | 5.7 | 20.0 |
| | FFP3B | 8 | 11.4 | 11.4 | 31.4 |
| | FFP3C | 16 | 22.9 | 22.9 | 54.3 |
| | FFP4B | 5 | 7.1 | 7.1 | 61.4 |
| | FFP4C | 27 | 38.6 | 38.6 | 100.0 |
| | Total | 70 | 100.0 | 100.0 | |

As demonstrated in **Figure 22,** the highest bleeding volume was observed in the group under 20 years of age, with a mean of 916.7 ml. Notably, 94.7% of these patients sustained high-energy traumas, such as car and motorcycle accidents. Following this group, patients aged 71–80 years had the second-highest average bleeding volume of 765.8 ml. This age group remains relatively active in daily activities; however, a significant proportion of these patients were on long-term antithrombotic therapy.

Interestingly, the age group of 81–90 years exhibited a much lower average bleeding volume of 227.8 ml. Most patients in this category sustained ground-level falls, which accounted for their lower bleeding volumes compared to other groups.

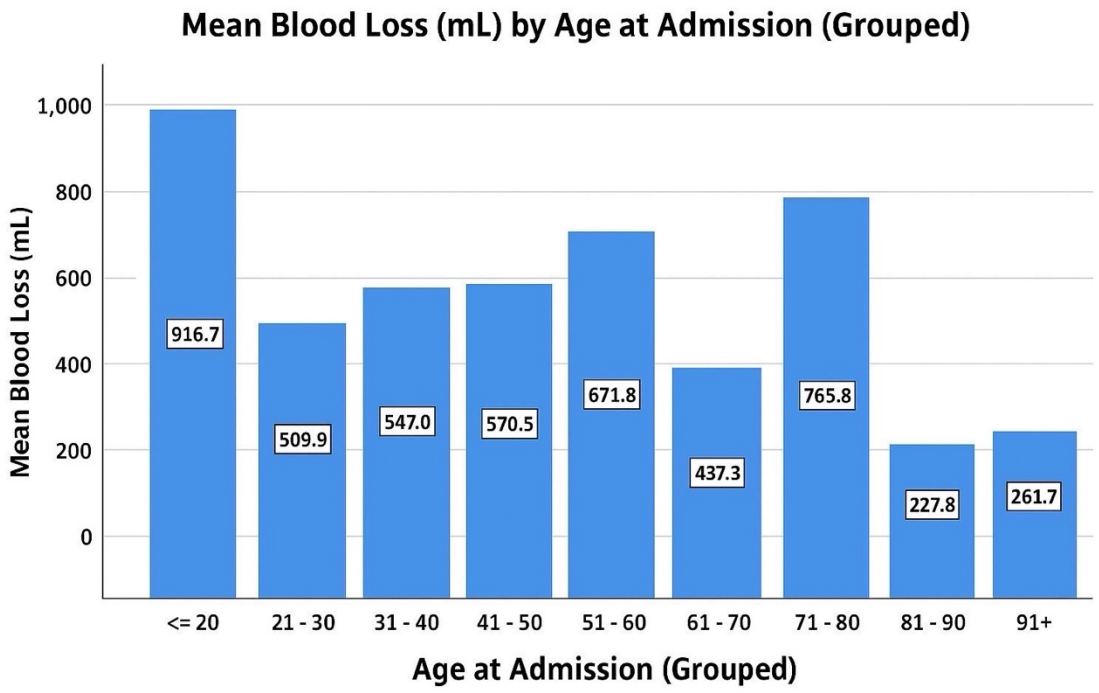


**Figure 22: Mean bleeding volume (in ml) across different age categories.** The chart illustrates the average bleeding volume at admission for patients grouped into age ranges. Younger patients (≤20 years) exhibited the highest mean bleeding volume (916.7 ml), while older age groups (81–90 years) showed significantly lower mean bleeding volumes (227.8 ml).

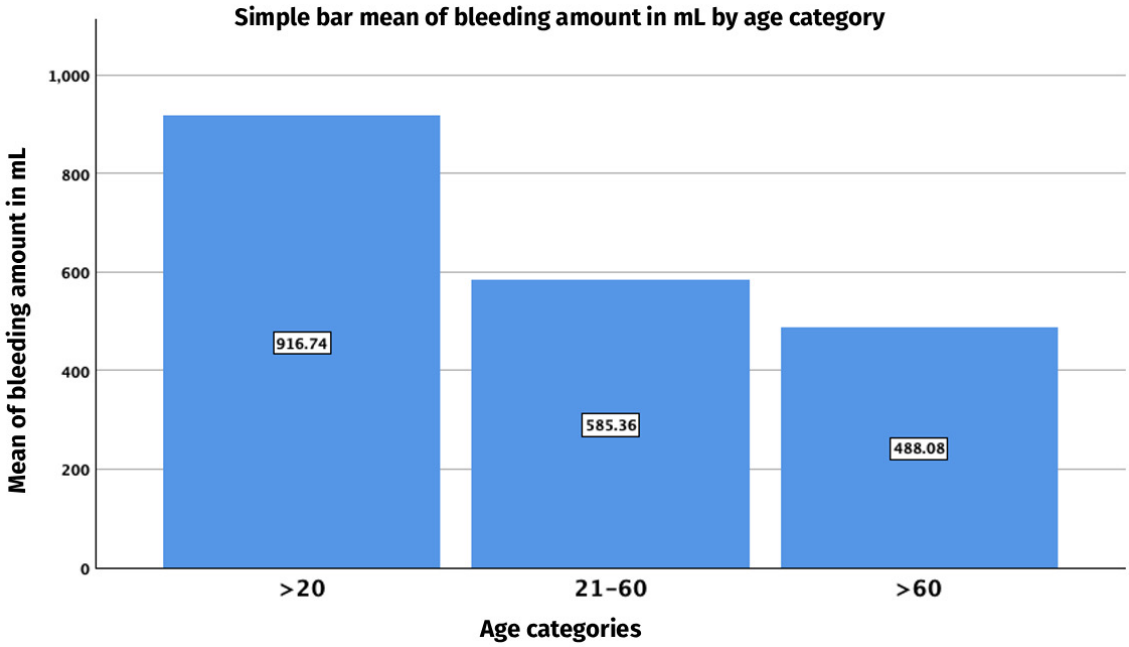


**Figure 23: Distribution of mean bleeding volume (in ml) across subcategorised patient age groups.** The chart shows that patients under 20 years of age exhibited the highest mean bleeding volume (916.74 ml), followed by patients aged 21–60 years (585.36 ml), and patients over 60 years (488.08 ml).

When subcategorized, patients under 20 years had the highest average bleeding volume of 916.7 ml, followed by patients aged 21–60 years, who had an average bleeding volume of 585.36 ml. These findings are summarized in **Figure 23.**

When analyzing the bleeding volume in specific groups of pelvic fractures, it was observed that patients with complex Type C fractures exhibited the highest bleeding volumes at the time of admission (Table 5). For instance, patients with a C3.3 AO pelvic fracture had an average bleeding volume of 1,124.5 ml, while those with a C3.2 AO pelvic fracture had an average bleeding volume of 813.01 ml. Following these groups were patients with a C2.1 AO pelvic fracture, who had an average bleeding volume of 762.8 ml.

**Table 5: Distribution of bleeding amount in different groups of patients according to the AO Classification.**

| Dependent Variable: Bleeding amount in ml | | | |
|---|---|---|---|
| AO | Mean | Std. Deviation | N |
| A61-B1.1 | 437.95087 | 338.480844 | 15 |
| A61-B1.3 | 131.61100 | 30.392864 | 2 |
| A61-B2.1 | 855.45500 | 205.077912 | 4 |
| A61-B2.2 | 247.74000 | 73.482537 | 2 |
| A61-B2.3 | 543.72000 | 695.066929 | 4 |
| A61-B3.1 | 585.84267 | 167.144456 | 3 |
| A61-C1.1 | 696.70567 | 616.046365 | 9 |
| A61-C1.2 | 287.66500 | 165.749574 | 4 |
| A61-C1.3 | 282.32000 | . | 1 |
| A61-C2.1 | 762.82522 | 436.540221 | 9 |
| A61-C2.2 | 458.37233 | 181.039563 | 3 |
| A61-C3.1 | 567.67080 | 380.330849 | 5 |
| A61-C3.2 | 813.01500 | 964.599716 | 2 |
| A61-C3.3 | 1124.49800 | 427.152414 | 6 |
| Total | 591.92377 | 455.465064 | 69 |

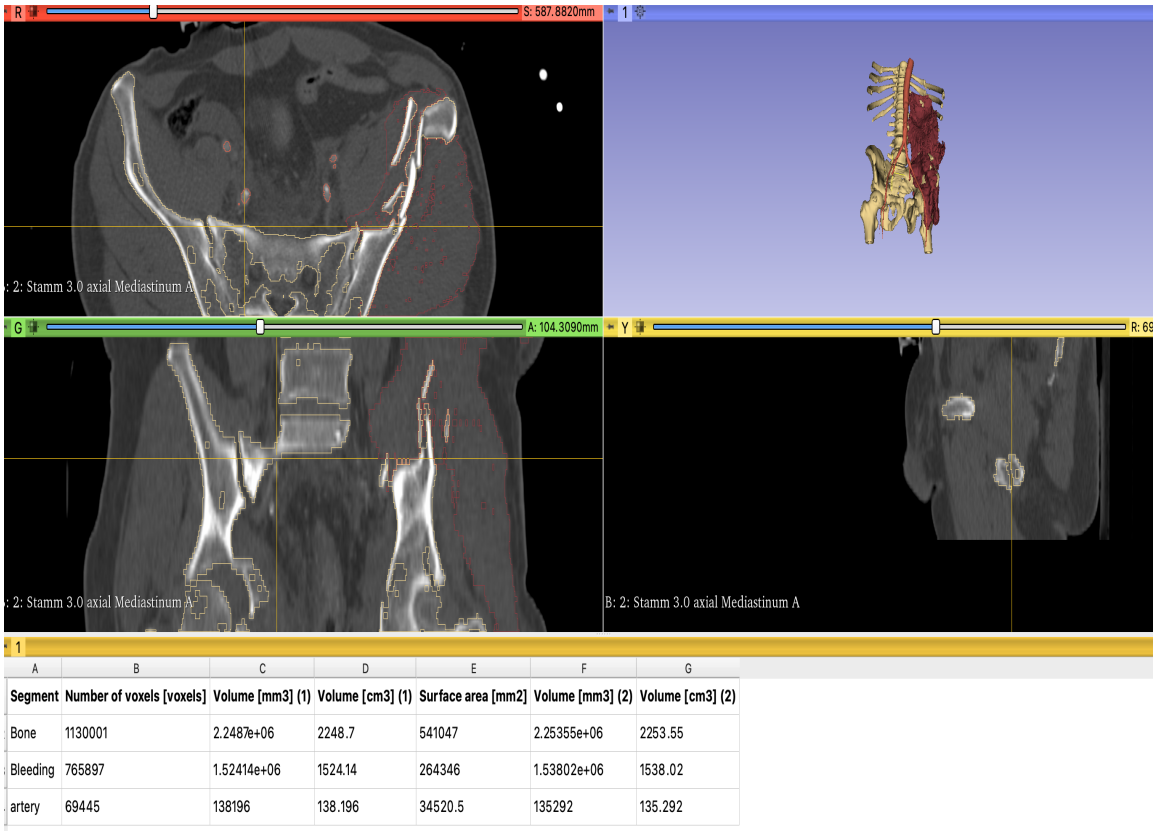


| Segment | Number of voxels [voxels] | Volume [mm3] (1) | Volume [cm3] (1) | Surface area [mm2] | Volume [mm3] (2) | Volume [cm3] (2) |
|---|---|---|---|---|---|---|
| Bone | 1130001 | 2.2487e+06 | 2248.7 | 541047 | 2.25355e+06 | 2253.55 |
| Bleeding | 765897 | 1.52414e+06 | 1524.14 | 264346 | 1.53802e+06 | 1538.02 |
| artery | 69445 | 138196 | 138.196 | 34520.5 | 135292 | 135.292 |

**Figure. 24: Example of a patient with pelvic fracture type C2.1 with bleeding from the one of the branches of the ileal arteries with big hematoma**

**Table 6: Showing the GCS Score in patients with pelvic fracture at the day at admission in the ED.**

| GCS | | | | | |
|---|---|---|---|---|---|
| | | Frequency | Percent | Valid Percent | Cumulative Percent |
| Valid | 3 | 19 | 27.1 | 27.1 | 27.1 |
| | 4 | 1 | 1.4 | 1.4 | 28.6 |
| | 8 | 1 | 1.4 | 1.4 | 30.0 |
| | 10 | 3 | 4.3 | 4.3 | 34.3 |
| | 11 | 1 | 1.4 | 1.4 | 35.7 |
| | 12 | 2 | 2.9 | 2.9 | 38.6 |
| | 13 | 3 | 4.3 | 4.3 | 42.9 |
| | 14 | 8 | 11.4 | 11.4 | 54.3 |
| | 15 | 32 | 45.7 | 45.7 | 100.0 |
| | Total | 70 | 100.0 | 100.0 | |

The Glasgow Coma Scale (GCS) is frequently assessed in polytraumatized patients, including those with pelvic fractures. In this study, 27.1% (19 patients) had a GCS score of 3, indicating severe neurological impairment **(Table 6).** Conversely, 45.7% (32 patients) achieved a GCS score of 15, representing normal neurological function.

Similar to the AO Classification, more complex fracture patterns in the FFP Classification are associated with greater bleeding volumes. For example, patients in the FFP4B group had an average bleeding volume of 827.5 ml, while those in the FFP3C group had an average bleeding volume of 814.2 ml. A detailed distribution of bleeding volumes across FFP subgroups is shown in **Figure 25.**

Regarding systolic blood pressure in patients with pelvic fractures, 63 patients (90.00%) had a systolic blood pressure exceeding 89 mmHg at admission, while 5 patients (7.14%) had pressures between 75 and 89 mmHg. Only 2 patients (2.86%) presented with systolic blood pressure below 75 mmHg. Despite these differences, all three groups exhibited similar blood loss, with an average bleeding volume of 593.7 ml. This comparison is illustrated in **Figure 26.**

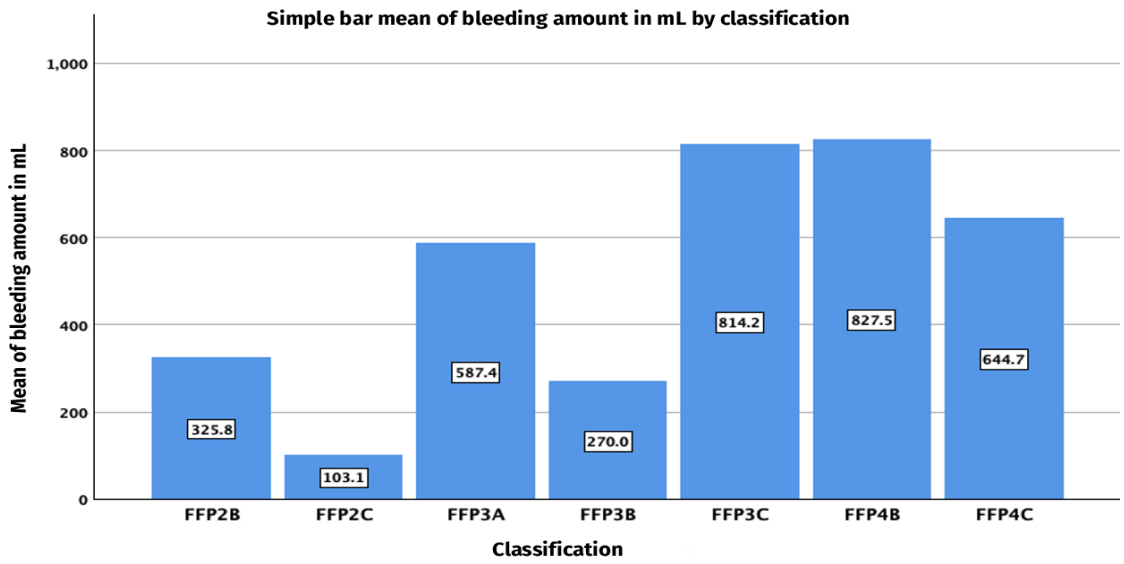


**Figure 25: Distribution of bleeding volume (in ml) across different patient groups classified according to the FFP Classification.** The chart highlights the mean bleeding volume for each subgroup, with FFP4B showing the highest mean bleeding volume at 827.5 ml, followed byFFP3C at 814.2 ml.

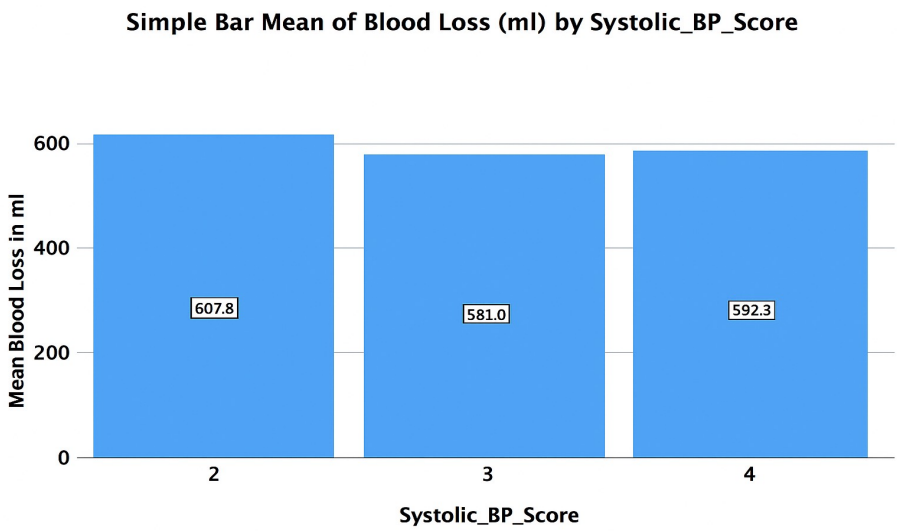


**Figure 26: Distribution of blood loss (in ml) across three groups of patients classified by systolic blood pressure at admission.** The groups represent systolic blood pressure scores: >89 mmHg (607.8 ml), 75–89 mmHg (581.0 ml), and <75 mmHg (592.3 ml). The chart demonstrates similar average blood loss across the groups, irrespective of systolic blood pressure levels.

According to the admission records, patients were assessed using the Trauma and Injury Severity Score (TRISS), which incorporates the Injury Severity Score (ISS), the Revised Trauma Score (RTS), and patient age. For patients aged 55 years or older, an age factor of 1 was applied; otherwise, it was set to 0. The mean TRISS score for the cohort was 5.69 (±1.70). The predicted mortality rate based on the TRISS score was 5.69%, while the observed mortality rate was significantly lower, at 1.44% **(Figure 27).**

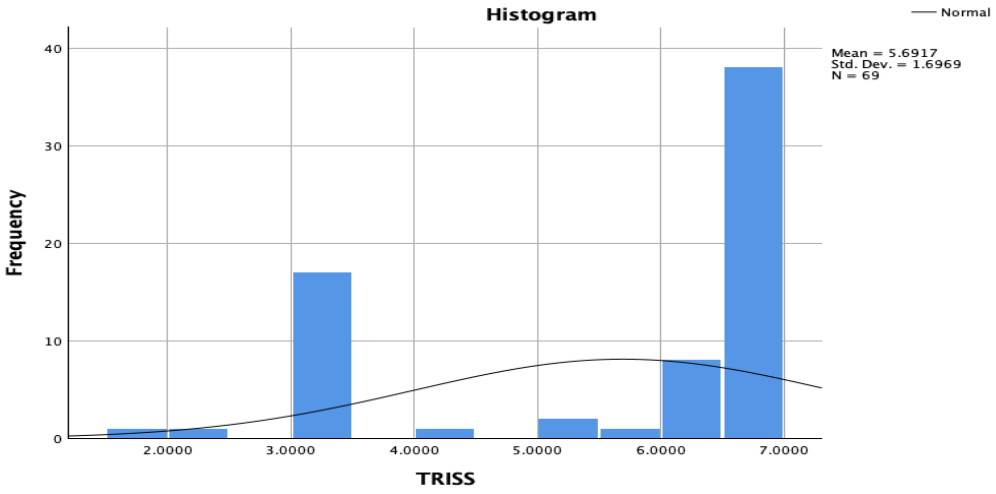


**Figure 27: Distribution of Trauma and Injury Severity Score (TRISS) among admitted patients.** The histogram illustrates the severity of injuries, with a mean TRISS value of 5.69 (±1.70). The frequency of patients is shown across TRISS ranges, highlighting the prevalence of severe injuries in the study cohort.

# 5 Discussion

Pelvic fractures are relatively infrequent injuries, but their incidence is on the rise due to increased motorization and advancements in traffic infrastructure. These injuries are highly complex, presenting significant challenges in treatment and long-term management. The complexity of pelvic fractures often leads to residual disabilities, which can impair the post-acute recovery process (Pohlemann et al., 2021). Patients with pelvic fractures frequently experience a combination of physical and psychosocial disabilities. These impairments reduce their independence and economic productivity, resulting in a diminished quality of life (Giannoudis et al., 2007). The economic burden associated with pelvic fractures is substantial, encompassing both acute care and post-acute management phases. Treatment requires a multidisciplinary approach and prolonged hospital stays, particularly in intensive care units (ICUs). This places considerable strain on healthcare systems.

For instance, Wu et al. reported that patients with pelvic fractures combined with major vascular injuries had an average ICU stay of 11.8 ± 9.8 days (Wu et al., 2010). In comparison, the average ICU stay in this study for patients with complex pelvic fractures at the University Hospital in Giessen was significantly longer, at 17.12 ± 15.98 days. This disparity underscores the economic impact of providing optimal care for patients with severe pelvic injuries.

The consequences of pelvic fractures are particularly pronounced in young adults, who face significant disruptions to their personal and professional lives during the post-acute recovery phase. Many patients are unable to earn an independent living, pursue education, or form families during this time. Several studies have shown that even after hospital discharge or rehabilitation, patients with pelvic fractures struggle with daily activities, including household chores, community reintegration, and maintaining employment. Chronic pain and emotional challenges further exacerbate these difficulties, compounding the long-term impact on their lives (Lunsjo et al., 2007).

## *5.1 Polytrauma and Maximum Care Hospitals*

Due to the complexity and severity of their injuries, polytraumatized patients are typically admitted and treated in maximum-care hospitals. At the Department for Trauma, Hand, and Reconstructive Surgery, University of Giessen, established standards, including

adherence to the Advanced Trauma Life Support (ATLS) guidelines, ensure optimal treatment for these patients. Such standardized protocols are essential for managing the multifaceted injuries associated with polytrauma.

According to the German Statistical Federal Office, the number of injured persons rose by 5% (approximately 900 cases) in April 2023 compared to the previous year (Destatis, 2023). This increase suggests a corresponding rise in the incidence of polytraumatized patients with unstable pelvic and internal injuries, necessitating enhanced preparedness in trauma care centers.

### *5.2 Morbidity, Mortality, and Economic Burden*

Numerous epidemiological studies have highlighted the significant morbidity, mortality, disability and economic burden associated with pelvic fractures. In the United States, for instance, the mortality rate for pelvic fractures is reported to be 8.3%, with projections estimating an annual incidence of 3 million fractures and associated healthcare costs of $25.3 billion by 2025 (Miller et al., 2017).

In this study, the mortality rate observed in Middle Hesse between 2017 and 2023 was considerably lower, at 1.43%. This discrepancy may reflect differences in healthcare systems, trauma care protocols, or regional demographics. However, with an ageing population in Germany, the incidence of osteoporotic pelvic fractures resulting from low-energy trauma, such as ground-level falls, is steadily increasing.

### *5.3 Gender and Age Distribution*

This study revealed that 75.7% of the patients with pelvic fractures were male, corresponding to 53 male patients and 17 female patients. The average age of the patient group was 49.98 ± 21.47 years, with an age range of 15 to 88 years. The age distribution exhibited two distinct peaks: one among younger adults aged 18–35 and another among middle-aged individuals aged 50–60.

Similar findings were reported by Ghosh et al., who documented a male-to-female ratio of 56/19 (74.67% male). The youngest patient in their study was 17 years old, and the oldest was 85 years old, with a mean age of 37.57. Notably, patients below 50 constituted 82% of their study population (Ghosh et al., 2019). These similarities reinforce the demographic trends observed in pelvic fracture patients across different regions.

### *5.4 Mechanisms of Injury*

The mechanisms of injury in this cohort were dominated by high-energy trauma, with traffic accidents accounting for 57.14% (40/70) of cases. Among these, 20 patients were car occupants, 13 were motorcyclists, four were pedestrians hit by vehicles, two were cyclists, and one was a scooterist. Falls from heights exceeding three meters were the second most common cause, affecting 25.71% (18/70) of patients. Finally, 17.14% (12/70) of patients sustained pelvic fractures from low-energy trauma, such as falls from heights of less than three meters.

These findings underscore the significant role of high-energy trauma in pelvic fractures, with 82.86% of patients in this study sustaining injuries through mechanisms involving substantial force. In comparison, Ghosh et al. reported similar trends, with vehicle accidents accounting for 77.3% of cases and falls from heights contributing to 21.3% (Ghosh et al., 2019). These data highlight the continued need for targeted prevention strategies, particularly in high-risk scenarios such as traffic collisions and occupational hazards involving falls.

### *5.5 High-Energy Versus Low-Energy Trauma*

In this study, 82.86% of the patients sustained pelvic fractures due to high-energy trauma, while the remaining cases were attributed to low-energy trauma. This aligns with the findings of Ghosh et al., who reported that the most frequent mechanism of injury was vehicle accidents, accounting for 77.3% of cases, followed by falls from heights (21.3%) and falling objects (1.3%, a single case) (Ghosh et al., 2019).

### *5.6 Economic and Clinical Burden*

Andrich et al. demonstrated that pelvic fractures in older adults significantly increase the utilisation of inpatient healthcare services and lead to excess costs within the first year after injury (Andrich et al., 2015). Although partial and completely unstable pelvic fractures are relatively rare, they are particularly critical in polytraumatized patients due to their high mortality rates.

Severe pelvic injuries, such as those classified as AO Type B and C, can result in massive hemorrhage, with blood loss reaching up to 3,000 ml at a rate of 1,000 ml/h (Huittinen & Slätis, 1972). Hemorrhagic shock, driven by acute bleeding, accounts for 80% of all

deaths associated with pelvic fractures, underscoring the importance of early detection and management of bleeding sources (Papakostidis et al., 2012).

### *5.7 Challenges in Early Detection*

Despite advancements in trauma care, bleeding remains the leading cause of non-CNS-related deaths in pelvic fractures, with mortality rates ranging from 12.5% to 26.6% (Hagiwara et al., 2009). A major challenge is that injuries to pelvic vessels in hemodynamically compensated patients (e.g., those with partially unstable fractures) often remain undetected until the condition becomes critical. These delays significantly increase the risk of complications and mortality. Furthermore, no uniform methodology currently exists to quantify pelvic blood loss in polytraumatized patients with or without pelvic fractures accurately.

The data from this study revealed that 63 patients (90.00%) had a systolic blood pressure above 89 mmHg at admission, while 5 patients (7.14%) had systolic pressures between 75 and 89 mmHg, and only 2 patients (2.86%) presented with systolic pressures below 75 mmHg. This indicates that patients with partially unstable or unstable pelvic fractures can initially present with relatively normal systolic blood pressure, which may lead to diagnostic errors or delays in recognizing significant vascular injuries.

### *5.8 Hidden Shock and Diagnostic Innovations*

Circulatory instability in patients with pelvic ring injuries can be difficult to identify during the early stages of hemorrhage, particularly in younger patients who remain clinically compensated despite substantial blood loss (Kobayashi et al., 2014). Such patients may enter a state of "hidden shock," where retroperitoneal bleeding remains undetected until proven otherwise (Sola et al., 2021).

The need for improved diagnostic tools to quantify bleeding volumes and guide therapeutic interventions led to the exploration of 3D Slicer software in this study.

This method could optimize the timing and precision of therapeutic interventions by quickly estimating bleeding volumes and correlating them with fracture types. Moreover, it could add fracture type to the list of prognostic risk factors.

### *5.9 CT Volumetry: Historical and Current Applications*

CT CT volumetry was first described in 1982, though initially not as a tool for measuring bleeding volumes. The technique was primarily used to quantify organ volumes (Weinreb et al., 1982). Over time, its applications expanded to include measurements for various purposes, such as evaluating tumor size and comparing it with the remaining liver volume in patients with hepatic tumours (Nishie et al., 2003).

In the context of polytraumatized patients, CT volumetry has become an invaluable tool for quantifying pelvic blood loss, particularly when combined with 'crash' CT scans in emergency diagnostics. This study demonstrated that evaluating pelvic hematomas using CT volumetry can help predict fracture-related blood loss, transfusion requirements, and the need for angiography or transarterial embolization (TAE) (Sola et al., 2021).

### *5.10 3D CT Volumetry in Evaluating Bleeding Volumes*

3D CT volumetry has been widely utilised to estimate the validity of measurements for various clinical applications. For example, it has been employed to assess lung volumes reconstructed from thin-section multidetector-row CT images, with results compared to standard pulmonary function testing (Sugiura et al., 1999). Additionally, studies have examined the relationship between slice thickness and calculated volume in CT liver volumetry, allowing for differentiation based on slice thickness and three-dimensional imaging resolution (Heussel et al., 1999). However, the three-dimensional presentation of bleeding volumes, particularly intramuscular and free pelvic bleeding, had not been explored until the commencement of this study.

### *5.11 Methodology and Training*

Stringent inclusion and exclusion criteria were implemented to ensure robust results with minimal susceptibility to confounding factors. These criteria excluded patients with other potential bleeding sources in the abdomen or pelvic region, facilitating accurate comparison of CT datasets. The identified bleeding areas were verified in collaboration with a radiologist from the Department of Diagnostic and Interventional Radiology in Giessen, ensuring precise localization and segmentation of hemorrhagic regions.

Using the 3D Slicer software, this study successfully segmented and quantified free fluid or blood within the pelvic cavity and surrounding musculature. The quantification tool

automatically converted segmented volumes into cubic millimetres ($mm^3$), which were then expressed as millilitres (ml) for clinical interpretation.

The 3D Slicer program, however, cannot independently detect, measure, or segment bleeding volumes. As a result, the process requires a highly trained team to manually perform the segmentation. To address this, it was necessary an specialized training to understand the program's functionality, including injury detection, bleeding volume measurement, and segmentation of the pelvic region. Initially, the segmentation process required approximately four hours per patient, but with experience and training, this time was reduced to two hours.

### *5.12 Limitations of 3D Slicer for Clinical Use*

Despite its utility, several limitations restrict the application of 3D Slicer in emergency diagnostics. The time-intensive nature of segmentation is a critical drawback in urgent clinical settings, where rapid decisions are necessary. Moreover, human error during segmentation can result in false-positive or false-negative findings, leading to inaccurate diagnoses and potentially inappropriate treatments. Sensitivity and specificity may also vary between patients and investigators, further complicating its reliability.

To date, 3D Slicer has been primarily employed as a research tool and has not been integrated into routine clinical diagnostics or therapeutic workflows. In this study, particular attention was paid to the correlation between bleeding volumes, clinical conditions, and fracture classifications.

### *5.13 Bleeding Volume by Fracture Classification*

As detailed in the Results section, patients with complex C fractures exhibited the highest bleeding volumes at admission. For instance, patients with AO C3.3 fractures had an average bleeding volume of 1,124.5 ml, while those with C3.2 fractures recorded 813.01 ml. Similarly, patients with AO C2.1 fractures exhibited an average bleeding volume of 762.8 ml. Interestingly, C1.1 fractures showed a bleeding volume of 969.7 ml.

These findings suggest that patients with C3 fractures are more likely to experience higher bleeding volumes. The same pattern is observed in partially unstable fractures, such as

AO Types B1–B3. Early detection of bleeding is therefore essential, as it significantly correlates with clinical treatment, outcomes, and mortality.

### *5.14 Comparison with Prior Studies*

Similar trends have been documented by Veith et al., who reported average total blood loss volumes of 476 ml for C1-type fractures, 931 ml for C2-type fractures, and 1,005 ml for C3-type fractures (Veith et al., 2016). A key difference in their study was using the Osirix DICOM viewer (Version 5.8; Pixmea; Geneva, Switzerland) to delineate separate bleeding areas, including intramuscular, interstitial, and total blood volumes. Notably, interstitial free blood volumes were significantly higher in C3-type fractures (888 ± 663 ml) compared to C1-type fractures (392 ± 502.8 ml; $p < 0.05$). Total blood loss also showed a significant increase in C3 fractures compared to C1 fractures (1,005 ± 649 ml vs. 476 ± 535 ml; $p < 0.05$) (Veith et al., 2016).

### *5.15 Fragility Fracture Classification and Age-Related Variations*

Due to the growing scientific and clinical interest in the fragility fracture classification of the pelvis (FFP), this study included an analysis of the collected data according to FFP classification. Although the FFP system is primarily used for patients with osteoporosis or related conditions, the classification was applied here to investigate potential connections between fracture types, clinical outcomes, and mortality.

Similar to the AO Classification, more complex fracture patterns in the FFP system correlated with higher bleeding volumes. For example, patients with FFP4B fractures exhibited an average bleeding volume of 827.5 ml, while those with FFP3C fractures averaged 814.2 ml. Early detection of blood loss in such cases is critical, as it significantly influences clinical conditions, outcomes, and mortality.

### *5.16 Mechanisms of Injury and Clinical Impact*

High-energy trauma accounted for 82.86% of the pelvic fractures observed in this study, with the remainder resulting from low-energy trauma. The mechanism of injury greatly influenced injury patterns, outcomes, and prognoses.

Two patients initially admitted in stable condition were successfully resuscitated due to progressive, severe intrapelvic hemorrhage. Both patients had sustained high-energy

trauma in traffic accidents. Among the cohort, 10% (7/70) of patients took anticoagulants as long-term medication at the time of injury. Of these, two sustained high-energy trauma, while 5 had low-energy injuries, such as falls from heights <3 meters. Interestingly, despite the known increased bleeding risk associated with anticoagulants, no significant differences in bleeding volumes were observed between patients, when stratified by fracture type or injury mechanism.

A 2016 study reported that 10–15% of patients with pelvic fractures admitted to emergency departments presented in shock, with one-third eventually dying. Mortality rates in more recent reports have reached as high as 32%, primarily due to uncontrolled bleeding and physiological exhaustion (Starr et al., 2016).

### *5.17 Age-Related Variations in Pelvic Fractures*

The average age of patients in this study was 49.98 ± 21.47 years, with an age range of 15 to 88 years. The age distribution exhibited two peaks: one among younger adults aged 18–35 years and another among middle-aged individuals aged 50–60 years. Gender distribution revealed that 75.7% of the patients were male (53 males and 17 females).

These findings are similar to those reported by Veith et al., where the average age was 47 ± 19 years, but with a reversed gender distribution, as 60% of the cohort were female.

The age group under 20 years exhibited the highest average bleeding volume (916.7 ml), with 94.7% of these cases resulting from high-energy trauma, such as car and motorcycle accidents. The second-highest bleeding volume was observed in patients aged 71–80 years, averaging 765.8 ml. Most patients in this group were active in daily activities but were on long-term anticoagulant or antithrombotic therapy. A significant proportion of these patients sustained injuries from falls <3 meters and were subsequently treated for osteoporosis.

Conversely, patients aged 81–90 years had the lowest average bleeding volume (227.8 ml), primarily due to ground-level falls. These patients were diagnosed with complex osteoporotic pelvic fractures involving both intramuscular bleeding and free blood in the pelvic cavity.

### *5.18 Findings in the Literature*

In 2007, Burge et al. reported that pelvic ring fractures in the elderly accounted for 7% of all osteoporosis-associated fractures in the United States (Burge et al., 2007). Similarly, Mika et al. conducted a 22-year retrospective analysis, observing a significant decrease in the frequency of Type A fractures (from 84.8% to 43.9%) and a corresponding increase in Type B and C fractures (from 7.0% and 8.2% to 14.3% and 41.8%, respectively). They also noted that patients aged 60–70 years exhibited higher frequencies of Type B and C fractures compared to those over 70 years (Mika et al., 2021).

### *5.19 Treatment Strategies for Complex Pelvic Fractures*

The management of complex pelvic fractures increasingly involves a combination of surgical and radiological-interventional treatments, which is crucial for optimal patient outcomes. These advanced therapeutic combinations are typically available only in Level 1 Trauma Centers globally, where multidisciplinary expertise is accessible.

Historically, acute hemorrhage in unstable pelvic fractures was managed using external stabilization methods (e.g., external fixators or C-clamps) in combination with laparotomy and packing. However, these techniques were associated with high mortality and complication rates. Recent advancements in radiological interventions, such as transarterial embolization (TAE), have significantly improved outcomes by enabling precise hemorrhage control (Usui et al., 2024).

### *5.20 Advances in the Treatment of Unstable Pelvic Fractures*

Historically, acute bleeding in unstable pelvic fractures was managed using external stabilization methods, such as external fixators or C-clamps, combined with open laparotomy and packing. While these techniques were effective in controlling hemorrhage, they were associated with high mortality and complication rates. The need for less invasive and more efficient approaches led to the incorporation of radiological interventions as an alternative treatment strategy.

### *5.21 Current Radiological Interventions*

A recent review by Usui et al. (2024) provided a comprehensive overview of transcatheter arterial embolization (TAE) and other radiological interventions for hemorrhagic pelvic vessel injuries. Their findings highlighted the effectiveness of TAE in improving vital signs and reducing transfusion requirements, making it a valuable tool in managing pelvic fractures with severe bleeding.

Another advancement in trauma care is using the Resuscitative Endovascular Balloon Occlusion of the Aorta (REBOA) system. A 20-year experience reported in 2018 by Pieper et al.. demonstrated its effectiveness as a non-invasive aortic clamp for controlling life-threatening hemorrhage. Balloon inflation was performed in Zone 3 (between the lower renal artery and the aortic bifurcation), effectively stopping acute bleeding in patients with severe pelvic trauma. REBOA significantly improved systolic blood pressure from 60 mmHg (35–73) to 115 mmHg (91–128) ($p < 0.001$). However, a high rate of vascular complications (19%, $n = 5$) was reported, although no cases of amputation occurred (Pieper et al., 2018).The Department for Trauma, Hand and Reconstructive Surgery, University of Giessen, has recently implemented the REBOA system. Since 2023, it has been used in two cases within the Emergency Department (ED), with plans for broader application based on clinical indications.

### *5.22 Polytraumatized Patients and Injury Patterns*

Pelvic ring fractures, particularly partially unstable and unstable types, are often part of a complex injury pattern in polytraumatized patients. These patients frequently present in the ED with non-standard injury distributions involving multiple organ systems and long bones.

This study found that isolated pelvic fractures were the most common injury type, affecting 25 patients (35.7% of the cohort). Among patients with accompanying injuries:

- 13 patients (18.5%) had serial rib fractures, with lung contusions being the most common thoracic diagnosis
- 2 patients (2.9%) exhibited osseous injuries to the spine, specifically transverse process fractures of the 4th and 5th lumbar vertebrae, indicating pelvic involvement

- 11 patients (15.7%) had extremity injuries
- 6 patients (8.6%) sustained abdominal injuries

In these cases, significant blood loss was primarily attributed to pelvic fractures, underscoring their critical role in hemorrhage management.

### *5.23 Comparison with Epidemiological Studies*

Other epidemiological studies reveal similar findings regarding associated injuries. The thoracolumbar transition (TH11–L2) exhibited the highest incidence of fractures (68.8%), followed by injuries to the thoracic spine (TH1–TH10) at 18.3% and the lumbar spine (L3–L5) at 12.9% (Culemann, 2003). Schindler et al. (2023) reported that spinal fractures most commonly affect the thoracic (41.9%) and lumbar (55.8%) regions, with cervical spine injuries being less frequent (25.6%). Multiple-segment fractures occurred in 20% of cases. Additionally, combined limb injuries (fractures of the femur, tibia, humerus, or forearm) were observed in 74.5% of cases, with upper limbs involved in 55.7% and lower limbs in 67.1%. Approximately 22.9% of patients experienced fractures in both upper and lower limbs (Culemann, 2008).

### *5.24 Clinical Outcomes, Limitations, and Conclusion*

Clinical outcomes in polytraumatized patients are closely related to patient history and the presence of associated injuries. In this study, patients with isolated pelvic fractures or minor associated injuries (e.g., limb injuries) demonstrated a better likelihood of recovery. Conversely, patients with more complex patterns of injury required more extensive interdisciplinary management, underscoring the importance of involving multiple specialties in the treatment of polytraumatized patients. Hemorrhage control is a critical priority in such cases. Accurately determining the bleeding volume in patients with unstable pelvic fractures facilitates patient stabilization, optimizes fluid resuscitation, and helps prevent the lethal triad of trauma: acidosis, coagulopathy, and hypothermia. This highlights the role of advanced diagnostic and therapeutic strategies in improving clinical outcomes.

### *5.25 Study Limitations*

This retrospective study, like other analyses relying on large databases, has inherent limitations:

1. **Data Source Limitations**: Data collection relied on the German Trauma Registry, controlled through the ICD-10 Coding system. However, temporal trends, such as the impact of the COVID-19 pandemic, may have influenced the data quality or reporting.

2. **Accuracy of Clinical Measurements**: Notable limitations include challenges in accurately interpreting examinations, such as Glasgow Coma Scale (GCS) scores, and potential inaccuracies in patient data registration.

3. **Lack of Comparability**: Data generated using the 3D Slicer software cannot be directly compared with other settings or datasets, limiting generalizability.

4. **Exclusion of Post-Discharge Data**: The database only includes inpatient data, omitting complications or follow-up information after discharge, which could provide valuable insights into long-term outcomes.

**5. Time Constraints**: The time-intensive nature of 3D Slicer segmentation (up to two hours per case) is a significant limitation in emergency settings, where rapid diagnosis and treatment are critical. Additionally, the software cannot independently detect bleeding or express it in quantifiable units, relying heavily on trained personnel for manual segmentation.

### *5.26 Future Implications*

Quantifying bleeding volumes in pelvic fractures, where the bleeding source is confined to the pelvic region, could significantly impact trauma care algorithms. By excluding other potential bleeding sources through serial examinations, this method has the potential to refine treatment approaches and improve outcomes. The importance of recognizing severe trauma, often accompanied by vital function disorders, cannot be overstated. Timely and appropriate treatment requires a coordinated interdisciplinary approach. Collaboration between trauma surgeons, radiologists, anesthesiologists, and other specialists is essential for delivering patient-centered care.

### *5.27 Proposed Diagnostic and Therapeutic Algorithm*

A structured diagnostic and therapeutic algorithm is proposed to address the complexities of pelvic fracture management. This algorithm integrates fracture classification, bleeding

volume quantification using 3D Slicer, and clinical parameters to guide tailored interventions.

1. **Initial Assessment and Stabilization**

- Triage patients following ATLS guidelines
- Categorize hemodynamic status (stable, borderline, unstable)
- Use pelvic binders or C-clamps for immediate stabilization in unstable patients

2. **Imaging and Diagnosis**

- Perform X-rays for initial assessment
- Use contrast-enhanced CT for comprehensive evaluation
- Apply 3D Slicer to quantify bleeding volumes and assess fracture severity

3. **Risk Stratification and Treatment**

**High-risk**: Severe bleeding (>800 ml) or complex fractures (e.g., AO C3, FFP 4). Intervene with TAE or REBOA as indicated.

**Moderate risk**: Moderate bleeding (300–800 ml). Employ radiological or surgical stabilization.

**Low risk**: Stable hemodynamics and minor bleeding (<300 ml). Manage conservatively with rest and pain control.

4. **Monitoring and Follow-Up**

ICU monitoring for high- and moderate-risk patients.Enroll in rehabilitation programs post-discharge and monitor for complications. This algorithm offers a framework for personalizing patient care, improving clinical outcomes, and optimizing resource allocation.

Future research should focus on validating this algorithm in diverse clinical settings, exploring its cost-effectiveness, and integrating advanced technologies, such as AI-driven imaging, to enhance its efficiency and reliability.

# 6 Conclusion

In conclusion, this study represents the most comprehensive epidemiological analysis combined with experimental analysis of the blood loss of pelvic ring fractures conducted in the Region of Middle Hesse, Germany.

Through meticulous research, the authors have illuminated the critical factors contributing to poor outcomes associated with these injuries, as well as identified the concerning trend of increasing incidence of pelvic fractures. The findings from this research provide invaluable insights that may be instrumental in shaping future treatment protocols and enhancing patient care.

While the program applied in our analysis proved exceptionally effective, its implementation required considerable time investment. This highlights a dual aspect of our research: the significant potential for utilizing advanced diagnostic and analytic tools to further our understanding of pelvic fractures, juxtaposed with the challenges posed by the time-intensive nature of these methodologies. Such an effort underscores the necessity for ongoing research and the continued development of efficient tools that expedite data analysis and improve the overall quality of care provided to patients suffering from pelvic injuries.

Our findings have emphasized the essential need for a multidisciplinary approach in managing pelvic fractures, incorporating various specialties to address the complexities inherent in such cases. To improve patient outcomes and to keep pace with the escalating rates of pelvic fractures, a concerted effort is required - one that embraces innovation in diagnostic techniques and fosters collaboration among healthcare professionals. This research is a foundational step toward achieving those goals, advocating for further exploration and refinement of practices that will ultimately enhance the care and recovery processes for individuals affected by pelvic ring fractures in Middle Hesse and beyond.

# 7 References


1. Andrich, S., Haastert, B., Neuhaus, E., Frommholz, K., Arend, W., Ohmann, C., Grebe, J., Vogt, A., Brunoni, C., Jungbluth, P., Thelen, S., Dintsios, C.-M., Windolf, J., & Icks, A. (2021). Health care utilization and excess costs after pelvic fractures among older people in Germany. Osteoporosis International, 32(10), 2061–2072. https://doi.org/10.1007/s00198-021-05935-1
2. Blackmore, C. C., Jurkovich, G. J., Linnau, K. F., Cummings, P., Hoffer, E. K., & Rivara, F. P. (2003). Assessment of volume of hemorrhage and outcome from pelvic fracture. Archives of Surgery, 138(5), 504–508.
3. Breiman, R. S., Beck, J. W., Korobkin, M., Glenny, R., Akwari, O. E., Heaston, D. K., Moore, A. V., & Ram, P. C. (1982). Volume determinations using computed tomography. AJR American Journal of Roentgenology, 138(2), 329–333. https://doi.org/10.2214/ajr.138.2.329
4. Burge, R., Dawson-Hughes, B., Solomon, D. H., Wong, J. B., King, A., & Tosteson, A. (2007). Incidence and economic burden of osteoporosis-related fractures in the United States, 2005–2025. Journal of Bone and Mineral Research, 22(3), 465–475. https://doi.org/10.1359/jbmr.061113
5. Costantini, T. W., Coimbra, R., Holcomb, J. B., Catalano, R., Wolf, L. L., Myers, J. B., Biffl, W. L. (2016). Current management of hemorrhage from severe pelvic fractures: Results of an American Association for the Surgery of Trauma multi-institutional trial. Journal of Trauma and Acute Care Surgery, 80(5), 717–723. https://doi.org/10.1097/TA.0000000000000972
6. Culemann, U., Tosounidis, G., Reilmann, H., & Pohlemann, T. (2003). Beckenringverletzung: Diagnostik und aktuelle Behandlungsmöglichkeiten. Der Chirurg, 74(7), 687–700.
7. Culemann, U., Günther, K., Pohlemann, T., & Rüter, A. (2008). Beckenring und Hüftgelenk. In H. Scharf, A. Rüter, T. Pohlemann, I. Marzi, D. Kohn, & K. Günther (Eds.), Orthopädie und Unfallchirurgie (2nd ed., pp. 709–804). Urban & Fischer.
8. Darmanis, S., Lewis, A., Mansoor, A., & Bircher, M. (2007). Corona mortis: An anatomical study with clinical implications in approaches to the pelvis and acetabulum. Clinical Anatomy, 20(4), 433–439. https://doi.org/10.1002/ca.20390
9. Destatis (Statistisches Bundesamt). (2023). Press release No. 160 of 14 April 2023. https://www.destatis.de/EN/Press/2023/04/PE23_160_46241.html
10. Dong, Y., Peng, R., Kang, H., Song, K., Guo, Q., Zhao, H., Zhu, M., Zhang, Y., Guan, H., & Li, F. (2022). Global incidence, prevalence, and disability of vertebral fractures: A systematic analysis of the global burden of disease study 2019. Spine Journal, 22(5), 857–868.

11. Dzupa, V., Chmelova, J., Pavelka, T., Kautzner, J., & Kucera, T. (2009). Multicentric study of patients with pelvic injury: Basic analysis of the study group. Acta Chirurgiae Orthopaedicae et Traumatologiae Cechoslovaca, 76(5), 404–409.
12. Finiels, H., Finiels, P. J., Jacquot, J. M., & Strubel, D. (1997). Fractures du sacrum par insuffisance osseuse. Méta-analyse de 508 cas. Presse Médicale, 26(33), 1568–1573.
13. Ge, P. L., & Du, S. D. (2014). Advances in preoperative assessment of liver function. Hepatobiliary & Pancreatic Diseases International, 13(4), 361–370.
14. Ghosh, S., Aggarwal, S., Kumar, V., Patel, S., & Kumar, P. (2019). Epidemiology of pelvic fractures in adults: Our experience at a tertiary hospital. Chinese Journal of Traumatology, 22(3), 138–141. https://doi.org/10.1016/j.cjtee.2019.03.003
15. Giannoudis, P. V., Grotz, M. R., Tzioupis, C., Dinopoulos, H., Wells, G. E., & Bouamra, O. (2007). Prevalence of pelvic fractures, associated injuries, and mortality: The United Kingdom perspective. Journal of Trauma, 63(4), 875–883. https://doi.org/10.1097/01.ta.0000242259.67486.15
16. Gray, H. (2013). Gray's Anatomy. Arcturus Publishing.
17. Hodgson, S. (2009). AO principles of fracture management. Annals of the Royal College of Surgeons of England, 91(5), 448–449. https://doi.org/10.1308/rcsann.2009.91.5.448b
18. Hori, M., Suzuki, K., Epstein, M. L., & Baron, R. L. (2011). Computed tomography liver volumetry using 3-dimensional image data in living donor liver transplantation: Effects of the slice thickness on the volume calculation. Liver Transplantation, 17(12), 1427–1436. https://doi.org/10.1002/lt.22419
19. Iwano, S., Okada, T., Satake, H., & Naganawa, S. (2009). 3D-CT volumetry of the lung using multidetector row CT: Comparison with pulmonary function tests. Academic Radiology, 16(3), 250–256. https://doi.org/10.1016/j.acra.2008.09.019
20. Johnson, M. H., Chang, A., & Brandes, S. B. (2013). The value of digital rectal examination in assessing for pelvic fracture–associated urethral injury: What defines a high-riding or nonpalpable prostate? Journal of Trauma and Acute Care Surgery, 75(5), 913–915. https://doi.org/10.1097/TA.0b013e3182a68668
21. Journal of Orthopaedic Trauma. (2018). Special issue: AO classification of pelvic fractures. Journal of Orthopaedic Trauma, 32(Suppl. 1).
22. Kannus, P., Palvanen, M., Niemi, S., Parkkari, J., & Järvinen, M. (2000). Epidemiology of osteoporotic pelvic fractures in elderly people in Finland: Sharp increase in 1970–1997 and alarming projections for the new millennium. Osteoporosis International, 11(5), 443–448.
23. Lange, R. H., & Hansen, S. T. Jr. (1985). Pelvic ring disruptions with symphysis pubis diastasis: Indications, technique, and limitations of anterior internal fixation. Clinical Orthopaedics and Related Research, 201, 130–137.
24. Linstrom, N. J., Heiserman, J. E., Kortman, K. E., Crawford, N. R., Baek, S., Anderson, R. L., Pitt, A. M., Karis, J. P., Ross, J. S., Lekovic, G. P., & Dean, B. L. (2009). Anatomical and biomechanical analyses of the unique and consistent

locations of sacral insufficiency fractures. Spine, 34(4), 309–315. https://doi.org/10.1097/BRS.0b013e318191ea01

25. Maier, B., Ploss, C., & Marzi, I. (2010). Verletzungen der thorakolumbalen Wirbelsäule. Der Orthopäde, 39(3), 247–255. https://doi.org/10.1007/s00132-009-1542-3
26. McMinn, K. R., Thomas, E. V., Martin, K. R., Lee, M. M., Patel, R. A., & Smith, L. J. (2020). Psychological morbidity and functional impairment following traumatic pelvic injury. Injury, 51(4), 978–983. https://doi.org/10.1016/j.injury.2020.02.038
27. Oberkircher, L., Ruchholtz, S., Rommens, P. M., Hofmann, A., Büking, B., & Krüger, A. (2018). Osteoporotic pelvic fractures. Deutsches Ärzteblatt International, 115(5), 70–80. https://doi.org/10.3238/arztebl.2018.0070
28. Pereira, G. J. C., Damasceno, E. R., Dinhane, D. I., Bueno, F. M., Leite, J. B. R., & Ancheschi, B. C. (2017). Epidemiology of pelvic ring fractures and injuries. Revista Brasileira de Ortopedia, 52(3), 260–269.
29. Pfeifer, R., Tarkin, I. S., Rocos, B., & Pape, H. C. (2009). Patterns of mortality and causes of death in polytrauma patients—Has anything changed? Injury, 40(9), 907–911. https://doi.org/10.1016/j.injury.2009.05.006
30. Pieper, A., Thony, F., Brun, J., Rodière, M., Boussat, B., Arvieux, C., Tonetti, J., Payen, J. F., & Bouzat, P. (2018). Resuscitative endovascular balloon occlusion of the aorta for pelvic blunt trauma and life-threatening hemorrhage: A 20-year experience in a Level I trauma center. Journal of Trauma and Acute Care Surgery, 84(3), 449–453. https://doi.org/10.1097/TA.0000000000001794
31. Pizanis, A., Pohlemann, T., Burkhardt, M., Aghayev, E., & Holstein, J. H. (2013). Emergency stabilization of the pelvic ring: Clinical comparison between three different techniques. Injury, 44(12), 1760–1764.
32. Pohlemann, T., Regel, G., Bosch, U., Stief, C., & Tscherne, H. (1998). Notfallbehandlung und Komplextrauma. In H. Tscherne & T. Pohlemann (Eds.), Tscherne Unfallchirurgie, Band 4, Becken und Acetabulum (pp. 89–116). Springer-Verlag.
33. Rommens, P. M., & Hofmann, A. (2013). Comprehensive classification of fragility fractures of the pelvic ring: Recommendations for surgical treatment. Injury, 44(12), 1733–1744. https://doi.org/10.1016/j.injury.2013.06.023
34. Rommens, P. M., & Hofmann, A. (2023). The FFP-classification: From eminence to evidence. Injury, 54 (Suppl 3), S10–S19. https://doi.org/10.1016/j.injury.2021.09.016
35. Rollmann, M. F., Herath, S. C., Kirchhoff, F., Braun, B. J., Holstein, J. H., Pohlemann, T., Menger, M. D., & Histing, T. (2017). Pelvic ring fractures in the elderly now and then – a pelvic registry study. Archives of Gerontology and Geriatrics, 71, 83–88. https://doi.org/10.1016/j.archger.2017.03.007
36. Rossaint, R., Cerny, V., Coats, T. J., Duranteau, J., Fernández-Mondéjar, E., Gordini, G., Stahel, P. F., Hunt, B. J., Neugebauer, E., & Spahn, D. R. (2006).

Key issues in advanced bleeding care in trauma. Shock, 26(4), 322–331. https://doi.org/10.1097/01.shk.0000225403.15722.e9

37. Rossaint, R., Duranteau, J., Stahel, P. F., & Spahn, D. R. (2007). Nonsurgical treatment of major bleeding. Anesthesiology Clinics, 25(1), 35–48.
38. Schindler, C. R., Sturm, R., Hörauf, J. A., Marzi, I., & Störmann, P. (2023). The sequence of the treatment of combined fractures of the pelvis, spine, and extremities in polytraumatized patients. EFORT Open Reviews, 8(5), 372–381. https://doi.org/10.1530/EOR-23-0046
39. Sobantu, N. A., Skaal, L., & Tshabalala, M. D. (2017). Health related quality of life of patients post pelvic fractures in the Tshwane Academic Hospitals, Pretoria, South Africa. Sefako Makgatho Health Sciences University [Unpublished master's thesis].
40. Sunil, T. M., & Shetty, N. (2000). Indicators of morbidity in pelvic fractures. Indian Journal of Orthopaedics, 34(3), 168–172.
41. Tile, M. (1988). Pelvic ring fractures: Should they be fixed? Journal of Bone and Joint Surgery - British Volume, 70(1), 1–12. https://doi.org/10.1302/0301-620X.70B1.3276697
42. Usui, R., & Kondo, H. (2024). Transcatheter arterial embolization for hemorrhagic pelvic fracture: Review article. Interventional Radiology (Higashimatsuyama), 9 (3), 156–163. https://doi.org/10.22575/interventionalradiology.2023-0015
43. Veith, N. T., Klein, M., Köhler, D., Tschernig, T., Holstein, J., Mörsdorf, P., Pohlemann, T., & Braun, B. J. (2016). Blood loss in pelvic ring fractures: CT-based estimation. Annals of Translational Medicine, 4(19), 366. https://doi.org/10.21037/atm.2016.08.39
44. Verma, V., Sen, R. K., Tripathy, S. K., Aggarwal, S., & Sharma, S. (2020). Factors affecting quality of life after pelvic fracture. Journal of Clinical Orthopaedics and Trauma, 11(6), 1016–1024. https://doi.org/10.1016/j.jcot.2020.08.011
45. Westhoff, J., Laurer, H., Wutzler, S., Wyen, H., Mack, M., Maier, B., & Marzi, I. (2008). Interventionelle Notfallembolisation bei schweren Beckenfrakturen mit arterieller Blutung: Integration in den frühklinischen Behandlungsalgorithmus. Der Unfallchirurg, 111, 821–828.
46. Wortmann, M., Engelhart, M., Elias, K., Popp, E., Zerwes, S., & Hyhlik-Dürr, A. (2020). Resuscitative endovascular balloon occlusion of the aorta (REBOA): Aktuelles zu Material, Indikationen und Grenzen – ein Überblick. Die Chirurgie, 11, [online publication].
47. World Health Organization. (2011). Global health and aging. National Institute on Aging, National Institutes of Health. https://www.who.int/ageing/publications/global_health/en/
48. Wu, Y. T., Cheng, C. T., Tee, Y. S., Fu, C. Y., Liao, C. H., & Hsieh, C. H. (2020). Pelvic injury prognosis is more closely related to vascular injury severity than anatomical fracture complexity: The WSES classification for pelvic trauma

makes sense. World Journal of Emergency Surgery, 15(1), 48. https://doi.org/10.1186/s13017-020-00328-x

49. Yoshihara, H., & Yoneoka, D. (2014). Demographic epidemiology of unstable pelvic fracture in the United States from 2000 to 2009: Trends and in-hospital mortality. Journal of Trauma and Acute Care Surgery, 76(2), 380–385. https://doi.org/10.1097/TA.0b013e3182ab0cde

# 8 Summary

***Introduction***

Pelvic fractures, often resulting from high-energy trauma, pose significant challenges in emergency medicine and trauma surgery, particularly due to their association with substantial hemorrhage. The severity and complexity of these injuries necessitate accurate and timely assessment to guide management strategies. Traditionally, the emphasis on evaluating bleeding volume in pelvic fractures has focused on intrabdominal bleeding, with less attention given to intramuscular bleeding and fracture hematomas. Given the dynamic nature of hemorrhagic complications in trauma settings, this study explores the utility of 3D Slicer Volumetry in measuring bleeding volumes associated with unstable pelvic fractures, targeting primarily patients with Type B and Type C fractures.

***Goal***

The primary aim of this research is to leverage advanced imaging techniques through 3D Slicer Volumetry to quantify bleeding volumes in patients with partially and completely unstable pelvic fractures. The investigation specifically seeks to: (1) determine differences in bleeding volume between pelvic fractures classified as Type B versus Type C by the AO Classification system; (2) evaluate the efficacy of 3D Slicer Volumetry as a viable clinical tool for defining bleeding volume; and (3) assess whether the quantified intracavitary bleeding correlates with overall blood loss in these traumatic injuries.

***Material and Methods***

This retrospective study was carried out using data from 70 patients who sustained Type B or Type C pelvic fractures at the University Hospital of Giessen between 2016 and 2021. Inclusion criteria encompassed patients aged 14 years or older, experiencing stable clinical conditions upon arrival, and having undergone a full-body CT scan with contrast. Following data collection, 3D Slicer software was employed for the volumetric analysis of bleeding volumes, allowing interactive segmentation and comprehensive assessment of hematomas.

Statistical analysis utilized non-parametric methods, particularly the Mann-Whitney U test, to compare bleeding volumes and clinical parameters across different fracture types. Key variables included age, gender, mechanism of injury, and laboratory findings at admission.

***Results***

The findings indicate a predominance of pelvic fractures due to traffic accidents, encompassing 57.14% of cases. The average age of the patients was 49.98 years, with a male-to-female ratio of approximately 3:1. The mean volume of bleeding recorded was 591.9 ml (±455.4 ml). Notably, 42.86% of patients sustained Type B fractures, while the remainder had Type C fractures. Results demonstrated statistically significant differences in bleeding volumes between the two fracture types, with Type C fractures presenting greater hemorrhagic volumes.

Systolic blood pressure upon admission was primarily above 89 mmHg in 90% of patients, indicating a relatively stable hemodynamic state despite significant injuries. The average duration of hospitalization was 33.55 days, reflecting the complexity of treatments necessitated by unstable pelvic fractures.

***Discussion***

The results underscore the clinical relevance of accurately assessing bleeding volumes in pelvic fractures, which can significantly influence treatment pathways in trauma settings. The application of 3D Slicer Volumetry proved effective in providing precise measurements of bleeding volume, thus enhancing injury characterization. The observed trend of increased hemorrhage in Type C pelvic fractures reinforces the need for swift intervention and potential surgical exploration in cases of severe instability.

Additionally, the study emphasizes the variable responses of patients to trauma based on age and sex, highlighting the need for tailored assessment protocols. While the results reveal promising data regarding the quantification of bleeding volumes, further research is warranted to correlate volumetric data with clinical outcomes and resource allocation in trauma care.

***Conclusion***

This study demonstrates the feasibility and utility of using 3D Slicer Volumetry to evaluate bleeding volumes in patients with unstable pelvic fractures. The findings reveal critical differences in hemorrhagic profiles between fracture types, enhancing the understanding and management of pelvic injuries in trauma patients. Integration of advanced imaging techniques may facilitate improved outcomes through better-informed clinical decision-making in emergency trauma care. Future investigations should focus on longitudinal outcomes related to volumetric assessment and treatment effectiveness in pelvic fracture management.

# 9 Zusammenfassung

***Einführung***

Beckenfrakturen, die häufig durch hochenergetisches Trauma verursacht werden, stellen in der Notfallmedizin und Unfallchirgie erhebliche Herausforderungen dar, insbesondere aufgrund ihrer Assoziation mit erheblichen Blutungen. Die Schwere und Komplexität dieser Verletzungen erfordern eine genaue und zeitnahe Bewertung, um die Behandlungsstrategien zu steuern. Traditionell lag der Fokus auf der Bewertung des Blutungsvolumens bei Beckenfrakturen auf dem intraabdominalen Blutverlust, während intramuskuläre Blutungen und Frakturhämatome weniger Beachtung fanden. Angesichts der dynamischen Natur der hämorrhagischen Komplikationen in Traumazentren untersucht diese Studie den Einsatz der 3D Slicer Volumetrie zur Messung des Blutungsvolumens bei instabilen Beckenfrakturen, wobei der Schwerpunkt auf Patienten mit Typ B- und Typ C-Frakturen liegt.

***Ziel***

Das Hauptziel dieser Forschung ist es, fortschrittliche Bildgebungstechniken durch 3D Slicer Volumetrie zu nutzen, um das Blutungsvolumen bei Patienten mit teilweise und vollständig instabilen Beckenfrakturen zu quantifizieren. Die Untersuchung zielt speziell darauf ab: (1) Unterschiede im Blutungsvolumen zwischen Beckenfrakturen zu bestimmen, die nach dem AO-Klassifikationssystem als Typ B bzw. Typ C eingestuft sind; (2) die Wirksamkeit der 3D Slicer Volumetrie als praktikables klinisches Werkzeug zur Definition des Blutungsvolumens zu bewerten; und (3) zu beurteilen, ob das quantifizierte intrakavitär Blutungsvolumen mit dem Gesamtblutverlust bei diesen traumatischen Verletzungen korreliert.

***Material und Methoden***

Diese retrospektive Studie basierte auf Daten von 70 Patienten, die zwischen 2016 und 2021 an der Universitätsklinik Gießen eine Typ B- oder Typ C-Beckenfraktur behandelt wurden. Die Einschlusskriterien umfassten Patienten im Alter von 14 Jahren oder älter, die bei Eintreffen klinisch stabil waren und eine Ganzkörper-CT-Untersuchung mit Kontrastmittel durchlaufen hatten. Nach der Datenerhebung wurde die 3D Slicer-Software zur volumetrischen Analyse der Blutungsvolumina eingesetzt, die eine interaktive Segmentierung und umfassende Beurteilung von Hämatomen ermöglicht.

Für die statistische Analyse wurden nichtparametrische Methoden, insbesondere der Mann-Whitney-U-Test, verwendet, um Blutungsvolumina und klinische Parameter über verschiedene Frakturtypen hinweg zu vergleichen. Wichtige Variablen umfassten Alter, Geschlecht, Mechanismus der Verletzung und Laborbefunde bei der Aufnahme.

***Ergebnisse***

Die Ergebnisse zeigen, dass der Großteil der Beckenfrakturen durch Verkehrsunfälle verursacht wurde (57,14 % der Fälle). Das Durchschnittsalter der Patienten betrug 49,98 Jahre, wobei das Verhältnis von Männern zu Frauen etwa 3:1 betrug. Das durchschnittliche Blutungsvolumen betrug 591,9 ml (±455,4 ml). Bemerkenswerterweise waren 42,86 % der Patienten mit Typ-B-Frakturen klassifiziert, während der Rest Typ-C-Frakturen aufwies. Die Ergebnisse zeigten statistisch signifikante Unterschiede in den Blutungsvolumina zwischen den beiden Frakturtypen, wobei Typ-C-Frakturen größere Blutungsvolumina aufwiesen.

Der systolische Blutdruck bei der Aufnahme war bei 90 % der Patienten überwiegend über 89 mmHg, was auf einen relativ stabilen hämodynamischen Zustand trotz erheblicher Verletzungen hinweist. Die durchschnittliche Dauer des Krankenhausaufenthalts betrug 33,55 Tage, was die Komplexität der erforderlichen Behandlungen bei instabilen Beckenfrakturen widerspiegelt.

***Diskussion***

Die Ergebnisse unterstreichen die klinische Relevanz einer genauen Bewertung des Blutungsvolumens bei Beckenfrakturen, die einen erheblichen Einfluss auf die Behandlungswege in Notfallsituationen haben kann. Die Anwendung der 3D Slicer Volumetrie erwies sich als effektiv zur Bereitstellung präziser Messungen des Blutungsvolumens, was die Charakterisierung der Verletzungen verbessert. Der beobachtete Trend einer erhöhten Blutung bei Typ-C-Beckenfrakturen verstärkt die Notwendigkeit einer schnellen Intervention und potenziellen chirurgischen Exploration bei schweren Instabilitäten.

Darüber hinaus betont die Studie die unterschiedlichen Reaktionen der Patienten auf Traumata basierend auf Alter und Geschlecht und hebt die Notwendigkeit maßgeschneiderter Bewertungsprotokolle hervor. Während die Ergebnisse vielversprechende Daten zur quantitativen Bewertung von Blutungsvolumina liefern, sind weitere Untersuchungen erforderlich, um die volumetrischen Daten mit klinischen Ergebnissen und der Ressourcenallokation in der Notfallversorgung zu korrelieren.

***Fazit***

Diese Studie demonstriert die Machbarkeit und den Nutzen der Verwendung der 3D Slicer Volumetrie zur Bewertung von Blutungsvolumina bei Patienten mit instabilen Beckenfrakturen. Die Ergebnisse zeigen kritische Unterschiede in den hämorrhagischen Profilen zwischen den Frakturtypen und verbessern das Verständnis und die Behandlung von Beckenverletzungen bei Trauma-Patienten. Die Integration fortschrittlicher Bildgebungstechniken könnte die Ergebnisse durch besser informierte klinische Entscheidungen in der Notfallversorgung verbessern. Zukünftige Untersuchungen sollten sich auf die longitudinalen Ergebnisse in Bezug auf die volumetrische Bewertung und die Behandlungswirksamkeit im Management von Beckenfrakturen konzentrieren.

# 10 List of Figures

**Figure 1: Pelvic inlet and associated anatomical structures.** The figure illustrates the main anatomical landmarks of the pelvic inlet, including the sacro-iliac joint, pubic symphysis, ischiopubic ramus, and obturator foramen, among others. Adapted from Gray, Henry (2013), *Gray's Anatomy*, London, England: Arcturus Publishing. ……..……4

**Figure 2: Anatomical components of the pelvic bone.** (A) Medial surface of the pelvic bone, highlighting structures such as the iliac fossa, arcuate line, and pubic crest. (B) Lateral surface of the pelvic bone, illustrating features including the gluteal surface, anterior superior iliac spine, and acetabulum. Adapted from Gray, Henry (2013), *Gray's Anatomy*, London, England: Arcturus Publishing.……...……5

**Figure 3: Sacrum and sacro-iliac joint anatomy.** (A) Anterior view of the sacrum, illustrating key structures such as the anterior sacral foramina, promontory, and ala. (B) Posterior view of the sacrum, highlighting the sacral hiatus, sacral cornua, and posterior sacral foramina. (C) Lateral view of the sacrum, showing the superior articular process, articular facet for the hip bone, and the promontory. Adapted from Gray, Henry (2013), *Gray's Anatomy*, London, England: Arcturus Publishing…….....8

**Figure 4: Comparison of the bony pelvis between women and men.** (A) Female pelvis with a circular pelvic inlet and a wider pubic arch angle (80–85°). (B) Male pelvis with a heart-shaped pelvic inlet and a narrower pubic arch angle (50–60°). The inset illustrations depict an approximation of the pubic arch angle: the angle between the thumb and index finger for women, and the angle between the index and middle fingers for men. Adapted from Gray, Henry (2013), *Gray's Anatomy*, London, England: Arcturus Publishing…… ……..……9

**Figure 5: Muscles of the pelvic region (medial view of the right side of the pelvis).** The illustration highlights key muscles of the pelvic region, including the obturator internus, piriformis, coccygeus, and components of the levator ani (iliococcygeus, pubococcygeus, and puborectalis muscles). Additional structures shown include thetendinous arch, urogenital hiatus, and sacrospinous ligament, which has been partially cut for clarity. Adapted from Gray, Henry (2013), *Gray's Anatomy*, London, England: Arcturus Publishing…….11

**Figure 6: Branches of the internal iliac artery and associated structures (male pelvis).** The illustration highlights the internal iliac artery, which divides into the posterior and anterior trunks. Key branches of the posterior trunk include the iliolumbar artery, lateral sacral arteries, and superior gluteal artery, which supply the posterior abdominal wall, sacrum, and gluteal region. The vascular anatomy of the pelvis demonstrates the close relationship between arterial branches and surrounding structures. Adapted from Gray, Henry (2013), *Gray's Anatomy*, London, England: Arcturus Publishing. ……..……13

**Figure 7: Branches of the anterior trunk of the internal iliac artery in females.** This illustration highlights the arterial branching of the anterior trunk of the internal iliac artery, including the uterine artery, vaginal artery, umbilical artery, obturator artery, middle rectal artery, internal pudendal artery, and inferior gluteal artery. These arteries supply blood to the pelvic viscera, perineum, and adjacent structures. The medial umbilical ligament is also depicted, showing its continuation from the umbilical artery. Adapted from Gray, Henry (2013), *Gray's Anatomy*, London, England: Arcturus Publishing.…… ……...15

**Figure 8: Components and branches of the sacral and coccygeal plexuses.** This diagram illustrates the anatomical composition of the sacral and coccygeal plexuses, including contributions from the lumbosacral trunk (L4 and L5), ventral rami of S1 to Co, and their major branches. Key nerves such as the sciatic nerve, superior and inferior gluteal nerves, pudendal nerve, and pelvic splanchnic nerves are shown, along with their targets, including the musculus piriformis, levator ani, and external anal sphincter. Dorsal and ventral divisions are color-coded for clarity. Adapted from Gray, Henry (2013), *Gray's Anatomy*, London, England: Arcturus Publishing……..……16

**Figure 9a: Tile Classification of Pelvic Fractures. The illustration depicts the Tile** classification of pelvic fractures based on fracture stability and mechanism of injury. Type A: Stable fractures, including A1 (fractures not involving the pelvic ring) and A2 (stable, minimally displaced fractures of the ring). Adapted from Journal of the Royal Army Medical Corps (jramc.bmj.com)…….…….…….18

**Figure 9b: Tile Classification of Pelvic Fractures.** The illustration depicts the Tile classification of pelvic fractures based on fracture stability and mechanism of injury. Type B: Rotationally unstable but vertically stable fractures, subdivided into B1 (open book injuries), B2 (ipsilateral lateral compression), and B3 (contralateral lateral compression or bucket-handle injuries). Adapted from Journal of the Royal Army Medical Corps (jramc.bmj.com). ……..…19

**Figure 9c. Tile Classification of Pelvic Fractures.** The illustration depicts the Tile classification of pelvic fractures based on fracture stability and mechanism of injury. Type C: Rotationally and vertically unstable fractures, including C1 (unilateral instability), C2 (bilateral instability), and C3 (associated with acetabular fractures). Adapted from Journal of the Royal Army Medical Corps (jramc.bmj.com)……...……..20

**Figure 10a: Type 61A- Stable Fractures with Intact Posterior Arch.** This figure illustrates Type 61A fractures, which maintain posterior arch stability. Subgroups include avulsion fractures of the anterior superior iliac spine, anterior inferior iliac spine, or ischial tuberosity (61A1); iliac wing fractures and unilateral or bilateral anterior arch fractures (61A2); and transverse fractures of the sacrum or coccyx (61A3). *Adapted from J Orthop Trauma* • Volume 32, Number 1 Supplement, January 2018 (*Copyright © 2017 by AO Foundation, Davos, Switzerland; Orthopaedic Trauma Association, IL, US* www.jorthotrauma.com). ……...21

**Figure 10b: Type 61B - Partially Stable Fractures with Rotational Instability Depicts Type 61B fractures.** Characterized by incomplete posterior arch disruption and rotational instability. Subgroups include lateral compression fractures (LC1), open book fractures (APC1), and unilateral posterior injuries with varying rotational instability (LC2 and APC2). *Adapted from J Orthop Trauma* • Volume 32, Number 1 Supplement, January 2018 (*Copyright © 2017 by AO Foundation, Davos, Switzerland; Orthopaedic Trauma Association, IL, US* www.jorthotrauma.com). …….22

**Figure 10c: Type 61B (Continued) - Bilateral Posterior Injuries with Rotational Instability.** Shows bilateral posterior injuries (61B3) involving combinations of lateral compression (LC3) and external rotation instability (APC2). These injuries result in complex patterns of instability on both sides of the pelvis. *Adapted from J Orthop Trauma* • Volume 32, Number 1 Supplement, January 2018 (*Copyright © 2017 by AO Foundation, Davos, Switzerland; Orthopaedic Trauma Association, IL, US* www.jorthotrauma.com)..…….....……....23

**Figure 10d: Type 61C- Complete Posterior Arch Disruption (Unilateral).** Illustrates Type 61C fractures, where the posterior arch is completely disrupted. Subgroups include injuries through the iliac bone, sacroiliac joint, or sacrum (61C1). *Adapted from J Orthop Trauma* • Volume 32, Number 1 Supplement, January 2018 (*Copyright © 2017 by AO Foundation, Davos,*

*Switzerland; Orthopaedic Trauma Association, IL, US* www.jorthotrauma.com). ……..……24

**Figure 11: FFP Classification of Pelvic Ring Fractures.** This figure illustrates the FFP (Fragility Fracture of the Pelvis) classification, which categorizes fractures based on the location and displacement of pelvic ring injuries: FFP Type I: Anterior pelvic ring fractures only, with no involvement of the posterior pelvic ring. (A-C) Examples show variations in fracture patterns with corresponding radiographs and CT images. FFP Type II: Non-displaced posterior pelvic ring fractures, where the posterior ring is involved without significant displacement. (A-C) Subcategories illustrate different posterior injury patterns with detailed imaging. FFP Type III: Displaced unilateral posterior pelvic ring fractures, involving one side of the posterior ring with displacement. (A-C) Examples demonstrate unilateral posterior fractures with associated anterior ring involvement. FFP Type IV: Displaced bilateral posterior pelvic ring fractures, where both sides of the posterior ring show significant displacement. (A-C) Imaging highlights bilateral instability and severe disruptions in the pelvic ring. The figure integrates schematic illustrations, radiographs, and CT images to provide a comprehensive visualization of each FFP classification subtype. Injury. 2013;44(12):1733–44...……...……26

**Figure 12: REBOA during Non-Traumatic Cardiac Arrest (NTCA) can enhance hemodynamics and improve organ perfusion, particularly to the heart and brain, by occluding the aorta.** This placement allows for targeted redirection of blood flow, effectively managing hemorrhagic shock and stabilizing patients until further interventio.ns. It also facilitates advanced resuscitation techniques like ECMO, potentially improving survival rates in critical situations. Overall, REBOA serves as a valuable tool in emergency care for managing cardiac arrest. J.Clin.Med. 2022, 11(3),742; https://doi.org/10.3390/jcm11030742.....30

**Figure 13: Example of Segmentation and 3D Reconstruction in a Patient with Pelvic Bleeding.** The figure demonstrates a multi-planar CT segmentation and 3D reconstruction of a patient with pelvic bleeding. Top Left: Axial CT view showing the bleeding region highlighted in red. Top Right: 3D reconstruction illustrating the bleeding distribution in relation to the skeletal anatomy. Bottom Left: Coronal CT view emphasizing the extent of the hemorrhage and its anatomical relationships. Bottom Right: Sagittal CT view detailing the vertical spread of the bleeding along the pelvic structures. This visualization highlights the utility of the "Thresholding" function, helping us to distinguish the different tissues……...……..36

**Figure 14: Example of Segmentation and 3D Reconstruction in a Patient with Pelvic Bleeding.** The figure demonstrates a multi-planar CT segmentation and 3D reconstruction of a patient with pelvic bleeding. Top Left: Axial CT view showing the bleeding region highlighted in red. Top Right: 3D reconstruction illustrating the bleeding distribution in relation to the skeletal anatomy. Bottom Left: Coronal CT view emphasizes the hemorrhage's extent and its anatomical relationships. Bottom Right: Sagittal CT view detailing the vertical spread of the bleeding along the pelvic structures. This visualization highlights the utility of the "Smoothing and Closing" function, helping us to distinguish the different tissues.……. ……...……...37

**Figure 15: Example of Segmentation and 3D Reconstruction in a Patient with Pelvic Bleeding.** The figure demonstrates a multi-planar CT segmentation and 3D reconstruction of a patient with pelvic bleeding. Top Left: Axial CT view showing the bleeding region highlighted in red. Top Right: 3D reconstruction illustrating the bleeding distribution in relation to the skeletal anatomy. Bottom Left: Coronal CT view emphasizing the extent of the hemorrhage and its anatomical relationships. Bottom Right: Sagittal CT view detailing the vertical spread of the bleeding along the pelvic structures. This visualization highlights the utility of segmentation and 3D reconstruction for identifying and localizing hemorrhagic sites, crucial for surgical planning and trauma management. ….……..…38

**Figure 16: 3D Reconstruction and Quantification of Bleeding in a Patient with an Unstable Pelvic Fracture.** This figure illustrates the 3D reconstruction and segmentation of pelvic bleeding in a patient with an unstable pelvic fracture, combined with quantitative analysis of the bleeding volume: Top Left: Axial CT view highlighting the bleeding (red) and skeletal structures (yellow). Top Right: 3D reconstruction showing the spatial distribution of the bleeding relative to the pelvis. Bottom Left: Coronal CT view visualizing the vertical extent of the hemorrhage. Bottom Right: Sagittal CT view providing additional anatomical context of the bleeding region. Table: The table below quantifies the bleeding, presenting the number of voxels, volume in cubic millimeters (mm3), and cubic centimeters (cm3), as well as the surface area of the segmented structures (bone and clot). This quantification is critical for assessing injury severity and planning treatment strategies. …….39

**Figure 17: Histogram of Age at Admission.** The histogram illustrates the age distribution of the study population, highlighting two distinct peaks: one between 18 and 35 years and another between 50 and 60 years. The superimposed curve represents the normal distribution for comparison, with a mean age of 49.88 years and a standard deviation of ±21.47 years. The dataset includes a total of 69 patients, showcasing a wide age range from 15 to 88 years. This distribution indicates potential differences in injury patterns and demographics across age group. ……..41

**Figure 18: Distribution of patients based on the mechanism of injury.** The chart illustrates that 57.14% of pelvic fractures were caused by traffic accidents (blue segment), 25.71% resulted from falls exceeding three meters (green segment), and 17.14% were due to falls of less than three meters (red segment). ……...42

**Figure 19: Distribution of the total length of hospital stay (in days) for the patient group.** The mean duration of hospitalisation was 33.55 days, with a standard deviation of ±21.68. The histogram illustrates the frequency of hospital stays and includes a normal distribution curve for reference. ……..43

**Figure 20: Distribution of the amount of bleeding (in ml) in patients with pelvic fractures.** The mean bleeding volume was 591.9 ml, with a standard deviation of ±455.4 ml. The histogram depicts the frequency of bleeding volumes, overlaid with a normal distribution curve for reference. ……..44

**Figure 21: Distribution of systolic blood pressure in patients upon admission to the emergency room.** The majority of patients (63, 90.00%) had systolic blood pressure values above 89 mmHg. A smaller proportion of patients (5, 7.14%) had systolic pressures between 75 and 89 mmHg, while only 2 patients (2.86%) had systolic blood pressure below 75 mmHg. ……...…...44

**Figure 22: Mean bleeding volume (in ml) across different age categories.** The chart illustrates the average bleeding volume at admission for patients grouped into age ranges. Younger patients (≤20 years) exhibited the highest mean bleeding volume (916.7 ml), while older age groups (81–90 years) showed significantly lower mean bleeding volumes (227.8 ml). ……...……...47

**Figure 23: Distribution of mean bleeding volume (in ml) across subcategorised patient age groups.** The chart shows that patients under 20 years of age exhibited the highest mean bleeding volume (916.74 ml), followed by patients aged 21–60 years (585.36 ml), and patients over 60 years (488.08 ml). …….47

**Figure. 24:** Example of a patient with pelvic fracture type C2.1 with bleeding from the one of the branches of the ileal arteries with big hematoma…….……..49

**Figure 25: Distribution of bleeding volume (in ml) across different patient groups classified according to the FFP Classification.** The chart highlights the mean bleeding volume for each subgroup, with FFP4B showing the highest mean bleeding volume at 827.5 ml, followed by FFP3C at 814.2 ml. ……..……..50

**Figure 26: Distribution of blood loss (in ml) across three groups of patients classified by systolic blood pressure at admission.** The groups represent systolic blood pressure scores: >89 mmHg (607.8 ml), 75–89 mmHg (581.0 ml) and <75 mmHg (592.3 ml). The chart demonstrates similar average blood loss across the groups, irrespective of systolic blood pressure levels. ……..……51

**Figure 27: Distribution of Trauma and Injury Severity Score (TRISS) among admitted patients. Th**e histogram illustrates the severity of injuries, with a mean TRISS value of 5.69 (±1.70). The frequency of patients is shown across TRISS ranges, highlighting the prevalence of severe injuries in the study cohort. ……51

# 11 List of Tables

**Table 1.** Description of gender distribution. ……..……..…42

**Table 2.** Number and dispersion of accompanying injuries by patient with a pelvic fracture...…… …….……43

**Table 3.** Distribution of pelvic fracture type for patients according to the AO Classification. ……..……45

**Table 4.** Distribution of pelvic fracture type for patients according to the FFP Classification. ……..……46

**Table 5.** Distribution of bleeding amount in different groups of patients according to the AO Classification. …….....48

**Table 6.** Showing the GCS Score in patients with pelvic fracture at the day at admission in the ED. …….49

# 12 Abbreviation Index

$ - dollar

2D - two-dimensional

3D - three-dimensional

4D - four-dimensional

ABCDE – Airway- Breathing – Circulation – Disability - Exposure

AO - Arbeitsgemeinschaft für Osteosynthesefragen

ASA – American Society of Anesthesiologist

ATLS – Advanced Trauma Life Support

CT – computed tomography

CO - corporation

e.g. - example

ED – Emergency Department

FAST - Focused Assessment with Sonography for Trauma

FFP – Fragility fracture of pelvis

g/dl - Grams per decilitre

GCS – Glasgow Coma Scale

ICD - International Classification of Diseases

ICU – Intensive Care Unit

L - lumbar

ml - Milliliter

$mm^3$ - Cubic Millimeter

mm Hg - Millimeters of Mercury

MRI – magnetic resonance imaging

NSAID - nonsteroidal anti-inflammatory drugs

REBOA – Resuscitative Endovascular Balloon Occlusion of the Aorta

RTA - Road traffic accident

S – sacral

SD - Standard Deviation

SPSS - Statistical Package for the Social Sciences

TAE - Trans arterial embolisation

TH – thoracic

TRISS - Trauma and Injury Severity Score

X-Ray – Conventional Radiography

# 13 Ehrenwörtliche Erklärung

„Hiermit erkläre ich, dass ich die vorliegende Arbeit selbständig und ohne unzulässige Hilfe oder Benutzung anderer als der angegebenen Hilfsmittel angefertigt habe. Alle Textstellen, die wörtlich oder sinngemäß aus veröffentlichten oder nichtveröffentlichten Schriften entnommen sind, und alle Angaben, die auf mündlichen Auskünften beruhen, sind als solche kenntlich gemacht. Bei den von mir durchgeführten und in der Dissertation erwähnten Untersuchungen habe ich die Grundsätze guter wissenschaftlicher Praxis, wie sie in der „Satzung der Justus-Liebig-Universität Gießen zur Sicherung guter wissenschaftlicher Praxis“ niedergelegt sind, eingehalten sowie ethische, datenschutzrechtliche und tierschutzrechtliche Grundsätze befolgt. Ich versichere, dass Dritte von mir weder unmittelbar noch mittelbar geldwerte Leistungen für Arbeiten erhalten haben, die im Zusammenhang mit dem Inhalt der vorgelegten Dissertation stehen, und dass die vorgelegte Arbeit weder im Inland noch im Ausland in gleicher oder ähnlicher Form einer anderen Prüfungsbehörde zum Zweck einer Promotion oder eines anderen Prüfungsverfahrens vorgelegt wurde. Alles aus anderen Quellen und von anderen Personen übernommene Material, das in der Arbeit verwendet wurde oder auf das direkt Bezug genommen wird, wurde als solches kenntlich gemacht. Insbesondere wurden alle Personen genannt, die direkt und indirekt an der Entstehung der vorliegenden Arbeit beteiligt waren. Mit der Überprüfung meiner Arbeit durch eine Plagiatserkennungssoftware bzw. ein internetbasiertes Softwareprogramm erkläre ich mich einverstanden.“

Ort/Datum Unterschrift

## 14 Acknowledgements

I wish to extend my deepest and most heartfelt gratitude to Univ.-Prof. Dr. med. Dr. h.c. Christian Heiß and Prof. Dr. rer. nat. Thaqif El Khassawna for their exceptional guidance, insightful mentorship, and unwavering support throughout the course of this research. Their profound expertise, constructive critique, and dedication to scientific excellence have been pivotal in shaping the development and quality of this work. Their encouragement and patience have motivated me to persevere through challenges and have inspired me to pursue rigorous academic standards. I am also profoundly grateful to Univ.-Prof. Dr. Gabriele Krombach from the University Clinic for Radiology. Her generous support, professional guidance, and provision of essential patient data have been instrumental in enabling the practical aspects of this research.

At this juncture, I must emphasize that the completion of this thesis would not have been possible without the unwavering support and encouragement of my family. Their steadfast presence, wise counsel, and unconditional love have been the cornerstone of my academic journey. Their patience and understanding during difficult times provided me with the emotional stability necessary to overcome obstacles and remain focused on my goals. Their constant motivation, coupled with their financial support, has alleviated many burdens and allowed me to dedicate myself fully to my studies, research, and professional development

I wish to express my deepest appreciation to my wife, whose unwavering support and exemplary approach to learning have profoundly influenced my own attitudes toward education and professional growth. Her dedication, patience, and insightful advice have been crucial to my success. Her belief in my potential and continuous encouragement have provided me with the strength to persevere through demanding phases of this endeavor. This thesis is dedicated to her, as she has been my most significant source of inspiration and support. Furthermore, I want to dedicate this achievement to my children, whose innocence, curiosity, and unconditional love serve as a constant reminder of the importance of perseverance and dedication. Their presence has been a source of motivation and joy, fueling my commitment to contribute meaningfully to my field and to set an example for them. Lastly, I wish to extend my sincere appreciation to all my friends and colleagues for their unwavering friendship, encouragement, and moral support.